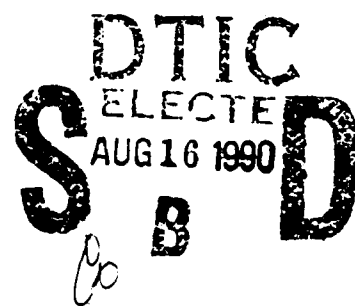WRDC-TR-90-3018

AD-A225 365

ROBUSTNESS OF FEEDBACK SYSTEMS WITH SEVERAL MODELLING ERRORS

James S. Freudenberg

University of Michigan
Ann Arbor, Michigan 48109

June 1990

Final Report for the Period March 1988 to March 1990

NOTICE

When Government drawings, specifications, or other data are used for any purpose other than in connection with a definitely Government-related procurement, the United States Government incurs no responsibility or any obligation whatsoever. The fact that the Government may have formulated or in any way supplied the said drawings, specifications, or other data, is not to be regarded by implication, or otherwise in any manner construed, as licensing the holder, or any other person or corporation; or as conveying any rights or permission to manufacture, use, or sell any patented invention that may in any way be related thereto.

This report is releasable to the National Technical Information Service (NTIS). At NTIS, it will be available to the general public, including foreign nations.

This technical report has been reviewed and is approved for publication.

SHARON A. HEISE, Capt, USAF
Project Engineer
Control Dynamics Branch
Flight Control Division

DAVID K. BOWSER, Chief
Control Dynamics Branch
Flight Control Division

FOR THE COMMANDER

H. MAX DAVIS, Assistant for
Research and Technology
Flight Control Division
Flight Dynamics Laboratory

REPORT DOCUMENTATION PAGE

Form Approved
OMB No. 0704-0188

1a. REPORT SECURITY CLASSIFICATION UNCLASSIFIED	1b. RESTRICTIVE MARKINGS N/A
2a. SECURITY CLASSIFICATION AUTHORITY N/A	3. DISTRIBUTION/AVAILABILITY OF REPORT Approved for Public Release; Distribution Unlimited
2b. DECLASSIFICATION/DOWNGRADING SCHEDULE N/A	

4. PERFORMING ORGANIZATION REPORT NUMBER(S) 025211-T-1	5. MONITORING ORGANIZATION REPORT NUMBER(S) WRDC-TR-90-3018

6a. NAME OF PERFORMING ORGANIZATION The University of Michigan	6b. OFFICE SYMBOL *(If applicable)*	7a. NAME OF MONITORING ORGANIZATION Flight Dynamics Laboratory (WRDC/FIGC) Wright Research and Development Center
6c. ADDRESS (City, State, and ZIP Code) EECS Department 4213 EECS Building Ann Arbor, MI 48109-2122		7b. ADDRESS (City, State, and ZIP Code) Wright-Patterson AFB, OH 45433-6553

8a. NAME OF FUNDING/SPONSORING ORGANIZATION Wright Research and Development Center	8b. OFFICE SYMBOL *(If applicable)* WRDC/FIGC	9. PROCUREMENT INSTRUMENT IDENTIFICATION NUMBER F33615-88-C-3601

8c. ADDRESS (City, State, and ZIP Code) Wright-Patterson AFB, OH 45433-6553	10. SOURCE OF FUNDING NUMBERS			
	PROGRAM ELEMENT NO. 61102F	PROJECT NO. 2304	TASK NO N2	WORK UNIT ACCESSION NO. 03

11. TITLE *(Include Security Classification)*

Robustness of Feedback Systems with Several Modelling Errors

12. PERSONAL AUTHOR(S)
James S. Freudenberg

13a. TYPE OF REPORT Final	13b. TIME COVERED FROM 3/88 TO 3/90	14. DATE OF REPORT (Year, Month, Day) 1990, June	15. PAGE COUNT 151

16. SUPPLEMENTARY NOTATION

17. COSATI CODES			18. SUBJECT TERMS *(Continue on reverse if necessary and identify by block number)*
FIELD	GROUP	SUB-GROUP	Robustness Multivariable Systems Feedback Designs
01	04		

19. ABSTRACT *(Continue on reverse if necessary and identify by block number)*

In this report we study robustness properties of linear multivariable feedback systems with several sources of modelling uncertainty. We assume that each source of uncertainty is modelled as a stable unstructured perturbation satisfying a frequency dependent norm bound. A stability margin for such an uncertainty description is furnished by the structured singular value. The structured singular value is obtained from a numerical optimization procedure. Consequently, it is difficult to obtain insight into the relation between its size and the plant, compensator, and design specifications upon which it depends. Our approach is to obtain such insight by deriving bounds and approximations to the structured singular value. The results we obtain are appealing in that they are both reasonably tight and in that they do provide the desired insight. We apply this insight first to understand the source of robustness difficulties associated with an ill-conditioned plant, and use the resulting information to develop a procedure for selecting weightings in LQG/LTR and H-infinity synthesis problems so that the structured singular value is minimized. — $\langle H^{\sim} f \rangle$

20. DISTRIBUTION/AVAILABILITY OF ABSTRACT [X] UNCLASSIFIED/UNLIMITED ☐ SAME AS RPT. ☐ DTIC USERS	21. ABSTRACT SECURITY CLASSIFICATION UNCLASSIFIED
22a. NAME OF RESPONSIBLE INDIVIDUAL Sharon A. Heise, Capt, USAF	22b. TELEPHONE (Include Area Code) (513)255-8683 22c. OFFICE SYMBOL WRDC/FIGCA

DD Form 1473, JUN 86   *Previous editions are obsolete.*

Project Summary

We study stability and performance robustness properties of linear multivariable feedback systems with several modelling errors. Each modelling error is assumed to be a stable unstructured perturbation that satisfies a frequency dependent norm bound but is otherwise arbitrary. The structured singular value is used to provide a stability margin for such an uncertainty description. Since the structured singular value is calculated via a numerical optimization procedure, it may be difficult to obtain insight into the relation between its size and the plant, compensator, and design specifications for the robustness problem. We derive bounds and approximations for the structured singular value as a method for providing such insight. Our results are applied first to analyze robustness difficulties that may be associated with an ill-conditioned plant, and next to develop design rules. In particular, we develop a procedure for selecting weightings to be used in the LQG/LTR and H^∞ synthesis problems so that the solutions to these optimization problems tends to minimize the structured singular value.

i

Contents

List of Figures

Chapter 1

Introduction

The problem of designing a feedback system to satisfy a performance specification and to be robustly stable against plant modelling errors is of fundamental importance in control theory. Indeed, over the last 10 years, this problem has received renewed attention, particularly in the context of multivariable systems (e.g. [DoS81], [SLH81], [Fra82], [Fra87], [Doy87], [Fra87]). Singular value analysis, based upon the singular value norm of a matrix transfer function, has served as an important tool for characterising both performance and stability robustness properties of a multivariable feedback system, and has allowed the generalisation of many useful concepts from classical feedback theory for scalar systems to multivariable systems.

Unfortunately, singular value analysis techniques are not applicable to many design problems of interest. For example, singular value robustness analysis is most useful when uncertainty is isolated at only one point in the system. When uncertainty and modelling errors are present at several points in the system, singular value analysis tends to yield estimates of stability robustness that are

1

either optimistic (by testing robustness against only one modelling error at a time) or pessimistic (by testing against a broader class of uncertainty than is actually present). Furthermore, singular value analysis is useful only for testing nominal performance properties of a system; obviously, performance should also be robust against modelling error. It may be shown [DWS82] that the robust performance problem is equivalent to one of stability robustness with an additional source of uncertainty that represents the performance specification. Hence, robust performance problems reduce to problems of stability robustness with respect to several sources of uncertainty, and the deficiencies of singular value analysis described above also apply to the analysis of robust performance.

To address the limitations of singular value analysis, Doyle ([Doy82], [DWS82]) introduced the structured singular value, an analysis tool that directly addresses the problem of stability robustness against several sources of modelling uncertainty, and thus also addresses the robust performance problem. Essentially, the structured singular value provides a precise stability margin against several simultaneous sources of modelling error.

With the aid of singular value and structured singular value analysis, several methodologies for the design of robust multivariable feedback systems have been proposed. Among these are LQG/LTR ([DoS81], [StA87]), H^∞ optimization [Fra87], and structured singular value synthesis [Doy85]. At present, each of these methodologies suffers from at least one shortcoming. For example, the LQG/LTR methodology is applicable only to robustness problems with one source of modelling error. This shortcoming is overcome by the structured singular value synthesis methodology; however, the latter methodology is experimental and tends

2

to generate exceedingly high order compensators.

It seems clear that additional insights into the properties of multivariable systems with several sources of uncertainty will be needed before a completely satisfactory design methodology can be developed. In particular, multivariable systems can possess robustness difficulties having no analogue in their scalar counterparts. For example, it has been observed by several researchers ([Ste84], [Ste85], [Ste87], [Doy87], [NeM87], [SMD88], [Fre89a], Fre89b]) that systems with ill-conditioned plants can cause robustness difficulties when modelling error is present at more than one loop location. Ill-conditioned plants arise in fields as diverse as aircraft control [Enn87] and chemical process control [SMD88]. From a systems viewpoint, ill-conditioning at a frequency means that the gain of the plant exhibits a strong directional dependence; i.e., certain input sinusoids at a frequency for which the plant is ill-conditioned will be amplified much more than will others. A thorough understanding of robustness problems caused by plant ill-conditioning is not yet available, nor is a design methodology capable of coping with these difficulties.

The work performed under this contract represents substantial progress toward understanding the robustness properties of multivariable systems with several sources of uncertainty, and toward design problems associated with an ill-conditioned plant. The springboard for the present work is provided by the results of [Fre89a, and [Fre89b]. To summarize these results briefly, the stability robustness problem with two sources of uncertainty is analyzed to determine when a system that is robust against each source of modelling error (assuming that the other is not present) can nevertheless be destabilised by small simul-

3

taneous modelling errors. These results are then applied to the ill-conditioned plant problem. A sensitivity analysis is performed to detect small modelling errors that strongly affect system stability robustness and performance. These modelling errors are then used to derive bounds upon the stability robustness margin, as quantified by the structured singular value. The significance of these bounds is that they express the interrelation among the plant directionality properties, the design specifications, and the compensator. This information suggests a strategy for compensator design to achieve robust performance and stability despite plant ill-conditioning.

The research described in this report contributes to the understanding of multivariable robustness problems in several ways. Our overall approach is summarised as follows. We shall study robustness problems that may be analysed using the Doyle's structured singular value (SSV). Because calculation of the SSV involves numerical optimisation procedures, it is difficult to obtain insight into the relation between its size and the plant, compensator, and design specifications. Such insight is useful for several reasons. First, one would like to identify combinations of plant properties and design specifications that are inherently difficult to satisfy. Second, one would like to have the capability to manipulate feedback properties, such as robustness and performance, by modifying the compensator. Our approach to obtaining such insight is to derive bounds and approximations to the SSV. To be useful, these bounds and approximations must be both reasonably accurate, and should also display the dependence of the SSV upon plant, compensator, and design specifications. Once such bounds and approximations have been derived, they are then analysed to provide insight

4

into fundamental design limitations, and to suggest compensation strategies. In particular, we incorporate the information gleaned from the bounds into a selection procedure for the weightings used in LQG/LTR, H^∞, and H^2 synthesis procedures.

The remainder of this report is outlined as follows. In Chapter 2 we shall derive bounds upon the SSV for robustness problems with two or three sources of uncertainty. The bounds with two sources of uncertainty improve those appearing in [Fre89a], and [Fre89b], while those with three sources of uncertainty are new. In Chapter 3, we analyze a specific robustness problem, that of output performance with respect to input uncertainty which is diagonal or block diagonal. Using a sensitivity analysis, as well as the bounds from Chapter 2 for three sources of uncertainty, we study the design difficulties posed by an ill-conditioned plant for such a robustness problem. In Chapter 4 we develop a framework for analysing robustness with respect to several sources of uncertainty. We identify certain *interaction parameters*, whose size determines the extent to which interactions among several modelling errors can cause robustness difficulty, and use these parameters to derive bounds upon the SSV. Chapters 5 and 6 are devoted to methods of incorporating insights obtained from our analyses into the H^∞ and LQG/LTR design methodologies. Chapter 7 contains directions for further research.

Chapter 2

Bounds on the Structured Singular Value with Two or Three Sources of Uncertainty

2.1 Introduction

The purpose of this chapter is to present bounds upon the structured singular value (SSV) with two or three sources of uncertainty. For two sources of uncertainty, our bounds improve those in [Fre89a] and [Fre89b]. For three sources of uncertainty, our bounds can be shown to improve those of Demmel [Dem88]. Applications of our bounds to specific classes of robustness problems will be found in Chapter 3 of this report.

The remainder of this chapter is organised as follows. Section 2.2 briefly reviews the structured singular value and its properties. Section 2.3 contains our main results, including both lower and upper bounds upon the 3-block structured singular value. These bounds are expressed in terms of a set of interaction parameters that essentially determine how several uncertainties can interact to

cause robustness difficulties. The research described in this chapter is discussed in [ChF89c].

2.2 Properties of the Structured Singular Value

We shall now briefly review those properties of the structured singular value used in this chapter; a complete discussion and examples are found in [Doy82]. The first step in the structured singular value analysis is to rearrange the block diagram of the feedback system into the form shown in Figure 2.1. The uncertainty matrix $\Delta(s)$ is assumed to lie in the set

$$\Delta = \{ \; \Delta(s) : \; \Delta(s) = \text{diag}[\Delta_1(s), \Delta_2(s), \cdots, \Delta_h(s)], \; \Delta_i \in C^{k_i \times k_i} \; and \; stable \; \}$$

(2.2.1)

It is often convenient to assume that system uncertainties have been scaled to satisfy the upper bound $\bar{\sigma}[\Delta_i(j\omega)] \leq \gamma, \; \forall\omega, \; \forall i$, and to introduce the set $\Delta_\gamma = \{ \; \Delta(s) : \; \Delta(s) \in \Delta \; and \; \bar{\sigma}[\Delta(j\omega)] \leq \gamma, \; \forall\omega \; \}$. The interconnection matrix

$$M(s) = [M_{ij}(s)] \;\; i,j = 1, 2, \cdots, k, \;\;\; M_{ij}(s) \in C^{k_i \times k_j}$$

(2.2.2)

is stable if the feedback system is nominally stable. At each frequency, the structured singular value, denoted $\mu[M]$, is defined[1] by [Doy82], [DWS82])[2]

$$\mu[M] = \begin{cases} 0 & det[I + M\Delta] \neq 0 \; \forall\Delta \in \Delta \\ 1/(\min_{\Delta \in \Delta}\{\bar{\sigma}[\Delta] : det[I + M\Delta] = 0\}) & otherwise \end{cases}$$

(2.2.3)

---

[1] Throughout this note, we suppress dependence upon frequency whenever appropriate.
[2] By a mild abuse of notation, the symbol Δ will occasionally be used to denote the set of constant complex matrices with block diagonal structure (2.2.1).
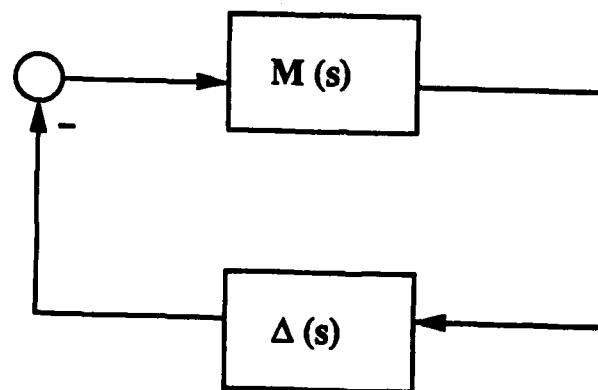
Figure 2.1: Block Diagram for Structured Singular Value Analysis

Hence, by definition, the reciprocal of the structured singular value is a frequency dependent stability margin with respect to uncertainty of the form (2.2.1), and a nominally stable feedback system will be robustly stable against all uncertainty in the set Δ_γ if and only if $\mu[M(j\omega)] < 1/\gamma$, $\forall \omega$.

The value of $\mu[M]$ can be calculated as follows. Define the set

$$D = \{\ diag[d_1 I_{k_1}, d_2 I_{k_2}, \cdots, d_k I_{k_k}] : d_i \in \mathbb{R}, d_i > 0\ \} \qquad (2.2.4)$$

where I_{k_i} denotes the identity matrix of dimension k_i. It was shown in [Doy82] that

$$\mu[M] \leq \inf_{D \in \mathcal{D}} \bar{\sigma}[DMD^{-1}] \qquad (2.2.5)$$

In particular, the upper bound $\inf_{D \in \mathcal{D}} \bar{\sigma}[DMD^{-1}]$ is equal to $\mu[M]$ when the system has three or fewer blocks of uncertainty, namely, $k \leq 3$. This fact may be used to derive bounds upon the structured singular value.

2.3 Lower and Upper Bounds of $\mu[M]$

In this section we present both lower and upper bounds on the 3-block structured singular value. For convenience, we shall first denote $\sigma_{ij} = \bar{\sigma}[M_{ij}]$, and introduce the following parameters that will be used subsequently in deriving the bounds.

$$
\begin{aligned}
\mu(i,j) &= \sqrt{\sigma_{ij}\sigma_{ji}}, \quad \forall i \neq j \\
\mu(i,j,k) &= (\sigma_{ij}\sigma_{jk}\sigma_{ki})^{1/3} \quad \forall i \neq j \neq k \\
\mu_1 &= \max_i \sigma_{ii} \\
\mu_2 &= \max_{i,j} \mu(i,j) \\
\mu_3 &= \max_{i,j,k} \mu(i,j,k)
\end{aligned}
\qquad (2.3.1)
$$

Interpretations of these parameters, which we shall term "interaction parameters," will become available as we develop bounds upon the structured singular

value. For motivation, let us postulate an analysis procedure wherein we test robustness against uncertainties taken first one at a time, then two at a time and finally all three at a time. We wish, in particular, to understand when two (or three) uncertainties can interact to cause robustness difficulties even though robustness is good with respect to uncertainties taken one (or two) at a time. It is well-known that the stability margin against Δ_i alone is equal to $1/\sigma_{ii}$ ([DWS82]. Hence the parameter μ_1 measures stability robustness against the uncertainties taken one at a time. Suppose next that we consider the effects of uncertainties taken two at a time. With no loss of generality, we may study this problem by setting $k = 2$ in (2.2.1-2).

Proposition 2.3.1 *Let* $k = 2$ *in (2.2.1-2), and suppose that the infimum in (2.2.5) is achieved. Then*

$$max \left\{ \mu_1, \, \mu_2 \right\} \leq \mu[M] \leq \mu_1 + \mu_2 \qquad (2.3.2)$$

Proof: In order to prove the lower bound, we note that $\mu[M] = \hat{\sigma}[\hat{D}M\hat{D}^{-1}]$ for some $\hat{D} = diag[d_1 I_{k_1}, d_2 I_{k_2}] \in \mathcal{D}$. It then follows that $\mu[M] \geq (d_i/d_j)\sigma_{ij}, \forall i, j$. Hence $\mu[M] \geq \sigma_{ii}$, and $\mu^2[M] \geq (d_i/d_j)\sigma_{ij} \cdot (d_j/d_i)\sigma_{ji} = \mu^2(i, j)$, thus establishing the lower bound. The proof for the upper bound is found in [Fre89a].

■

Remark 2.3.1: The upper bound in (2.3.2) first appeared in [Fre89a], and the lower bound is a tighter version of that in [Fre89a]. The statement and derivation of the improved lower bound are due to C. N. Nett (personal communication). The proof of this improved bound is significantly simpler than that of

the bound in [Fre89a], although the proof in [Fre89a] is conceptually appealing in that it provides the set of smallest destabilizing uncertainties.

Obviously, Proposition 2.3.1 can be extended to analyze the effects of any two uncertainties in the general k-block structured singular value problem. The parameter $\mu(i,j)$ essentially determines how the uncertainties Δ_i and Δ_j can interact to produce robustness difficulties; hence motivating the terminology *interaction parameter*. Note in particular that a stable system whose interconnection matrix has the form $M(s) = \begin{bmatrix} 0 & M_{12}(s) \\ M_{21}(s) & 0 \end{bmatrix}$ cannot be destabilized by either uncertainty acting alone; as pointed out in [Fre89a] and [NeU88[, $\mu[M] = \mu_2$ in this case.

We now extend this result to the 3-block structured singular value problem. Using Nett's technique to extend the lower bound in (2.3.2) is straightforward.

Proposition 2.3.2 *Let $k = 3$ in (2.2.1,2), and suppose that the infimum in (2.2.5) is achieved. Then,*

$$\mu[M] \geq \max \{\mu_1, \mu_2, \mu_3 \} \qquad (2.3.3)$$

■

Proof: It suffices to show $\mu[M] \geq \mu_3$. Following the same reasoning as in the proof of Proposition 3.1 leads to $\mu^3[M] \geq (d_i/d_j)\sigma_{ij} \cdot (d_j/d_k)\sigma_{jk} \cdot (d_k/d_i)\sigma_{ki}$, for some d_i, d_j, and d_k. Thus, $\mu^3[M] \geq \mu^3(i,j,k)$, $\forall i \neq j \neq k$.   ■

Remark 2.3.2: Note that this proof technique consists of finding a lower bound upon $\inf_{D \in \mathcal{D}} \bar{\sigma}[DMD^{-1}]$, and may be extended to derive similar lower bounds upon this quantity for the case of $k > 3$. Of course, this technique results in a

11

lower bound upon $\mu[M]$ only if the upper bound in (2.2.5) is an equality, and this is guaranteed only for $k = 2, 3$. Most algorithms (e. g., see [FaT86], [FaT88]) for computing the structured singular value actually compute this upper bound, which Doyle has conjectured is within 15% of the true value of $\mu[M]$ ([Doy82], [DLP86]). Hence, if Doyle's conjecture is correct, one might argue that extensions of Proposition 2.3.2 to $k > 3$ remain useful.

Remark 2.3.3: Alternately, one can also apply the techniques of [Fre89a] for the case $k = 2$ to derive lower bounds for $k \geq 3$. As in the case $k = 2$, the lower bound obtained in this way is not as sharp as (2.3.2). However, the technique is in principle generalizable to obtain lower bounds for arbitrary k.

Next, we present upper bounds upon $\mu[M]$. Toward this end, it is necessary to consider two cases.

Proposition 2.3.3 *Let $k = 3$ in (2.2.1,2).*

(a) Suppose $\mu_3 > 0$. Then

$$\mu[M] \leq \mu_1 + \mu_3 + \frac{\mu_2^2}{\mu_3} \qquad (2.3.4)$$

If $\mu_2/\mu_3 \leq 1$, then

$$\mu[M] \leq \mu_1 + \mu_2 + \mu_3 \qquad (2.3.5)$$

(b) Suppose $\mu_2 > 0$. Then

$$\mu[M] \leq \mu_1 + \mu_2 + \sqrt{3}\, max\, \{\mu_3, (\frac{\mu_3^3}{\mu_2})^{1/2}\} \qquad (2.3.6)$$

If $\mu_2/\mu_3 > 1$, then

$$\mu[M] \leq \mu_1 + (1 + \sqrt{3}\,)\mu_2 \qquad (2.3.7)$$

Proof of (a): With no loss of generality, we assume $\mu_3 = \mu(1,2,3)$. Our proof proceeds with the decomposition $M = M_0 + M_1 + M_2$, where $M_0 = diag[M_{11},\ M_{22},\ M_{33}]$,

$$M_1 = \begin{bmatrix} 0 & M_{12} & 0 \\ 0 & 0 & M_{23} \\ M_{31} & 0 & 0 \end{bmatrix} \quad and \quad M_2 = \begin{bmatrix} 0 & 0 & M_{13} \\ M_{31} & 0 & 0 \\ 0 & M_{32} & 0 \end{bmatrix} \qquad (2.3.8)$$

Note first that

$$\mu_3 = \inf_{D \in \mathcal{D}} \partial[DM_1D^{-1}]$$
$$= \inf_{d_1,d_2,d_3} max\left\{ \frac{d_1}{d_2}\sigma_{12},\ \frac{d_2}{d_3}\sigma_{23},\ \frac{d_3}{d_1}\sigma_{31} \right\}$$

The solution to this minimization problem is obtained by setting $\hat{d}_1 = 1$, $\hat{d}_2 = \sigma_{12}/\mu(1,2,3)$, $\hat{d}_3 = \mu(1,2,3)/\sigma_{31}$, leading to $\mu_3 = \mu(1,2,3)$. Next, notice that

$$\mu[M] \leq \inf_{D \in \mathcal{D}} \partial[DMD^{-1}] \leq \mu_1 + \partial[\hat{D}M_1\hat{D}^{-1}] + \partial[\hat{D}M_2\hat{D}^{-1}]$$

where

$$\partial[\hat{D}M_2\hat{D}^{-1}] = max\left\{ \frac{\hat{d}_1}{\hat{d}_3}\sigma_{13},\ \frac{\hat{d}_3}{\hat{d}_2}\sigma_{32},\ \frac{\hat{d}_2}{\hat{d}_1}\sigma_{21} \right\}$$
$$= max\left\{ \frac{\mu^2(1,2)}{\mu_3},\ \frac{\mu^2(2,3)}{\mu_3},\ \frac{\mu^2(1,3)}{\mu_3} \right\}$$
$$\leq \frac{\mu_2^2}{\mu_3}$$

This proves (2.3.4), and (2.3.5) immediately follows.

Proof of (b): Without loss of generality, we assume that $\mu_2 = \mu(1,2)$. Our proof proceeds with the decomposition $M = M_0 + M_3 + M_4$, where $M_0 = diag[M_{11},\ M_{22},\ M_{33}]$,

$$M_3 = \begin{bmatrix} 0 & M_{12} & 0 \\ M_{21} & 0 & 0 \\ 0 & 0 & 0 \end{bmatrix} \quad and \quad M_4 = \begin{bmatrix} 0 & 0 & M_{13} \\ 0 & 0 & M_{23} \\ M_{31} & M_{32} & 0 \end{bmatrix}$$

Clearly, $\mu[M] \le \mu_1 + \inf_{D \in \mathcal{D}} \{\bar{\sigma}[DM_3D^{-1}] + \bar{\sigma}[DM_4D^{-1}]\}$. Setting $\hat{d}_1 = 1$, $\hat{d}_2 = \sigma_{12}/\mu_2$ yields

$$\mu[M] \le \mu_1 + \mu_2 + \inf_{d_3, d_1 = \hat{d}_1, d_2 = \hat{d}_2} \bar{\sigma}[DM_4D^{-1}]$$

To solve the minimization problem in the right hand side, note that

$$\begin{aligned}
\inf_{d_3, d_1 = \hat{d}_1, d_2 = \hat{d}_2} \bar{\sigma}[DM_4D^{-1}] &= \inf_{d_3} \max \left\{ d_3 \bar{\sigma}[M_{31}, (1/\hat{d}_2)M_{32}], \frac{1}{d_3}\bar{\sigma}\left[\begin{array}{c} M_{13} \\ \hat{d}_2 M_{23} \end{array} \right] \right\} \\
&\le \inf_{d_3} \max \left\{ d_3\sqrt{\sigma_{31}^2 + (1/\hat{d}_2)^2 \sigma_{32}^2}, (1/d_3)\sqrt{\sigma_{13}^2 + \hat{d}_2^2 \sigma_{23}^2} \right\}
\end{aligned}$$

The last minimization problem has the solution $\hat{d}_3 = [(\sigma_{13}^2 + \hat{d}_2^2\sigma_{23}^2)/(\sigma_{31}^2 + (1/\hat{d}_2)^2\sigma_{32}^2)]^{1/4}$. Substituting the value of $\hat{d}_2$ yields

$$\begin{aligned}
\bar{\sigma}[\hat{D}M_4\hat{D}^{-1}] &\le \left[\mu^4(2,3) + \mu^4(1,3) + \frac{\mu^6(1,2,3)}{\mu_2^2} + \frac{\mu^6(1,3,2)}{\mu_2^2} \right]^{1/4} \\
&= \left[\left(\mu^2(2,3) - \mu^2(1,3)\right)^2 + \left(\frac{\mu^3(1,2,3)}{\mu_2} + \frac{\mu^3(1,3,2)}{\mu_2} \right)^2 \right]^{1/4} \\
&\le \left[(\mu_3^2)^2 + \left(2\frac{\mu_3^3}{\mu_2} \right)^2 \right]^{1/4} \\
&\le \sqrt{\mu_3^2 + 2\frac{\mu_3^3}{\mu_2}}
\end{aligned}$$

This proves (2.3.6), and (2.3.7) follows immediately. ∎

Just as the parameter μ_2 measures how the effects of two uncertainties can interact to cause robustness difficulties, so does μ_3 measure the problems caused by interactions among all three uncertainties. Indeed, suppose that the system interconnection matrix has the form of $M_1(s)$, or $M_2(s)$, defined as in (2.3.8). Since $\mu_1 = \mu_2 = 0$, neither of these systems can be destabilized by uncertainties acting individually or in pairs. However, each system can be destabilized by

14

a combination of Δ_1, Δ_2, and Δ_3. The following corollary is an immediate consequence of (2.3.3) and (2.3.4).

Corollary 2.3.4 *Let M_1 and M_2 be defined as in (2.3.8). Then,*

(a)

$$\mu[M_1] = \mu(1,2,3) \tag{2.3.9}$$

(b)

$$\mu[M_2] = \mu(1,3,2) \tag{2.3.10}$$

Hence the first upper bound (2.3.4) is useful in the case that the most significant difficulty is due to the interaction of all three uncertainties, while the second upper bound (2.3.6) is useful in the case that the most significant difficulty is due to the interaction of just two of the uncertainties. An interesting open problem is whether a single upper bound exists which is useful in both cases and is not prohibitively messy.

2.4 Concluding Remarks

In this chapter we have derived both lower and upper bounds upon the structured singular value with respect to three blocks of uncertainty. Our bounds are expressed in terms of a set of parameters that determine how two or three uncertainties can interact to cause robustness difficulties. These bounds appear to give reasonably tight estimates of the structured singular value. Specifically, the upper bounds were shown to be within a factor of three of the lower bound on one occasion, while within a factor of $2 + \sqrt{3}$ (≈ 3.73) on the other. It is interest-

ing to note that our bounds are substantially tighter, and have more interesting interpretations, than those developed in [Dem88].

More importantly, our bounds may be used to study various robustness analysis and design problems. In applying these bounds, we found that the blocks M_{ij} of the interconnection matrix will be mutually interrelated, and, as in [Fre89a], it is important to analyze this interrelation to obtain design insight.

We conclude this chapter by pointing out the potential extensions of these bounds to the k-block structured singular value, with $k > 3$. Many of the present results can be extended; however, the technique used to derive the lower bounds may not. The major obstacle in achieving this, of course, is the invalidity of the equality $\mu[M] = \inf_{D \in \mathcal{D}} \bar{\sigma}[DMD^{-1}]$ in the general case.

Chapter 3

Robust Performance with Respect to Diagonal Input Uncertainty

3.1 Introduction

In this chapter we shall apply the results of Chapter 2 to a specific class of robust performance problems. For motivation, consider the problem of maintaining the output sensitivity function small, to achieve disturbance attenuation, despite the presence of unstructured multiplicative uncertainty at the plant input. Analysis of this problem has exposed potential design difficulties when the plant transfer function matrix is *ill-conditioned* at frequencies near crossover. By "ill-conditioned," we mean that the gain of the plant, at a frequency of interest, exhibits a strong directional dependence: some input signals will be amplified much more than will others. Although no conclusive proof has yet appeared, anecdotal evidence suggests that ill-conditioned plants may be inherently difficult to robustly control, at least for certain types of plant uncertainty, and

that the size of the plant condition number is an indicator of the degree of the difficulty in achieving robustness [Fre89a], [Fre89b], [NeM87], [SMD88], [Ste85], [Ste87], [SkM87].

The tentative conclusion that an ill-conditioned plant is inherently difficult to robustly control depends critically upon the assumption that the input uncertainty is *unstructured*, and can therefore introduce coupling among different plant inputs. Often, however, physical considerations dictate that it is more reasonable to assume that uncertainty *cannot* introduce such coupling, or can introduce coupling *only* among a subset of the inputs. Examples arise in diverse applications, such as process control [SkM87], [SMD88] and aircraft control [Enn87]. This property is modelled mathematically by assuming that the input uncertainty has a diagonal or block diagonal structure. In [SMD88], it is demonstrated via examples that ill-conditioned plants can *sometimes* cause design difficulties when input uncertainty is constrained to be diagonal (i.e., to introduce no coupling between inputs), but that sometimes no such difficulty is encountered. Appealing physical explanations of this phenomenon are presented in [SMD88], and the extent of the potential robustness difficulty depends upon the input directionality properties of the plant, as well as its condition number. It is also remarked [SkM87] that the plant *relative gain array* may be a useful indicator of potential robustness difficulty for this problem. The analysis in [SkM87], [SMD88] focuses in particular upon robustness difficulties that can be encountered through use of a compensator that explicitly inverts the plant model.

Our purpose in this chapter is to provide a framework useful for analysing the degree of difficulty inherent in the robust performance problem when the input

18

uncertainty is modelled as a diagonal or block diagonal matrix. An outline of our results follows. In Section 3.2, we introduce notation and define the robust performance problem of maintaining the output sensitivity function small despite the presence of block diagonal uncertainty at the plant input. Section 3.3 contains initial results: we calculate the first- and second-order effects of the input uncertainty upon the output sensitivity function, and point out conditions on the closed-loop shapes which must be satisfied if these effects are to be kept small. In Section 3.4, we review the use of the *structured singular value* [Doy82] as a test for robust performance. Since the interrelation among the plant, compensator, uncertainty structure, and size of the structured singular value is rather complicated, we use the *frequency dependent bounds* upon the structured singular value derived in Chapter 2 to provide useful insights into this interrelation. These bounds are stated in terms of *interaction parameters*; keeping these parameters small is approximately equivalent to satisfying the goal of robust performance. Furthermore, the interaction parameters are very closely related to the first- and second-order effects of input uncertainty that were calculated in Section 3.3. Next, in Section 3.5, we analyze the problem of keeping the interaction parameters small, and show that the difficulty of this problem depends upon a *robustness indicator* which is a function of both the plant condition number and its input directionality properties. In Section 3.6, we briefly discuss and compare the relative gain array to our new robustness indicator. Examples are given in Section 3.7, and concluding remarks are made in Section 3.8. The research described in this chapter is discussed in [ChF89a].

3.2 The Robust Performance Problem

Consider the linear time-invariant feedback system depicted in Figure 3.1. The transfer functions $P(s)$ and $F(s)$ are those of the plant model and compensator, respectively. We shall assume[1] that the plant has n inputs and outputs, and that $det P(s) \not\equiv 0$. The signals $r(s)$, $d(s)$, and $y(s)$ are the reference input, disturbance input, and system output, respectively. Define the *input open-loop transfer function, sensitivity function, and complementary sensitivity function*:

$$L_I(s) = F(s)P(s), \quad S_I(s) = [I + L_I(s)]^{-1}, \quad T_I(s) = L_I(s)[I + L_I(s)]^{-1} \quad (3.2.1)$$

and the *output open-loop transfer function, sensitivity function, and complementary sensitivity function*:

$$L_O(s) = P(s)F(s), \quad S_O(s) = [I + L_O(s)]^{-1}, \quad T_O(s) = L_O(s)[I + L_O(s)]^{-1} \quad (3.2.2)$$

The following notation will be used. Let RH^∞ denote the set of proper rational matrices that are stable, i.e. that have no poles in the closed right half plane. Given $G(s) \in RH^\infty$, define $\|G\|_\infty = \sup_\omega \bar{\sigma}[G(j\omega)]$, where $\bar{\sigma}[\cdot]$ denotes the largest singular value of a matrix [GoV83]. Define also the set

$$\mathbf{D}_\gamma = \{G(s) \in RH^\infty : \quad \|G\|_\infty < \gamma\} \quad (3.2.3)$$

When we refer to a matrix in $\mathbf{D}_\gamma$, the dimensions will be clear from the context. Finally, we suppress dependence upon frequency whenever convenient.

---

[1] Our results extend to nonsquare plants that satisfy the relevant assumption of left or right invertibility.
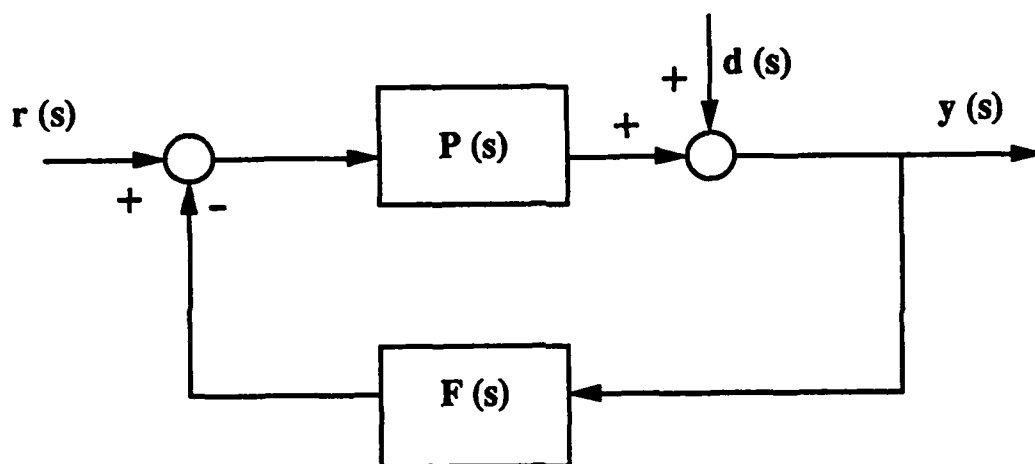
Figure 3.1: Feedback Configuration

We now describe the design specifications that our system is to satisfy. Suppose that the true plant is given by

$$P'(s) = P(s)[I + R_I(s)\Delta_I(s)] \tag{3.2.4}$$

The matrix $\Delta_I(s)$ may lie anywhere in a set of form

$$\Delta_\gamma = \left\{ diag[\Delta_1, \Delta_2] : \Delta_1 \in \mathbf{C}^{k \times k}, \ \Delta_2 \in \mathbf{C}^{(n-k) \times (n-k)}, \ \Delta_i \in \mathbf{D}_\gamma, \ i = 1, 2 \right\} \tag{3.2.5}$$

where $0 \leq k \leq n$. We say that each Δ_i is an *unstructured uncertainty*. The matrix $R_I(s) = diag[r_1(s)I_k, \ r_2(s)I_{n-k}]$ is dimensioned compatibly with $\Delta_I(s)$ (I_k and I_{n-k} are identity matrices). The weighting functions $r_1(s)$ and $r_2(s)$ are chosen to be stable and to have stable inverses, and are used to model the *frequency dependence of the level of uncertainty*.

Our first design goals are to achieve nominal internal stability (cf. [Vid85], Section 5.1) and to maintain stability robust against the uncertainty described by (3.2.4). Using standard arguments (e.g., see [DoS81], [DWS82]), it is straightforward to show that stability will be robust against arbitrary $\Delta_i \in \mathbf{D}_\gamma$ *alone* (i.e., with $\Delta_j \equiv 0$, $j \neq i$) if and only if

$$\|r_i E_i^H T_I E_i\|_\infty < 1/\gamma \tag{3.2.6}$$

where $E_1 = \begin{bmatrix} I_k \\ 0 \end{bmatrix}$, $E_2 = \begin{bmatrix} 0 \\ I_{n-k} \end{bmatrix}$. Assessing stability robustness against *both* uncertainties simultaneously requires use of the structured singular value [Doy82], and will be deferred until Section 3.4.

We also wish to satisfy the nominal performance goal of reducing the effect of the disturbance input upon the system output. We say that this goal is achieved

if

$$\|r_2 S_O\|_\infty < 1 \qquad (3.2.7)$$

where $r_2(s)$ is a weighting function whose size indicates the relative importance of disturbance reduction at each frequency. Next, we demand that performance be robust against uncertainty. Hence, for a given γ, we require that

$$\|r_2 S_O'\|_\infty < 1, \ \forall \Delta_I \in \Delta_\gamma \qquad (3.2.8)$$

where $S_O' = [I + P'F]^{-1}$.

We shall need to use the *singular value decomposition* [GoV83] of the plant to describe its directionality properties; for a detailed discussion, see e.g., [FrL86], [Fre89a], and [Fre90]. Let the singular value decomposition of the plant transfer function, evaluated at a fixed frequency, be denoted $P = WTZ^H$, where $T = diag[\tau_1, \tau_2, \cdots, \tau_n]$, $W = [w_1, w_2, \cdots, w_n]$, and $Z = [z_1, z_2, \cdots, z_n]$. The diagonal elements of T are termed the singular values of P, and are ordered so that $\bar{\sigma}[P] = \tau_1 \geq \tau_2 \geq \cdots \geq \tau_n = \underline{\sigma}[P] \geq 0$. The columns of the unitary matrices W and Z are termed the left and right singular vectors, respectively. The largest and smallest singular values of $P(j\omega)$ have interpretations as the largest and smallest possible gains at frequency ω. The condition number of the plant is defined as $\kappa[P] = \bar{\sigma}[P]/\underline{\sigma}[P]$. If the condition number is very large at a frequency, then the gain of the system is strongly directional at that frequency, and the plant is said to be *ill-conditioned* [GoV83].

It will prove convenient to adopt the following notation. Consider a matrix whose columns form an orthonormal basis for a k-dimensional subspace of $\mathbf{C}^n$. We denote the matrix by an uppercase letter (or a lowercase letter in the case

23

$k = 1$), and the associated subspace by the boldface version of the same letter (e.g., the columns of $X \in \mathbb{C}^{m \times k}$ form an orthonormal basis for the k-dimensional subspace $\mathbf{X} \subset \mathbb{C}^m$).

Finally, we need to define a specific class of compensators which we shall term *plant-inverting compensators*. Such compensators were discussed in [Fre89b], [Fre90], [SkM87], and are useful in revealing design difficulties associated with ill-conditioned plants. A plant-inverting compensator $F(s)$ is of the form

$$F(s) = l(s)P^{-1}(s) \qquad (3.2.9)$$

where $l(s)$ is a scalar transfer function selected so that $F(s)$ is proper. Obviously, use of a plant-inverting compensator requires that the plant be stable and have a stable inverse. For later reference, note that with such a compensator the two sets of transfer functions (3.2.1-2) are identical. We shall denote these by $L_O(s) = L_I(s) = l(s)I$, $S_O(s) = S_I(s) = s(s)I$, and $T_O(s) = T_I(s) = t(s)I$, where $s(s) = 1/(1 + l(s))$ and $t(s) = l(s)/(1 + l(s))$.

3.3 First- and Second-Order Effects of Input Uncertainty upon Output Sensitivity

The robust performance problem posed in the preceding section requires that the output sensitivity function be kept small despite the presence of block diagonal uncertainty at the plant input. In this section we shall study this problem by investigating the first- and second-order effects of input uncertainty upon output sensitivity. As we shall show in Section 3.4, an understanding of only the first- and second-order effects is sufficient to allow development of qualitative design

rules for this robust performance problem.

Lemma 3.3.1 *Assume that P' has the form defined in (3.2.3-4). Then $S_O' = [I + P'F]^{-1}$ has the form $S_O' = S_O + S_O^1 + S_O^2 + O(\Delta_I^3)$, where*

$$S_O^1 = -S_O P R_I \Delta_I P^{-1} T_O \qquad (3.3.1)$$

and

$$S_O^2 = S_O P R_I \Delta_I T_I R_I \Delta_I P^{-1} T_O \qquad (3.3.2)$$

■

Proof: The proof follows from straightforward manipulations as in the proof of Lemma 4 of [Fre89a].

■

Lemma 3.3.1 allows an approximate decomposition of S_O' into the sum of the zeroth order term S_O, first order term S_O^1, and second order term S_O^2. Achieving robust performance requires that S_O^1 and S_O^2 be kept small. Let us initially consider the first order effects.

Proposition 3.3.2 *Suppose that $\Delta_I \in \Delta_\gamma$. Then*

$$\sup_{\Delta_I \in \Delta_\gamma} \bar{\sigma}[S_O^1] \leq \gamma \sum_{i=1}^{2} \mid r_i \mid \bar{\sigma}[S_O P E_i] \bar{\sigma}[E_i^H P^{-1} T_O] \qquad (3.3.3)$$

and

$$\sup_{\Delta_I \in \Delta_\gamma} \bar{\sigma}[S_O^1] \geq \gamma \max_i \mid r_i \mid \bar{\sigma}[S_O P E_i] \bar{\sigma}[E_i^H P^{-1} T_O] \qquad (3.3.4)$$

Proof: The upper bound follows by noting that ■

$$S_O^1 = -r_1 S_O P E_1 \Delta_1 E_1^H P^{-1} T_O - r_2 S_O P E_2 \Delta_2 E_2^H P^{-1} T_O \qquad (3.3.5)$$

25

and applying the triangle inequality. The lower bound follows from (3.3.5) by noting that

$$\sup_{\Delta_I \in \Delta_\gamma} \bar{\sigma}[S_O^1] \geq \sup_{\Delta_I \in \Delta_\gamma, \ \Delta_2 = 0} \bar{\sigma}[S_O^1]$$

and constructing a "worst case" Δ_1 as in the proof of Lemma 5, [Fre89a].

■

It is clear that the terms[2] $|r_i| \bar{\sigma}[S_O P E_i] \bar{\sigma}[E_i^H P^{-1} T_O]$ characterize the first order effects of uncertainty at the plant input upon the output sensitivity function. Hence, to achieve robust performance, it is necessary that keeping these terms small be made a design objective.

The remainder of this section is devoted to exploring the second order effects of input uncertainty upon the output sensitivity function.

Proposition 3.3.3 *Suppose that* $\Delta_I \in \Delta_\gamma$. *Then*

$$\sup_{\Delta_I \in \Delta_\gamma} \bar{\sigma}[S_O^2] \leq \gamma^2 \sum_{j=1}^{2} \sum_{i=1}^{2} |r_i r_j| \bar{\sigma}[S_O P E_i] \bar{\sigma}[E_i^H T_I E_j] \bar{\sigma}[E_j^H P^{-1} T_O] \qquad (3.3.6)$$

■

Proof: The proof follows from noting that

$$
\begin{aligned}
S_O^2 &= r_1^2 S_O P E_1 \Delta_1 E_1^H T_I E_1 \Delta_1 E_1^H P^{-1} T_O \\
&\quad + r_1 r_2 S_O P E_1 \Delta_1 E_1^H T_I E_2 \Delta_2 E_2^H P^{-1} T_O \qquad (3.3.7) \\
&\quad + r_2 r_1 S_O P E_2 \Delta_2 E_2^H T_I E_1 \Delta_1 E_1^H P^{-1} T_O \\
&\quad + r_2^2 S_O P E_2 \Delta_2 E_2^H T_I E_2 \Delta_2 E_2^H P^{-1} T_O
\end{aligned}
$$

---

[2]In Section 3.4, we shall show that these terms, as well as those discussed following Proposition 3.3.3, are closely related to our interaction parameters.

and applying the triangle inequality.

∎

Proposition 3.3.3 shows that the second order effects are characterized by the terms $| r_i r_j | \bar{\sigma}[S_O P E_i] \bar{\sigma}[E_i^H T_I E_j] \bar{\sigma}[E_j^H P^{-1} T_O]$. Hence keeping these terms small should also be included as a design objective. In this regard, we notice that the first and fourth terms in (3.3.7) will tend to be small if the robust stability bounds (3.2.6) are satisfied and if the first-order effects of uncertainty are small. Analysis of the second and third terms in (3.3.7) is more problematic, and we shall return to this point at the close of Section 3.4.

It is straightforward to extend the results of this section to analyze the first- and second-order effects of input uncertainty modelled as an $m \times m$ block diagonal matrix.

3.4 Structured Singular Value Analysis of the Robust Performance Problem

The first step in applying structured singular value analysis is to reformulate the robust performance problem as an equivalent robust stability problem by introducing a fictitious modelling uncertainty to represent the performance specification [DWS82]. For our problem, this is accomplished by supposing that the true plant is given by

$$\tilde{P}(s) = [I + r_s(s)\Delta_s(s)]^{-1} P(s)[I + R_I(s)\Delta_I(s)] \tag{3.4.1}$$

where the input uncertainty is the same as in (3.2.3-5), $\Delta_3(s)$ is stable, and the weighting function $r_3(s)$ is identical with that in (3.2.7). As discussed in [Doy82], [DWS82], the next step is to define

$$\Delta = diag[\Delta_1, \Delta_2, \Delta_3] \qquad (3.4.2)$$

and

$$M = \begin{bmatrix} r_1 E_1^H T_I E_1 & r_1 E_1^H T_I E_2 & -r_1 E_1^H P^{-1} T_O \\ r_2 E_2^H T_I E_1 & r_2 E_2^H T_I E_2 & -r_2 E_2^H P^{-1} T_O \\ -r_3 S_O P E_1 & -r_3 S_O P E_2 & r_3 S_O \end{bmatrix} \qquad (3.4.3)$$

By definition [Doy82], the structured singular value, denoted $\mu[M(j\omega)]$, is the reciprocal of a frequency dependent stability margin with respect to all three sources of uncertainty. Define $\mu_\infty[M] = \sup_\omega \mu[M(j\omega)]$. A nominally stable feedback system will be robustly stable against all uncertainties of the form (3.4.2) with Δ_i an arbitrary member of $\mathbf{D}_\gamma$ if and only if $\mu_\infty[M] < 1/\gamma$. In terms of the original robust performance problem, we have that $\|r_3 S_O'\|_\infty \leq 1/\gamma$ for all $\Delta_I \in \Delta_\gamma$ if and only if $\mu_\infty[M] < 1/\gamma$ [DWS82]. For the rest of this section, we will discuss only the equivalent robust stability problem.

To obtain insight into the robust stability problem, we will work with a set of frequency dependent bounds upon the structured singular value. To simplify notation, we denote the block elements of M by M_{ij}, and define

$$\sigma_{ij} = \bar\sigma[M_{ij}] \qquad (3.4.4)$$

and

$$\mu_1 = \max_i \sigma_{ii} \qquad (3.4.5)$$

Hence the system is robustly stable against the uncertainty Δ_i *alone* if and only if $\sigma_{ii}(j\omega) < 1/\gamma$, $\forall\omega$.

28

Next, we define the *interaction parameters* (cf. Chapter 2)

$$\mu(i,j) \;=\; \sqrt{\sigma_{ij}\sigma_{ji}}\,, \quad \forall i \neq j \tag{3.4.6}$$

$$\mu(i,j,k) \;=\; (\sigma_{ij}\sigma_{jk}\sigma_{ki})^{1/3}\,, \quad \forall i \neq j \neq k \tag{3.4.7}$$

$$\mu_2 \;=\; \max_{i,j}\mu(i,j) \tag{3.4.8}$$

$$\mu_3 \;=\; \max_{i,j,k}\mu(i,j,k) \tag{3.4.9}$$

The interaction parameter $\mu(i,j)$ determines to what extent the effects of the two uncertainties Δ_i and Δ_j can interact to produce robustness difficulties. The robust stability problem obtained by setting $\Delta_k = 0$ can be studied using structured singular value techniques applied to the matrix obtained by deleting the kth block row and column of M. Denote this matrix by $M|_{i,j}$. The following result is an immediate corollary to Proposition 2.3.1.

Proposition 3.4.1 *Choose* $i \neq j \neq k$. *Then*

$$max\,\{\,\sigma_{ii},\,\sigma_{jj},\,\mu(i,j)\,\} \leq \mu[M|_{i,j}] \leq max\,\{\,\sigma_{ii},\,\sigma_{jj}\,\} + \mu(i,j) \tag{3.4.10}$$

∎

For our problem, the interaction parameters in (3.4.6) are

$$\mu(1,2) \;=\; \sqrt{\bar{\sigma}[r_1 E_1^H T_I E_2]\bar{\sigma}[r_2 E_2^H T_I E_1]} \tag{3.4.11}$$

$$\mu(1,3) \;=\; \sqrt{\bar{\sigma}[r_3 S_O P E_1]\bar{\sigma}[r_1 E_1^H P^{-1} T_O]} \tag{3.4.12}$$

$$\mu(2,3) \;=\; \sqrt{\bar{\sigma}[r_3 S_O P E_2]\bar{\sigma}[r_2 E_2^H P^{-1} T_O]} \tag{3.4.13}$$

To illustrate, let us return to the problem of robust stability against block diagonal uncertainty at the plant input. Recall that the system is robustly stable against Δ_i alone ($i = 1, 2$) if and only if (3.2.6) is satisfied. The system will be

29

robustly stable against Δ_1 and Δ_2 together if and only if $\mu_\infty[M|_{1,2}] < 1/\gamma$. It follows from Proposition 3.4.1 that, in addition to keeping the diagonal blocks of T_I small, it is also necessary to keep the *product* of the off-diagonal blocks small. The latter requirement is to prevent destabilizing interactions between Δ_1 and Δ_2.

The interaction parameters $\mu(1,3)$ and $\mu(2,3)$ each have an analogous interpretation. Suppose that stability is robust with respect to Δ_1 and Δ_3 individually. Then, to maintain robust stability against the combined effects of these two uncertainties, it is necessary and sufficient that $\mu(1,3)$ be kept small. An inspection of Proposition 3.3.2 reveals that this requirement is equivalent to keeping the first order effects of Δ_1 upon output sensitivity small. Similar comments apply to the combined effects of Δ_2 and Δ_3.

We next consider the combined effects of all three uncertainties. The following proposition is a restatement of Propositions 2.3.2 and 2.3.3, combined here for convenience.

Proposition 3.4.2 *Consider μ_1, μ_2, and μ_3 defined in (3.4.4-9). Then*

(i)

$$\mu[M] \geq max\ \{\mu_1, \mu_2, \mu_3\} \qquad (3.4.14)$$

(ii) Suppose that $\mu_3 \neq 0$. If $\mu_2/\mu_3 \leq 1$, then

$$\mu[M] \leq \mu_1 + \mu_2 + \mu_3 \qquad (3.4.15)$$

(iii) Suppose $\mu_2 \neq 0$. If $\mu_3/\mu_2 \leq 1$, then

$$\mu[M] \leq \mu_1 + 2.74\mu_2 \qquad (3.4.16)$$

For later reference, we note that for our problem,

$$\mu(1,2,3) = \left(\bar{\sigma}[r_1 E_1^H T_I E_2] \bar{\sigma}[r_3 S_O P E_1] \bar{\sigma}[r_2 E_2^H P^{-1} T_O] \right)^{1/3} \qquad (3.4.17)$$

and

$$\mu(1,3,2) = \left(\bar{\sigma}[r_2 E_2^H T_I E_1] \bar{\sigma}[r_3 S_O P E_2] \bar{\sigma}[r_1 E_1^H P^{-1} T_O] \right)^{1/3} \qquad (3.4.18)$$

From an inspection of Proposition 3.3.3 and the ensuing discussion, it follows that keeping μ_1, μ_2 and μ_3 small is equivalent to keeping the zeroth-, first-, and second-order effects of input uncertainty upon output sensitivity small. Note in particular that $\mu(1,2,3)$ and $\mu(1,3,2)$ correspond to the second and third terms in (3.3.7). This shows that the essentials of the robust performance problem are captured by our analysis of the first- and second-order effects of input uncertainty upon the output sensitivity function.

3.5 A Robustness Indicator

In the previous section we have defined interaction parameters that must be kept small if performance is to be robust. We now derive a *robustness indicator* whose size determines the potential difficulty of this task. To simplify the exposition, it will prove convenient to assume that the singular value decomposition of the plant may be partitioned as

$$P = W_1 T_1 Z_1^H + W_2 T_2 Z_2^H \qquad (3.5.1)$$

where $T_1 = diag[\tau_1, \tau_2, \cdots, \tau_l]$, $T_2 = diag[\tau_{l+1}, \tau_{l+2}, \cdots, \tau_n]$, $W_1, Z_1 \in \mathbf{C}^{n \times l}$, and $W_2, Z_2 \in \mathbf{C}^{n \times (n-l)}$. We shall further assume that $\tau_l \gg \tau_{l+1}$, and refer to the plant as consisting of "high and low gain subsystems" [FrL86] with input directions Z_1 and output directions W_1. Finally, we shall assume that the gain in each subsystem is *uniform*: $\tau_1 = \tau_l$, and $\tau_{l+1} = \tau_n$. If any of the above assumptions fail to hold, analysis may be performed using the dyadic form of the plant singular value decomposition, and steps toward accomplishing this will be indicated in the sequel.

We next need to describe how well the plant input directions are aligned with the two blocks of uncertainty. We do this by introducing an angular measure of the distance between the subspaces Z_i containing the inputs to the high- and low-gain *subsystems of the plant* and the subspaces E_i containing the inputs to and outputs from each block of uncertainty. Consider the subspaces Z_1, Z_2, E_1, and E_2, and let $q = min\{k, l\}$. As discussed in Section 2 of [FrL86] and the references cited therein, the *principal angles* [BjG73], [GoV83] $\bar{\alpha} = \alpha_1 \geq \alpha_2 \geq \cdots \geq \alpha_q = \underline{\alpha}$, $\alpha_i \in [0, \pi/2]$, between the subspaces Z_1 and E_1 are a measure of the angular distance between these two subspaces, and thus also between their orthogonal complements Z_2 and E_2. These angles have the following useful characterizations.

Lemma 3.5.1 *Consider the matrix*

$$E^H Z = \begin{bmatrix} E_1^H Z_1 & E_1^H Z_2 \\ E_2^H Z_1 & E_2^H Z_2 \end{bmatrix} \tag{3.5.2}$$

Assume[3] *that $k+l \leq n$. Then there exist compatibly dimensioned unitary matrices*

---

[3]Otherwise $(n - l) + (n - k) \leq n$, and the decomposition may be obtained by renumbering and replacing k with $n - k$ and l with $n - l$.

32

$U = diag[U_1, \ U_2]$ and $V = diag[V_1, \ V_2]$ such that

(i) if $k \geq l$, then

$$U^H E^H Z V = \begin{bmatrix} C & \vdots & -S & 0 & 0 \\ 0 & \vdots & 0 & I_{k-l} & 0 \\ \cdots & \cdots & \cdots & \cdots & \cdots \\ S & \vdots & C & 0 & 0 \\ 0 & \vdots & 0 & 0 & I_{n-(k+l)} \end{bmatrix} \qquad (3.5.3)$$

(ii) if $k \leq l$, then

$$U^H E^H Z V = \begin{bmatrix} C & 0 & \vdots & -S & 0 \\ \cdots & \cdots & \cdots & \cdots & \cdots \\ S & 0 & \vdots & C & 0 \\ 0 & I_{l-k} & \vdots & 0 & 0 \\ 0 & 0 & \vdots & 0 & I_{n-(k+l)} \end{bmatrix} \qquad (3.5.4)$$

where $C = diag[\cos \alpha_1, \ \cos \alpha_2, \ \cdots, \ \cos \alpha_q]$ and $S = diag[\sin \alpha_1, \ \sin \alpha_2, \ \cdots, \ \sin \alpha_q]$.

∎

Proof: A straightforward generalization of the *C-S Decomposition* of a general unitary matrix, which is presented in [Ste77], [GoV83].

Comparing (3.5.2) with (3.5.3-4), it follows that the singular values of $E_1^H Z_1$ are equal to the *cosines* of the principal angles, while the singular values of $E_1^H Z_2$ are equal to the *sines* of the principal angles and (possibly) unity, and so forth. This proves significant, as it follows from (3.3.1) and (3.5.1) that the first-order effects of input uncertainty upon the output sensitivity function depend upon both the plant condition number and the matrices $E_i^H Z_j$, $i, \ j = 1, 2$. The following lemma makes this statement precise.

Lemma 3.5.2 *Suppose that the plant is partitioned as in (3.5.1). Then, from*

(3.3.1), it follows that

$$S_O^1 = -r_1 S_O W_1 T_1 Z_1^H E_1 \Delta_1 E_1^H Z_2 T_2^{-1} W_2^H T_O$$

$$-r_2 S_O W_1 T_1 Z_1^H E_2 \Delta_2 E_2^H Z_2 T_2^{-1} W_2^H T_O \qquad (3.5.5)$$

$$+other\ terms$$

Note that the first two terms in this expansion are proportional in size to the plant condition number. Hence, if the plant is ill-conditioned, the first-order effects in (3.3.1) are potentially large. By the uniform gain assumption, the "other terms" in this expansion[4] are not proportional to the plant condition number, and thus are of less significance. Also, this result shows that the extent to which plant ill-conditionedness can cause design difficulty depends upon the alignment between the subspaces E_1 and Z_1. To illustrate, consider S_O^1 as the series connection of $S_O P$, $R_I \Delta_I$ and $P^{-1} T_O$ (c.f. (3.3.1)). Potential design difficulties arise whenever the uncertainty can introduce coupling between the high- (low-) gain subsystems of P and P^{-1}. For example, if $k = l = n/2$, then no coupling will be introduced if the alignment is perfect (i.e., $\bar{\alpha} = 0$ or $\alpha = \pi/2$). Certain combinations of the dimensions k, l, and n will *always* result in coupling, regardless of how the subspaces are aligned. For an example, consider $k = 1, l = 2,$ and $n = 4$. Also, a limiting case is when $k = n$, for which the uncertainty is no longer block diagonal and the analysis reduces to that of [Fre89a]. The potential robustness difficulties arising from these and other combinations of k, l, and n can be best summarized by considering the interaction parameters $\mu(1,3)$ and $\mu(2,3)$.

Proposition 3.5.3 *Suppose that the partition (3.5.1) and the uniform gain as-*

---

[4]It is straightforward to calculate these terms explicitly. Since the resulting expressions are lengthy, they are omitted for purpose of brevity.

sumption hold, and that $k + l \leq n$. Then

$$\mu^2(1,3) \geq \underline{\sigma}[S_O]\underline{\sigma}[T_O]\rho_{13}[P] \tag{3.5.6}$$

$$\mu^2(2,3) \geq \underline{\sigma}[S_O]\underline{\sigma}[T_O]\rho_{23}[P] \tag{3.5.7}$$

where

$$\rho_{13}[P] = |r_1 r_3| \kappa[P] \begin{cases} \cos\underline{\alpha}, & k > l \\ \cos\underline{\alpha}\sin\bar{\alpha}, & k \leq l \end{cases} \tag{3.5.8}$$

$$\rho_{23}[P] = |r_2 r_3| \kappa[P] \begin{cases} \sin\bar{\alpha}, & k+l < n, \ k \geq l \\ \cos\underline{\alpha}\sin\bar{\alpha}, & k+l = n, \ k \geq l \\ 1, & k+l < n, \ k < l \\ \cos\underline{\alpha}, & k+l = n, \ k < l \end{cases} \tag{3.5.9}$$

Furthermore, for $i = 1, 2$,

$$\mu^2(i,3) \leq \bar{\sigma}[S_O W_1]\bar{\sigma}[W_2^H T_O]\rho_{i3}[P] + \text{other terms} \tag{3.5.10}$$

∎

Proof: Using standard norm inequalities and the fact that W is a unitary matrix yields

$$\mu^2(1,3) \geq |r_1 r_3| \underline{\sigma}[S_O]\underline{\sigma}[T_O]\bar{\sigma}[T_i Z_i^H E_1]\bar{\sigma}[E_1^H Z_j T_j^{-1}]$$

Setting $i = 1$, $j = 2$ and applying the uniform gain assumption gives

$$\mu^2(1,3) \geq |r_1 r_3| \underline{\sigma}[S_O]\underline{\sigma}[T_O]\kappa[P]\bar{\sigma}[Z_1^H E_1]\bar{\sigma}[E_1^H Z_2],$$

from which (3.5.6) follows. Proof of (3.5.7) is similar. The upper bound (3.5.10) follows by substituting (3.5.1) into (3.4.12-13) and applying norm properties.

∎

It follows from (3.5.6-7) that robustness is potentially poor at any frequency for which the *robustness indicator*

$$\rho[P] \triangleq \max_i \rho_{i3}[P] \qquad (3.5.11)$$

is large. At such frequencies, it is necessary that the output loop-transfer function be shaped so that $\underline{\sigma}[S_O]\underline{\sigma}[T_O]$ is small. Since the "other terms" in (3.5.10) are *not* proportional to the plant condition number, it follows that $\mu(i,3)$ may be kept small by requiring the product $\bar{\sigma}[S_O W_1]\bar{\sigma}[W_2^H T_O]$ to be small. Comparison with (3.5.5) shows that this strategy is equivalent to keeping the first-order effects of Δ_1 and Δ_2 small. For purpose of comparison with the results of [Fre89a], [Fre89b], [Fre90], and [Ste87] we note that the case of *unstructured* input uncertainty corresponds to setting $k = n$ in (3.2.5). In this case the weighting r_2 is irrelevant and $\bar{\alpha} = 0$, and hence the robustness indicator assumes a correspondingly simple form:

$$\rho[P] = | r_1 r_3 | \kappa[P] \qquad (3.5.12)$$

which depends solely upon the plant condition number.

In summary, we have shown that if the robustness indicator (3.5.11) is large, then performance robustness is potentially poor. The analysis is limited, however, in that it is based solely upon the interaction parameters $\mu(i,3)$, and thus solely upon the first order effects of uncertainty. It remains to be determined whether performance robustness can be potentially poor because of the second-order effects of uncertainty, even if the first-order effects are negligible. This question translates approximately into that of determining whether the interaction parameters $\mu(i,j,k)$ can be large even if μ_1 and μ_2 are small. A somewhat

surprising result, which is applicable to systems with two inputs and two outputs, shows that keeping the interaction parameters μ_1 and μ_2 small tends to insure that μ_3 is small as well.

Proposition 3.5.4 *Let $n = 2$, and let μ_1, μ_2 and μ_3 be defined in (3.4.4-9). Then*

$$\mu_3 \leq 1.62 \max \{ \mu_1, \mu_2 \} \qquad (3.5.13)$$

Proof: See Appendix A.

∎

Suppose that the goals of nominal performance and robust stability against diagonal input uncertainty are satisfied, so that μ_1 is small. Then it follows from Propositions 3.4.2 and 3.5.4 that the goal of achieving robust performance essentially translates into that of keeping μ_3 small. It follows, therefore, that the robustness indicator does adequately reflect the potential difficulty of achieving robust performance. Finally, although it seems reasonable to conjecture that Proposition 3.5.4 can be extended to the general case of block 2×2 uncertainty, the proof of this proposition does not readily generalize, and the conjecture is left for future research.

In what follows we shall discuss the robustness difficulties associated with a plant-inverting compensator. Note first that the interaction parameter $\mu_3 = 0$ in this case, so that the discussions following Proposition 3.5.4 are rendered moot. To explain these difficulties, we first recall the following result of Stein [Ste87], who explicitly calculates the structured singular value resulting from use of a plant-inverting compensator in the case of *unstructured* uncertainty.

Proposition 3.5.5 [Ste87] *Assume that $k = n$ in (3.2.5), and that $F(s)$ is given by (3.2.9). Then*

$$\mu^2[M] = |r_1 t|^2 + |r_3 s|^2 + |r_1 t| \cdot |r_3 s| \cdot (\kappa[P] + 1/\kappa[P]) \qquad (3.5.14)$$

Hence, it follows that, for a fixed loop shape $l(s)$, the structured singular value will increase as the square root of the robustness indicator (3.5.12).

We next develop a corresponding result for the present problem. For notational simplicity, we consider only the special case $k = l = n/2$, for which $\rho[P] = \max_i |r_i r_3| \kappa[P] \cos \underline{\alpha} \sin \bar{\alpha}$. Noticing that $\mu_3 = 0$, $\mu(1,2) = 0$, the bounds given in (3.4.14) and (3.4.16) can be utilized. However, stronger results may be obtained due to the special structure of the interconnection matrix.

Proposition 3.5.6 *Assume that $k = l = n/2$ in (3.2.5), and that the partition (3.5.1) and the uniform gain assumption hold. Let $F(s)$ be given as in (3.2.9). Then*

$$\max\{\mu_1, \mu_2\} \le \mu[M] \le \mu_1 + \sqrt{2}\,\mu_2 \qquad (3.5.15)$$

where

$$\begin{aligned}
\mu_1 &= \max\{|r_1 t|, |r_2 t|, |r_3 s|\} \\
\mu_2 &= \max\{\mu(1,3), \mu(2,3)\}
\end{aligned} \qquad (3.5.16)$$

Furthermore,

$$\mu^2(i,3) \ge |r_i t| \cdot |r_3 s| \kappa[P] \cos \underline{\alpha} \sin \bar{\alpha} \qquad (3.5.17)$$

and

$$\mu^2(i,3) \le |r_i t| \cdot |r_3 s| \left(\kappa[P] \cos \underline{\alpha} \sin \bar{\alpha} + \cos^2 \underline{\alpha} + \sin^2 \bar{\alpha} + (1/\kappa[P]) \cos \underline{\alpha} \sin \bar{\alpha} \right)$$

$$(3.5.18)$$

Proof: See Appendix B.

∎

Hence again, we see that for a fixed loop shape, the structured singular value will increase with the square root of the robustness indicator (3.5.11). The main difference is that now the robustness indicator depends not only upon the plant condition number, but also upon the alignment angles. Motivated by these analyses and those in [SkM87], it is of particular interest to develop an intuitive explanation of the design difficulties associated with such a compensator. Toward this end, note that when the plant has the form (3.5.1), such a compensator also has a decomposition into high and low gain subsystems. In the absence of uncertainty, the high (or low) gains of the compensator cancel the low (or high) gains of the plant *exactly*. However, with uncertainty present, this cancellation will be exact *only if* the alignment conditions are satisfied (and hence the robustness indicators are zero). Otherwise, the uncertainty can cause the high (or low) gains of the plant and compensator to multiply one another, so that the resulting series connection of plant, uncertainty, and compensator is significantly different from its nominal value. Remarks similar to these are presented in [SMD88], and physical interpretations are presented for robustness problems associated with high-purity distillation columns. Our results above are appealing in that they allow these potential difficulties to be quantified in terms of the principal angles.

Finally, if the uniform gain assumption fails to hold, then analysis can proceed using the dyadic form of the plant singular value decomposition: $P =$

39

$\sum_{i=1}^{n} r_i w_i z_i^H$. Indeed, calculations similar to those in Proposition 3.5.3 yield

$$\mu^2(i, 3) \geq \mid r_i r_3 \mid \underline{\sigma}[S_O]\underline{\sigma}[T_O] \cdot (r_j/r_k)\|z_j^H E_i\| \cdot \|E_i^H z_k\| \tag{3.5.19}$$

where $\|z_j^H E_i\|$ and $\|E_i^H z_k\|$ are the cosines of the angles between the subspaces z_j and E_1, and z_k and E_1, respectively. Hence $\rho[P] = \max_i \rho_{i3}[P]$, where

$$\rho_{i3}[P] = \max_{j,k} \mid r_i r_3 \mid (r_j/r_k)\|z_j^H E_i\| \cdot \|E_i^H z_k\| \tag{3.5.20}$$

is a useful generalization of the robustness indicator to this more general situation.

3.6   The Relative Gain Array

The Relative Gain Array (RGA) [Bri66] is widely used in the process control industry to analyse interactions in multivariable systems. A number of authors have studied robustness difficulties associated with plants having large elements in the RGA. (For discussions of these results and lists of references, see [NeM87], [SkM87].) Skogestad and Morari [SkM87] have demonstrated that the RGA is useful as an indicator of potential design difficulty for the problem of maintaining performance robust against *diagonal* multiplicative uncertainty at the plant input. In particular, they show that the RGA is a less conservative indicator than is the plant condition number for this particular problem. On the other hand, they also show that the RGA can be optimistic, and can sometimes fail to detect potential difficulties when the plant has large off-diagonal elements (cf [SkM87]). Our purpose in this section is to compare our robustness indicator with the RGA, and to show that ours does not suffer from this shortcoming. It

suffices to consider the case $n = 2$, and to assume that the weightings in (3.2.4) are unity.

For our purpose, the RGA is a matrix

$$RGA = \begin{bmatrix} \lambda_{11} & \lambda_{12} \\ \lambda_{21} & \lambda_{22} \end{bmatrix} \tag{3.6.1}$$

where $\lambda_{22} = \lambda_{11}$, $\lambda_{12} = \lambda_{21} = 1 - \lambda_{11}$, $\lambda_{11} = 1/\left(1 - \frac{p_{12}p_{21}}{p_{11}p_{22}}\right)$ and p_{ij}, $i, j = 1, 2$ are the elements of the plant transfer function matrix. For $n = 2$, the subspaces Z_1 and E_1 are one-dimensional and thus will be denoted as z_1 and e_1, here e_1 and e_2 correspond to the vectors $e_1 = \begin{bmatrix} 1 \\ 0 \end{bmatrix}$ and $e_2 = \begin{bmatrix} 0 \\ 1 \end{bmatrix}$. The robustness indicator is

$$\rho[P] = \kappa[P] \cos \alpha \sin \alpha \tag{3.6.2}$$

here α denotes the principal angle between the subspaces z_1 and e_1. The following is adapted from [SkM87].

Proposition 3.6.1 *Suppose that uncertainty has the form of (3.2.1) with $n = 2$, $k = 1$. Then the output open-loop transfer function can be written as $L_O' = (I + E)PF$, where E is an error term:*

$$E = P\Delta_I P^{-1} \tag{3.6.3}$$

Furthermore,

$$\sup_{\Delta_I \in \Delta_\gamma} \bar{\sigma}[E] \geq \gamma \max_{i,j} |\lambda_{11}| \cdot |\frac{p_{ij}}{p_{jj}}| \tag{3.6.4}$$

Proof: The proof follows from noting that [SkM87]

$$P\Delta_I P^{-1} = \begin{bmatrix} \lambda_{11}\Delta_1 + \lambda_{12}\Delta_2 & -\lambda_{11}(p_{12}/p_{22})(\Delta_1 - \Delta_2) \\ -\lambda_{11}(p_{21}/p_{11})(\Delta_1 - \Delta_2) & \lambda_{21}\Delta_1 + \lambda_{22}\Delta_2 \end{bmatrix} \tag{3.6.5}$$

∎

41

It follows from (3.6.4) with $i = j$ that large values of the relative gain $| \lambda_{11} |$ correspond to systems that are very sensitive to uncertainty. However, small values of $| \lambda_{11} |$ need not necessarily correspond to systems that are insensitive. Indeed, counterexamples can readily be constructed using a triangular P matrix whose largest element is on the off-diagonal (e.g., p. 2328, [SkM87]).

Expressing the plant output with respect to the basis consisting of the left singular vectors of the plant displays the role played by the condition number and input directionality properties of the plant.

Proposition 3.6.2 *Consider the error term (3.6.3):*

$$\sup_{\Delta_I \in \Delta_\gamma} \bar{\sigma}[E] \geq \gamma \max_{i,j,k}(\tau_j/\tau_k) \mid z_j^H c_i \mid \cdot \mid c_i^H z_k \mid \tag{3.6.6}$$

and

$$\sup_{\Delta_I \in \Delta_\gamma} \bar{\sigma}[E] \leq 4\gamma \max_{i,j,k}(\tau_j/\tau_k) \mid z_j^H c_i \mid \cdot \mid c_i^H z_k \mid \tag{3.6.7}$$

∎

Proof: The proof follows by applying norm properties to the error term $\bar{\sigma}[E]$, and noting that $\bar{\sigma}[E] = \bar{\sigma}[W^H E W]$, where

$$W^H E W = \begin{bmatrix} \sum_{i=1}^2 z_1^H c_i \Delta_i c_i^H z_1 & \kappa[P] \sum_{i=1}^2 z_1^H c_i \Delta_i c_i^H z_2 \\ (1/\kappa[P]) \sum_{i=1}^2 z_2^H c_i \Delta_i c_i^H z_1 & \sum_{i=1}^2 z_2^H c_i \Delta_i c_i^H z_2 \end{bmatrix} \tag{3.6.8}$$

∎

In particular, it follows from (3.6.2) and (3.6.6) that

$$\sup_{\Delta_I \in \Delta_\gamma} \bar{\sigma}[E] \geq \gamma \rho[P] \tag{3.6.9}$$

42

Finally, the upper bound (3.6.7) shows that the error term cannot be significantly larger than $\bar{\sigma}[\Delta_I]$ if the robustness indicator is small.

3.7 Examples

The authors of [SMD88] illustrated the design difficulties of ill-conditioned plants using simplified models of the LV and DV configurations of a distillation column. Both configurations result in an ill-conditioned plant, and both display robustness problems when a plant-inverting compensator is used and the input uncertainty is assumed to be *unstructured*. If, however, the input uncertainty is assumed to be diagonal, then only the LV-configuration continues to pose robustness problems when a plant-inverting compensator is used. Based upon an analysis of the directionality properties of the plants, the authors of [SMD88] presented an intuitively appealing explanation of this phenomenon. Our intent in this section is to demonstrate, using our robustness indicator, that the DV-configuration is indeed less difficult to robustly control when the input uncertainty is diagonal.

The plant models for both configurations are given by

$$P_{LV}(s) = [1/(75s + 1)] \begin{bmatrix} 0.878 & -0.864 \\ 1.082 & -1.096 \end{bmatrix} \qquad (3.7.1)$$

and

$$P_{DV} = [1/(75s + 1)] \begin{bmatrix} -0.878 & 0.014 \\ -1.082 & -0.014 \end{bmatrix} \qquad (3.7.2)$$

respectively. The condition numbers are constant with frequency: $\kappa[P_{LV}] = 141.7$, $\kappa[P_{DV}] = 70.8$. The weighting functions used in [SMD88] are $r_1(s) = r_2(s) = r(s) = 0.2(5s + 1)/(0.5s + 1)$, and $r_3(s) = 0.5(10s + 1)/10s$. These

43

data readily verify that the robustness indicator for the case of *unstructured* uncertainty (cf (3.5.12)) is large. By Proposition 3.5.5, a plant-inverting compensator will therefore yield poor robustness properties, and this was indeed verified in [SMD88] using Bode plots of the structured singular value. When a *diagonal* uncertainty structure is assumed, however, the robustness indicator is given by (3.6.2). The principal angles for the two configurations are $\alpha_{LV} = 45^0$ and $\alpha_{DV} = 0^0$, respectively. Hence only the LV-configuration poses potential robustness difficulties, a fact also verified in [SMD88] using the structured singular value plots.

To further illustrate the dependence of the structured singular value upon the plant input directions, we alter the directions of the LV-configuration and in the meanwhile keep its condition number unchanged. Define

$$P_\theta(s) = P_{LV}(s)R, \qquad R = Z \begin{bmatrix} \cos\theta & -\sin\theta \\ \sin\theta & \cos\theta \end{bmatrix} \tag{3.7.3}$$

where $Z = \begin{bmatrix} \cos 45^0 & -\sin 45^0 \\ \sin 45^0 & \cos 45^0 \end{bmatrix}$ is a matrix of the right singular vectors for $P_{LV}(j\omega)$ [SMD88]. Hence, the robustness indicator for this new plant is

$$\rho[P_\theta] = |rr_3|\kappa[P_{LV}]\cos\theta\sin\theta \tag{3.7.4}$$

Plots of the structured singular value for the compensator[5] $F(s) = (0.7/s)P_\theta^{-1}(s)$ versus different values of θ are shown in Figure 3.2, and indeed we see that these plots are consistent with the analyses in Section 3.5.

Finally, we note that the problem of aligning the plant input directions is one

---

[5]Note that this compensator was discussed in [SMD88] for $\theta = 45^0$ and when the input uncertainty is unstructured.
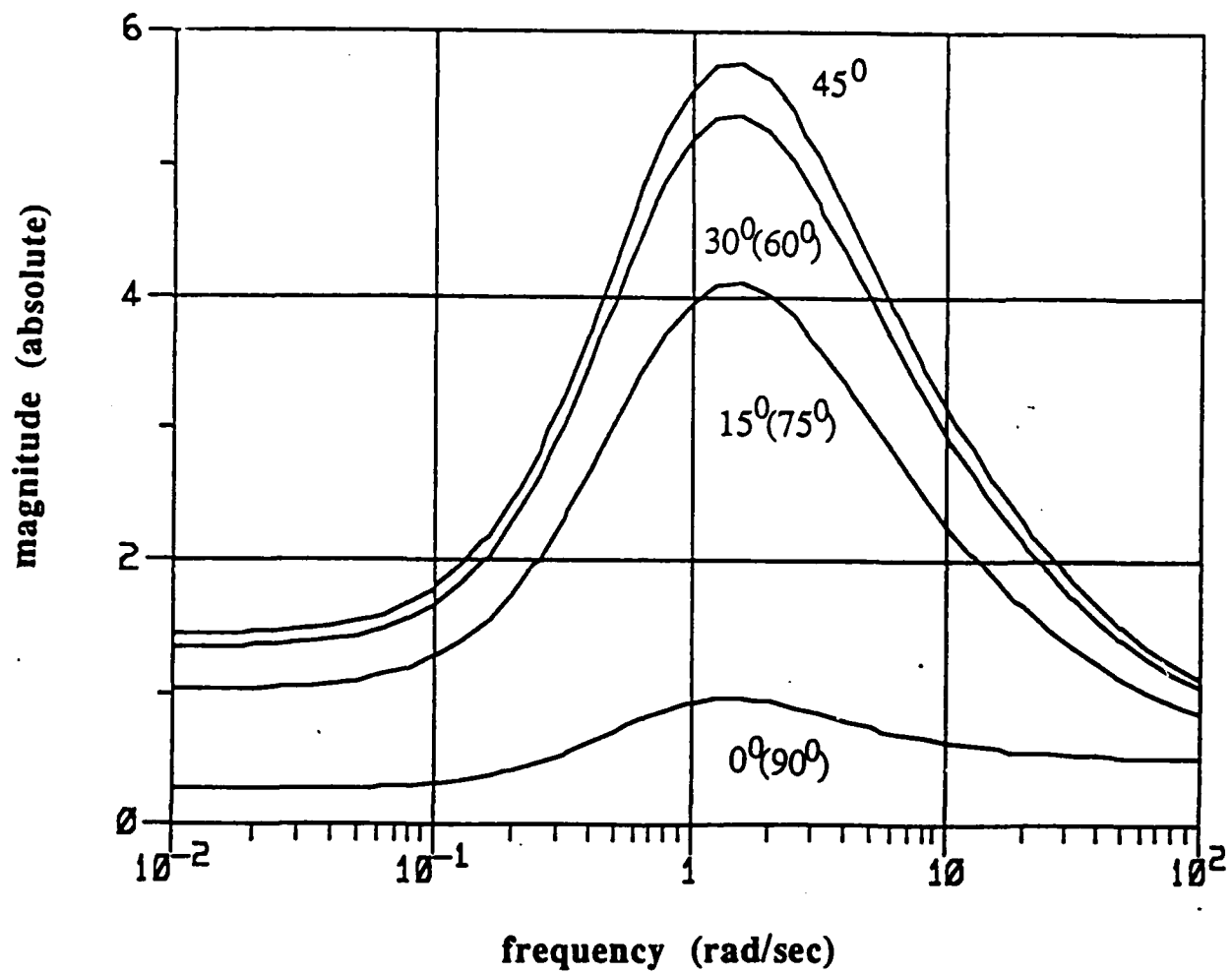
Figure 3.2: SSV Plots for Plant-Inverting Compensators with Respect to P_ϕ.

of plant *configuration* rather than that of compensation. This follows because the input uncertainty is assumed to be located between the plant and compensator.

3.8   Concluding Remarks

In this Chapter we have studied a robust performance problem that arises when the transfer function of plant model is ill-conditioned and the modelling uncertainty at the plant input has block diagonal structure. Our analysis shows that design goals should include keeping the first- and second-order effects of input uncertainty upon the output sensitivity function small in order to achieve robust performance, and this poses potential design difficulties for plants having large robustness indicators.

Chapter 4

Several Sources of Modelling Uncertainty

4.1 Introduction

An important problem in feedback design is to insure robustness of stability and performance with respect to several sources of modelling uncertainty. A useful stability margin for an important class of modelling uncertainties can be calculated using Doyle's structured singular value (SSV) [Doy82], [DWS82]. By plotting the structured singular value as a function of frequency, robustness difficulties associated with a given design can be reliably detected. However, because the structured singular value is a complicated function of the plant, compensator and uncertainty description, it is sometimes difficult to obtain design insights using only such a plot. For example, if the system has a poor stability margin, one would like to know how this may be improved by adjusting the compensator. Moreover, some feedback design problems are inherently difficult, and one would also like to know whether one is faced with such a problem and, if so, how a

compensator may be selected to achieve a judicious tradeoff among conflicting design objectives. The computation of the structured singular value via numerical optimization (cf. [FaT86], [FaT88], [Hel88], [PFD88]) renders such insights difficult to obtain.

Our goal in the present paper is to develop results that should be useful in obtaining insights into robustness problems associated with several modelling uncertainties. To motivate our approach, let us consider a procedure whereby we assess stability robustness sequentially, first with respect to uncertainties taken one at a time, then taken two at a time, and so forth. As we proceed, we may find that a system which is robust against all combinations of k or fewer uncertainties can nevertheless be destabilized by combinations of $k + 1$, possibly small, uncertainties. Evidently, such an instability must be caused by a harmful interaction among these $k + 1$ uncertainties. It is therefore of practical interest to have a methodology for determining the existence and strength of such interactions. Our analysis below will identify a set of interaction parameters, which appear to be useful for this task.

Essentially, our approach in this chapter is a generalization of that taken in Chapters 2 and 3. We provide additional interpretations of the earlier results, and lay the groundwork for applying our general approach to other design problems.

The remainder of this chapter is outlined as follows. In Section 4.2, we review the definition and properties of the structured singular value. In Section 4.3 we define the interaction parameters and show they are related to Mason's gain rule. In Section 4.4 we derive bounds upon the structured singular value expressed in

terms of these parameters. Section 5 contains an analysis of the aforementioned robust performance problem, and we conclude our discussion in Section 4.6. Some of the results described in this chapter are discussed in [ChF89b] and [ChF90].

4.2 Preliminaries: Properties of the Structured Singular Value

The first step in the structured singular value analysis is to rearrange the block diagram of the feedback system into the form shown in Figure 2.1. The *uncertainty matrix* $\Delta(s)$ is assumed to lie in the set[1]

$$\Delta_\gamma = \{diag[\Delta_i(s)] : \; \Delta_i \in C^{n_i \times n_i} \text{ and stable, } \|\Delta_i\|_\infty < \gamma, \, i = 1, 2, \cdots, N \}$$

$$(4.2.1)$$

where $\|\Delta_i\|_\infty = \sup_\omega \bar{\sigma}[\Delta_i(j\omega)]$, and $\bar{\sigma}[\cdot]$ denotes the largest singular value, or the Euclidean norm of a matrix. The *interconnection matrix* $M(s)$ is a function of the nominal plant model, the compensator, and weighting matrices introduced to normalize the size of the uncertainties. It is stable if the feedback system is nominally stable. At each frequency, the structured singular value, denoted $\mu[M]$, is defined[2] by [Doy82].

$$\mu[M] = \begin{cases} 0 & det[I + M\Delta] \neq 0 \; \forall \Delta \in \Delta_\infty \\ 1/(\min_{\Delta \in \Delta_\infty} \{\bar{\sigma}[\Delta] : det[I + M\Delta] = 0\}) & otherwise \end{cases}$$

$$(4.2.2)$$

---

[1] We assume throughout this chapter that all Δ_i's in (4.2.1) are distinct. The general case of repeated Δ_i's is treated in [Doy82], [PFD88].

[2] We shall suppress dependence upon frequency whenever appropriate, and shall occasionally abuse notations by using the symbol Δ_γ to denote the set of constant complex matrices with block diagonal structure (4.2.1).

Define $\mu_\infty[M] = \sup_\omega \mu[M(j\omega)]$. Then, if the feedback system in Figure 2.1 is nominally stable, it will be robustly stable against all uncertainty in the set Δ_γ if and only if $\mu_\infty[M] < 1/\gamma$.

Further properties of the structured singular value are summarized in the following; for a complete discussion, see [Doy82]. Define the sets

$$D = \{\ diag[d_1 I_{n_1}, d_2 I_{n_2}, \cdots, d_N I_{n_N}] : d_i \in \mathbb{R},\ d_i > 0\ \}\qquad (4.2.3)$$

where I_{n_i} denotes the identity matrix of dimension n_i, and

$$U = \{\ diag[u_1, u_2, \cdots, u_N] : \|u_i\| = 1,\ u_i \in \mathbb{C}^{n_i \times 1}\ \}\qquad (4.2.4)$$

The following facts provide tools for evaluating the structured singular value.
Fact 4.2.1 [Doy82]

$$\mu[M] \le \inf_{D \in D} \bar{\sigma}[DMD^{-1}]\qquad (4.2.5)$$

Fact 4.2.2 [Doy82] Let $\rho[\cdot]$ denote the spectral radius of a matrix. Then,

$$\mu[M] = \max_{X,Y \in U} \rho[X^H M Y]\qquad (4.2.6)$$

Note in particular, the upper bound ' (4.2.5) is equal to $\mu[M]$ when the system has three or fewer blocks of uncertainty, namely, $N \le 3$.

We shall partition the interconnection matrix into blocks whose dimensions are compatible with those of the uncertainty:

$$M(s) = [M_{ij}(s)],\quad i,j = 1,2,\cdots,N,\quad M_{ij}(s) \in \mathbb{C}^{n_i \times n_j}\qquad (4.2.7)$$

and define $\sigma_{ij} = \bar{\sigma}[M_{ij}]$. It will often be convenient to consider the simplified stability robustness problem obtained by assuming that a subset of the uncertainty

blocks Δ_i are equal to zero. We introduce the following notation to describe such a problem. Let $Z_N = \{1, 2, \cdots, N\}$, and define

$$\aleph_k = \{\{i_1, \cdots, i_k\} : i_1, \cdots, i_k \in Z_N, i_1 \neq \cdots \neq i_k\} \qquad (4.2.8)$$

The cardinality of $\aleph_k$ is $\begin{pmatrix} N \\ k \end{pmatrix}$. We shall assume that the elements of $\aleph_k$ have been ordered in some fashion, and shall denote these elements by J_{ki}, $i = 1, 2, \cdots, \begin{pmatrix} N \\ k \end{pmatrix}$. Hence for each i, J_{ki} is a subset of Z_N with k *distinct* elements (see Example 4.3.1 for an illustration). Define

$$\Delta_\gamma|_{J_{ki}} = \{\Delta : \Delta \in \Delta_\gamma, \Delta_j = 0, \forall j \notin J_{ki}\} \qquad (4.2.9)$$

and

$$M|_{J_{ki}} = \{\text{interconnection matrix } M \text{ (4.2.7) with the } jth \text{ block row}$$
$$\text{and column set equal to zero, } \forall j \notin J_{ki}.\} \qquad (4.2.10)$$

Then, it follows readily that the feedback system pictured in Figure 2.1 is robustly stable against all uncertainties of the form (4.2.9) if and only if $\mu_\infty[M|_{J_{ki}}] < 1/\gamma$. For example, suppose that only *one* of the Δ_i's in (4.2.1) is nonzero; i.e., suppose that we consider the set $J_{1i} = \{i\}$. Then, it follows from the definition (4.2.2) that the feedback system in Figure 2.1 is robustly stable against all uncertainties in the set $\Delta_\gamma|_{J_{1i}}$ if and only if $\sigma_{ii}(j\omega) < 1/\gamma$, $\forall \omega$.

4.3 Interaction Parameters

From the analysis at the close of the preceding section, it follows that if the only nonzero blocks of the interaction matrix are those on the diagonal, then

$\mu[M] = \max_i \sigma_{ii}$. In general, however, nonzero off-diagonal blocks will introduce interactions between blocks of uncertainty, and thus will affect the size of the structured singular value. In this section we introduce a set of *interaction parameters* whose magnitudes are a function of the off-diagonal blocks of M, and we shall argue that these parameters determine the extent to which interactions among two or more blocks of uncertainty can cause stability robustness problems.

Consider the set of all possible permutations of the elements of all possible k-dimensional subsets of Z_N:

$$P_k = \{(i_1 i_2 \cdots i_k) : i_1, \cdots, i_k \in J_{bi}, \ J_{bi} \in \aleph_k\} \tag{4.3.1}$$

Note that the cardinality of P_k is equal to $\binom{N}{k} \cdot (k-1)!$. We shall assume that the elements of P_k have been ordered in some fashion, and shall denote these elements by Π_{bij}, $i = 1, 2, \cdots, \binom{N}{k}$, $j = 1, 2, \cdots, (k-1)!$. Given one of the subsets $J_{bi} \in \aleph_k$, and a permutation Π_{bij} of the elements of that subset, define the corresponding *interaction parameter of order k*:

$$\mu(\Pi_{bij}) = (\sigma_{i_1 i_2} \sigma_{i_2 i_3} \cdots \sigma_{i_k i_1})^{1/k} \tag{4.3.2}$$

and denote the largest of these by

$$\mu_k = \max_{\Pi_{bij} \in P_k} \mu(\Pi_{bij}) \tag{4.3.3}$$

Define also the corresponding *loop of length k*:

$$L(\Pi_{bij}) = (-1)^{k+1} M_{i_1 i_2} \Delta_{i_2} M_{i_2 i_3} \Delta_{i_3} \cdots M_{i_k i_1} \Delta_{i_1} \tag{4.3.4}$$

Two loops $L(\Pi_{bij})$ and $L(\Pi_{lmn})$ are said to be *nontouching* if $J_{bi} \cap J_{lm} = \emptyset$.

52

Note that there is a one-to-one correspondence between the set of loops and the set of interaction parameters.

Furthermore, the gain in each loop is related to the size of the corresponding interaction parameter.

Proposition 4.3.1: Consider a permutation Π_{kij} of the integers J_{ki}, and the associated loop $L(\Pi_{kij})$. Then

$$\sup_{\Delta \in \Delta_J} \bar{\sigma}[(\Pi_{kij})] = \gamma^k \mu^k(\Pi_{kij}) \tag{4.3.5}$$

∎

Example 4.3.2 Let us illustrate our notations using the following example. Consider $N = 3$, $Z_N = \{1, 2, 3\}$.

Loops of length 1:

$$\aleph_1 = \{\{1\}, \{2\}, \{3\}\}, \ J_{1i} = \{i\}, \ \Pi_{1i1} = (i)$$
$$L(\Pi_{1i1}) = M_{ii}\Delta_i, \ \mu(\Pi_{1i1}) = \sigma_{ii}, \ \mu_1 = \max_i \sigma_{ii}$$

Loops of length 2:

$$\aleph_2 = \{\{1, 2\}, \{1, 3\}, \{2, 3\}\}$$
$$J_{21} = \{1, 2\}, \ J_{22} = \{1, 3\}, \ J_{23} = \{2, 3\}$$
$$\Pi_{211} = (12), \ \Pi_{221} = (13), \ \Pi_{231} = (23)$$
$$L(\Pi_{211}) = -M_{12}\Delta_2 M_{21}\Delta_1$$
$$L(\Pi_{221}) = -M_{13}\Delta_3 M_{31}\Delta_1$$
$$L(\Pi_{231}) = -M_{23}\Delta_3 M_{33}\Delta_2$$
$$\mu(\Pi_{211}) = \sqrt{\sigma_{12}\sigma_{21}}$$
$$\mu(\Pi_{221}) = \sqrt{\sigma_{13}\sigma_{31}}$$
$$\mu(\Pi_{231}) = \sqrt{\sigma_{23}\sigma_{32}}$$
$$\mu_2 = \max_{i,j} \sqrt{\sigma_{ij}\sigma_{ji}}, \ i \neq j$$

Loops of length 3:

$$\aleph_3 = \{\{1,2,3\}\}, \ J_{31} = \{1,2,3\}$$
$$\Pi_{311} = (123), \ \Pi_{312} = (132)$$
$$L(\Pi_{311}) = M_{12}\Delta_2 M_{23}\Delta_3 M_{31}\Delta_1$$
$$L(\Pi_{312}) = M_{13}\Delta_3 M_{32}\Delta_2 M_{21}\Delta_1$$
$$\mu(\Pi_{311}) = (\sigma_{12}\sigma_{23}\sigma_{31})^{1/3}$$
$$\mu(\Pi_{312}) = (\sigma_{13}\sigma_{32}\sigma_{21})^{1/3}$$
$$\mu_3 = \max_{i,j,k}(\sigma_{ij}\sigma_{jk}\sigma_{ki})^{1/3}, \ i \neq j \neq k$$

To illustrate $\Delta_\gamma|_{J_{ki}}$ and $M|_{J_{ki}}$, consider J_{22}. Then

$$M|_{J_{22}} = \begin{bmatrix} M_{11} & 0 & M_{13} \\ 0 & 0 & 0 \\ M_{31} & 0 & M_{33} \end{bmatrix}$$

and

$$\Delta_\gamma|_{J_{22}} = \left\{ \begin{bmatrix} \Delta_1 & 0 & 0 \\ 0 & 0 & 0 \\ 0 & 0 & \Delta_3 \end{bmatrix} : \ \|\Delta_1\|_\infty < \gamma, \ \|\Delta_3\|_\infty < \gamma \right\}$$

When all the uncertainties are scalars, then so are the blocks of M, and the preceding definition of a loop reduces to that used in *Mason's gain formula* (e.g., Theorem 9.15.20, [ZaD63]), which may be applied to obtain a useful expression for $\det[I + M\Delta]$.

Proposition 4.3.3 *Assume that $n_i = 1$, $i = 1, 2, \cdots, N$ in (4.2.1). Then,*

$$\det[I + M\Delta] = 1 + G^1(\Delta) + G^2(\Delta) + \cdots + G^N(\Delta) \tag{4.3.6}$$

where

$$G^k(\Delta) = \sum_{j=1}^{(k-1)!\binom{N}{k}} \sum_{i=1} L(\Pi_{kij}) + R^k(\Delta) \tag{4.3.7}$$

and $R^k(\Delta)$ is a sum of products of nontouching loops of length $< k$, with the property that each product contains exactly k Δ_i's.

Proof: From Mason's formula, it follows that $\det(I + M\Delta)$ can be expanded into a sum of products of nontouching loops. The result is obtained by grouping

54

these products into an appropriate $G^k(\Delta)$, depending upon how many Δ_i's each product contains.

∎

It is clear, by construction, that each $G^k(\Delta)$ represents the kth order effects of uncertainty upon $\det(I + M\Delta)$. Furthermore, each $G^k(\Delta)$ is a sum of terms involving loops of length $\leq k$. Since the maximum gain in each loop is determined by the corresponding interaction parameter (Proposition 4.3.1), it follows that if the interaction parameters of order $\leq k$ are small, then the kth order effects will be small also. We summarize this observation by appealing to the limiting case.

Proposition 4.3.4: Let M and Δ be defined as in Section 4.2, with $n_i = 1, i = 1, \ldots, N$. Suppose that

$$\mu_l = 0 \ , \quad l = 1, \ldots, k \tag{4.3.8}$$

Then, $\forall \Delta \in \Delta_\infty$,

$$G^l(\Delta) = 0, l = 1, \ldots, k \tag{4.3.9}$$

∎

Keeping the interaction parameters of order $\leq k$ small is not, in general, a *necessary* condition for insuring that the kth order effects of uncertainty are small. The reason for this is that the preceding analysis takes only gain information into account. The following example illustrates this point.

Example 4.3.5: Consider the following interconnection matrix for $N = 3$,

$n_i = 1$, $i = 1, 2, 3$:

$$M = \begin{bmatrix} 0 & 1 & 1 \\ -1 & 0 & 1 \\ 1 & 1 & 0 \end{bmatrix}.$$

In this case $\mu_3 = 1$, but $G^3(\Delta) = 0$. This example shows that the third-order effects of uncertainty may equal zero even though the interaction parameters of order three are nonzero.

$\blacksquare$

As we shall see, in the multivariable case directionality as well as phase information is ignored. More importantly, our analysis implicitly assumes that the M_{ij}'s are mutually independent. In fact, they are each functions of the plant, compensator, and weightings. The implications of this fact will be discussed in Section 4.5.

Extending Proposition 4.3.3 to the multivariable case is possible using the formula for the determinant of a block partitioned matrix (e.g., [Kai80], p. 650). However, the complexity of the ensuing expressions renders analysis problematic. We choose to adopt an alternate approach, by reducing the multivariable problem to one with scalar blocks. To do this we must invoke a preliminary result.

Lemma 4.3.6: Consider the matrices M and Δ defined in Section 4.2 evaluated at a fixed frequency. Suppose there exists $\Delta \in \Delta_\infty$ such that (i) $\det[I + M\Delta] = 0$ and (ii) $\bar{\sigma}[\Delta] = \alpha$. Then there exists $\hat{\Delta} \in \Delta_\infty$ satisfying (i) and (ii) with the additional property that $\hat{\Delta} = \text{diag} \hat{\Delta}_i$, where $\hat{\Delta}_i = y_i x_i^H \delta_i$, where $\delta_i \in \mathbb{C}$, $y_i, x_i \in \mathbb{C}^{n_i}$, and $\|y_i\|_2 = \|x_i\|_2 = 1$.

Proof: Follows from the results in Section 4 of [Doy82]. $\blacksquare$

One consequence of the above lemma is that the definition of the structured singular value in Section 4.2 may be modified by replacing the minimization over $\Delta \in \Delta_\infty$ with a minimization over $\delta_i, x_i,$ and y_i. Define modified interconnection and uncertainty matrices by

$$\overline{M} = \{\overline{M}_{ij} = x_i^H M_{ij} y_j : i, j = 1, \ldots N\} \tag{4.3.10}$$

and

$$\overline{\Delta} = \text{diag}\{\delta_i I_{n_i} : i = 1, \ldots, N\} \tag{4.3.11}$$

Corollary 4.3.7: Consider M and Δ defined in Section 4.2. Then

$$\min_{\Delta \in \Delta_\infty} \{\bar{\sigma}[\Delta] : \det[I + M\Delta] = 0\} = \min_{x_i, y_i, \delta_i} \{\bar{\sigma}[\overline{\Delta}] : \det[I + \overline{M}\overline{\Delta}] = 0\} \tag{4.3.12}$$

∎

It follows from (4.3.12) that Proposition 4.3.4 may be extended to multivariable systems. Specifically, we may apply Proposition 4.3.3 to $\det[I + \overline{M}\overline{\Delta}]$, and define $\overline{G}^i(\overline{\Delta})$ analogously with (4.3.7).

Proposition 4.3.8: Consider M and Δ defined in Section 4.2, the corresponding interaction parameters (4.3.2-3), and the matrices $\overline{M}$ and $\overline{\Delta}$ defined by (4.3.10-11). Suppose that

$$\mu_l = 0, \quad l = 1, \ldots, k \tag{4.3.13}$$

Then, $\forall \delta_i \in \mathbb{C}, \ i = 1, \ldots, N$,

$$\overline{G}^l(\overline{\Delta}) = 0 \quad l = 1, \ldots, k \tag{4.3.14}$$

∎

Proof: Each $\overrightarrow{G}^l(\Delta)$ is the sum of products of nontouching loops of order $\leq l$. Since $|\overline{M}_{ij}| \leq \overline{\sigma}[M_{ij}]$, it follows from Proposition 4.3.1 that (4.3.13) implies (4.3.14).

∎

Let us now derive a result which emphasizes the difficulty inherent in analyzing robustness for a system with a large number of uncertainties. Consider an analysis procedure whereby we analyze robustness against uncertainties taken one at a time, then two at a time, and so forth. At the kth step of this procedure, one might find that the system is robustly stable against all combinations of *fewer* than k uncertainties, but may be destabilized by some combinations of k *small* uncertainties. The following result describes the extreme case of this phenomenon.

Proposition 4.3.9: Given a permutation $\Pi_{Nij} = (i_1 i_2 \cdots i_N) \in P_N$, consider the set of interconnection matrices

$$\mathcal{M}(\Pi_{Nij}) = \begin{cases} M_{i_1 i_2} \neq 0, M_{i_2 i_3} \neq 0, \ldots, M_{i_N i_1} \neq 0 \\ M_{lm} = 0, \text{ otherwise} \end{cases} \tag{4.3.15}$$

Then, for all $M \in \mathcal{M}(\Pi_{Nij})$,

$$\mu_k = 0, \quad k = 1, 2, \ldots, N-1 \tag{4.3.16}$$

and

$$\mu_N = \mu(\Pi_{Nij}) > 0 \tag{4.3.17}$$

Furthermore,

$$\mu[M|_{J_{k,i}}] = 0, \quad k = 1, \ldots, N-1, i = 1, \ldots \binom{N}{k} \qquad (4.3.18)$$

and

$$\mu[M] = \mu_N \qquad (4.3.19)$$

$\blacksquare$

It follows from (4.3.16-17) and our earlier discussion that the 1st, 2nd, ... $(N-1)$st effects of uncertainty upon $\det(I + M\Delta)$ are equal to zero. Furthermore, stated in words, (4.3.18-19) imply that a system whose interconnection matrix satisfies (4.3.15) *cannot* be destabilized by any combination of fewer than all N uncertainties.

Proof: It follows easily from (4.3.15) and the definition of the μ_k's that (4.3.16-17) are satisfied. It is also straightforward to verify that (4.3.18) holds. From Proposition 4.3.8, we see that

$$\begin{aligned}
\det[I + \overline{M}\Delta] &= 1 + \overline{G}^N(\Delta) \\
&= 1 + \overline{M}_{i_1 i_2}\overline{M}_{i_2 i_3} \cdots \overline{M}_{i_N i_1}\delta_1\delta_2 \cdots \delta_i
\end{aligned}$$

Selecting the x_i's and y_i's so that $\overline{M}_{i_1 i_2} = \overline{\sigma}[M_{i_1 i_2}], \ldots, \overline{M}_{i_N i_1} = \overline{\sigma}[M_{i_N i_1}]$ and setting $\delta_i = (\mu(\Pi_{Nij}))^{1/N}$, $i = 1, \ldots, N-1$ and $\delta_N = -(\mu(\Pi_{Nij}))^{1/N}$ yields $\det[I + \overline{M}\Delta] = 0$. Hence $\mu[M] \geq \mu(\Pi_{Nij})$. But it is easy to verify that if $\max_i |\delta_i| < 1/\mu(\Pi_{Nij})$, then $\det[I + \overline{M}\Delta] \neq 0$. Hence (4.3.19) is satisfied.

$\blacksquare$

4.4 Bounds on the Structured Singular Value

In this section we derive bounds upon the structured singular value defined in (4.2.2). We first note that most algorithms (e.g., [FaT86], [FaT88], [Hel88]) for computing the structured singular value actually compute the upper bound in (4.2.5), which Doyle [Doy82] has conjectured is within 15% of the true value of $\mu[M]$. Hence, instead we derive bounds upon the quantity $\inf_{D \in \mathcal{D}} \bar{\sigma}[DMD^{-1}]$ and argue that the qualitative information furnished by these bounds remain useful in our methodology.

Proposition 4.4.1 *Suppose that the infimum in (4.2.5) is achieved. Then,*

$$\inf_{D \in \mathcal{D}} \bar{\sigma}[DMD^{-1}] \geq max\left\{ \mu_1, \mu_2, \cdots, \mu_n \right\} \tag{4.4.1}$$

Proof: First note that $\inf_{D \in \mathcal{D}} \bar{\sigma}[DMD^{-1}] = \bar{\sigma}[\hat{D}M\hat{D}^{-1}]$ for some $\hat{D} = diag[d_1 I_{n_1}, d_2 I_{n_2},$

$\cdots, d_N I_{n_N}] \in \mathcal{D}$, if the infimum is achieved. It then follows that $\inf_{D \in \mathcal{D}} \bar{\sigma}[DMD^{-1}] \geq (d_i/d_j)\sigma_{ij}, \forall i, j$. Hence

$$\left(\inf_{D \in \mathcal{D}} \bar{\sigma}[DMD^{-1}] \right)^k \geq (d_{i_1}/d_{i_2})\sigma_{i_1 i_2} \cdot (d_{i_2}/d_{i_3})\sigma_{i_2 i_3} \cdots (d_{i_k}/d_{i_1})\sigma_{i_k i_1}$$

$$= \mu^k(\Pi_{k;j})$$

$\forall \Pi_{k;j} \in \mathcal{P}_k$. This completes the proof.

■

We note that this proof technique consists of finding a lower bound upon the quantity $\inf_{D \in \mathcal{D}} \bar{\sigma}[DMD^{-1}]$, and thus results in lower bounds upon the structured singular value for the case of $N \leq 3$ (cf. Chapter 2). It follows that these lower

bounds can be used in analyzing the effects of any two or three uncertainties in the structured singular value problem for $N > 3$. Specifically,

$$\mu[M] \geq max\left\{\mu_1, \mu_2, \mu_3\right\} \qquad (4.4.2)$$

Alternately, one can also use (4.2.6) to derive lower bounds upon the structured singular value, as done in [Fre89a] for the case $N = 2$. However, the bounds obtained in this way are *sometimes* complicated and thus may obscure information we desire from the interaction parameters.

Proposition 4.4.2 *Suppose $\mu_N > 0$. Then*

$$\mu[M] \leq \mu_N \sum_{k=1}^{N}\left(\frac{\mu_k}{\mu_N}\right)^k \qquad (4.4.3)$$

Furthermore, if $\mu_k/\mu_N \leq 1$, $\forall k$, then

$$\mu[M] \leq \sum_{k=1}^{N} \mu_k \qquad (4.4.4)$$

Proof: See Appendix C.

∎

Proposition 4.4.2 provides an upper bound useful in the case that the most significant effects are due to the interaction of all N uncertainties, i.e., $\mu_k \leq \mu_N$, $\forall k = 1, 2, \cdots, N - 1$. Bounds useful in other cases may also be derived by following a procedure suggested in Chapter 2. Note, however, that the bounds obtained in such cases may involve significant complexity, especially when the number of uncertainties is large. To summarize, it follows from these lower and upper bounds that large values of the interaction parameters can lead to a large structured singular value, and thus robustness problems. This, indeed, is consistent with our analysis in the preceding section. Consequently, the bounds derived

61

in this section along with the analysis in the preceding section do show that the interaction parameters can qualitatively characterize robustness properties. A useful application is to analyze these parameters to gain design insights into a given problem, as in [Fre89a], [ChF89a], and [ChF89b]. In applying this methodology, it is significant to note that the blocks M_{ij} of the interconnection matrix will be mutually interrelated, and, as in the cited references, it is important to analyze this interrelation to obtain design insights.

4.5 An Analysis Example

We now illustrate our analysis procedure by studying a three-block structured singular value problem. Consider the linear time-invariant feedback system depicted in Figure 3.1. The transfer functions $P(s)$ and $F(s)$ are those of the plant model and compensator, respectively. We shall assume[3] that the plant is square, and that $detP(s) \not\equiv 0$. The signals $r(s)$, $d(s)$, and $y(s)$ are the reference input, disturbance input, and system output, respectively. Define the *input open loop transfer function, sensitivity function, and complementary sensitivity function*:

$$L_I(s) = F(s)P(s), \; S_I(s) = [I + L_I(s)]^{-1}, \; T_I(s) = L_I(s)[I + L_I(s)]^{-1} \quad (4.5.1)$$

and the *output open loop transfer function, sensitivity function, and complementary sensitivity function*:

$$L_O(s) = P(s)F(s), \; S_O(s) = [I + L_O(s)]^{-1}, \; T_O(s) = L_O(s)[I + L_O(s)]^{-1} \quad (4.5.2)$$

---

[3]Our results extend to nonsquare plants that satisfy the relevant assumption of left or right invertibility.

We consider a benchmark robust performance problem studied in [Fre89a], [Fre89b], [SMD88] and [Ste87] with an *additional* source of modelling error which we take to be an unstructured additive uncertainty. As discussed in [DWS82], such a performance robustness problem can be treated as an equivalent robust stability problem against the actual sources of plant uncertainty plus an additional source of *fictitious* uncertainty used to represent the performance specification. In this regard, the present problem is equivalent to the problem of maintaining stability robust against plant uncertainty in the form of

$$P_{\delta}(s) = [I + r_2(s)\Delta_2(s)]^{-1}[P(s) + r_3(s)\Delta_3(s)][I + r_1(s)\Delta_1(s)] \qquad (4.5.3)$$

which corresponds to the block diagram depicted in Figure 4.1. Here $r_i(s)$, $i = 1,2,3$, are stable, minimum phase scalar weighting functions used to describe how the uncertainties and performance requirement vary with frequency, and $\Delta_i(s)$, $i = 1,2,3$ are unstructured uncertainties which satisfy $\|\Delta_i\|_\infty < \gamma$. Note that $\Delta_1(s)$ and $\Delta_3(s)$ are actual sources of plant uncertainty, while $\Delta_2(s)$ is the fictitious uncertainty used to represent the performance specification. Our nominal performance goal will be achieved if the output sensitivity function satisfies a frequency dependent bound

$$\|r_2 S_O\|_\infty < 1/\gamma \qquad (4.5.4)$$

and the *robust performance* goal will be satisfied if $\forall \Delta_1$, Δ_3, $\|\Delta_1\|_\infty < \gamma$, $\|\Delta_3\|_\infty < \gamma$,

$$\|r_3 S_O'\|_\infty < 1/\gamma \qquad (4.5.5)$$

with $S_O' = [I + P'F]^{-1}$ and $P' = [P + r_3\Delta_3][I + r_1\Delta_1]$
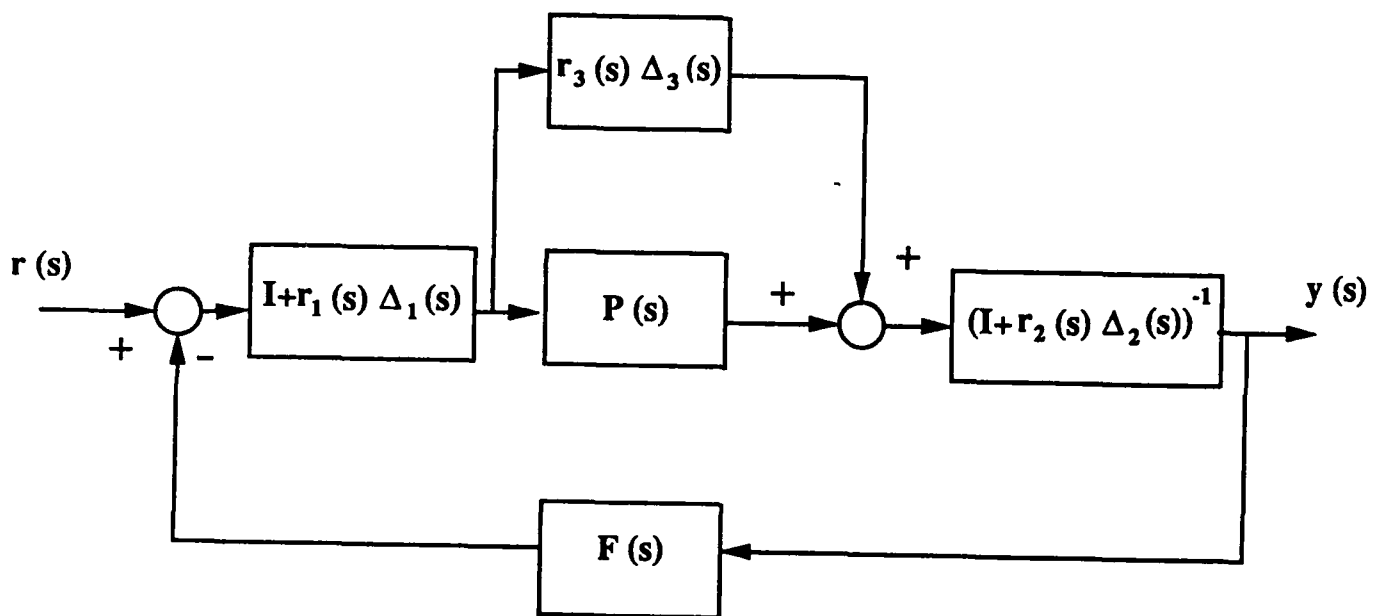
Figure 4.1: Feedback System with Three Modelling Uncertainties

We shall now discuss the stability robustness problem in detail. For purposes of illustration, we shall mainly demonstrate this procedure which centers at analysing the interaction parameters; a complete derivation of design insights for this robust performance problem is found in [ChF89b].

We now formulate this stability robustness problem as a three-block structured singular value problem. Our first task is to find the corresponding interconnection matrix. Manipulating the block diagram in Figure 4.1 yields

$$M = \begin{bmatrix} r_1 T_I & -r_1 T_I P^{-1} & r_1 T_I P^{-1} \\ -r_2 S_O P & r_2 S_O & -r_2 S_O \\ -r_3 S_I & -r_3 T_I P^{-1} & r_3 T_I P^{-1} \end{bmatrix} \tag{4.5.6}$$

Next, we need to identify the interaction parameters defined in (4.3.2-3), and for convenience we shall adopt the ordering of these parameters given as in Example 4.3.2:

$$\begin{aligned}
\mu_1 &= max \left\{ \bar{\sigma}[r_1 T_I], \bar{\sigma}[r_2 S_O], \bar{\sigma}[r_3 T_I P^{-1}] \right\} \\
\mu(\Pi_{211}) &= \sqrt{\bar{\sigma}[r_2 S_O P]\bar{\sigma}[r_1 T_I P^{-1}]} \\
\mu(\Pi_{221}) &= \sqrt{\bar{\sigma}[r_3 S_I]\bar{\sigma}[r_1 T_I P^{-1}]} \\
\mu(\Pi_{231}) &= \sqrt{\bar{\sigma}[r_2 S_O]\bar{\sigma}[r_3 T_I P^{-1}]} \\
\mu(\Pi_{311}) &= \left(\bar{\sigma}[r_1 T_I P^{-1}]\bar{\sigma}[r_2 S_O]\bar{\sigma}[r_3 S_I]\right)^{1/3} \\
\mu(\Pi_{312}) &= \left(\bar{\sigma}[r_1 T_I P^{-1}]\bar{\sigma}[r_2 S_O P]\bar{\sigma}[r_3 T_I P^{-1}]\right)^{1/3}
\end{aligned} \tag{4.5.7}$$

We first analyse the effects that are due to each *individual* uncertainty. Note that if the feedback system is nominally stable, then it will be robustly stable against Δ_1 alone if and only if $\|r_1 T_I\|_\infty < 1/\gamma$ [DoS81]. Similar statements apply to Δ_2 and $\|r_2 S_O\|_\infty$, and to Δ_3 and $\|r_3 T_I P^{-1}\|_\infty$. Hence μ_1 summarizes stability robustness with respect to each of the three uncertainty sources individually.

Next, we analyze the effects of uncertainties taken two at a time. The effect of interactions between Δ_1 and Δ_2 is quantified by $\mu[M|_{J_{21}}]$ and has been studied

65

in [Fre89a], [Fre89b]. Applying the bound (4.4.2-3) for $N = 2$ to this problem, it follows that the parameter $\mu(\Pi_{211})$ determines the extent to which these two uncertainties can interact to cause stability robustness difficulties even if the system is robustly stable against Δ_1 and Δ_2 individually. To prevent this undesirable effect imposes a *nontrivial* problem, for merely requiring $\bar{\sigma}[r_1 T_I]$ and $\bar{\sigma}[r_2 S_O]$ to be small does not imply that $\mu(\Pi_{211})$ is also small. To this point, let the plant *condition number* [GoV83] be defined by $\kappa[P(j\omega)] = \bar{\sigma}[P(j\omega)]/\underline{\sigma}[P(j\omega)]$.

Proposition 4.5.1 [Fre89a] *Let $\mu(\Pi_{211})$ be defined in (4.5.7). Then, at each frequency,*

$$\mu(\Pi_{211}) \leq \sqrt{\kappa[P]} \cdot \sqrt{\bar{\sigma}[r_1 T_I] \bar{\sigma}[r_2 S_O]} \qquad (4.5.8)$$

Since the bound (4.5.8) may be tight [Fre89a], it follows that stability robustness against Δ_1 and Δ_2 together is potentially much worse than that against each of these two *individually* at frequencies for which the plant is ill-conditioned ($\kappa[P] \gg 1$). It was shown in [Fre89a], [Fre89b] that requiring $\mu(\Pi_{211})$ to be small imposes more stringent constraints upon the closed-loop transfer functions than those that are due to the stability robustness requirements with respect to Δ_1 or Δ_2 alone (i.e., $\|r_1 T_I\|_\infty < 1/\gamma$, $\|r_2 S_O\|_\infty < 1/\gamma$, respectively).

Similarly, we analyze the combined effects of uncertainties Δ_2 and Δ_3.

Proposition 4.5.2 *Let $\mu(\Pi_{231})$, μ_1 be defined in (4.5.7). Then, at each frequency,*

$$\mu[M|_{J_{23}}] \leq 2\mu_1 \qquad (4.5.9)$$

∎

66

Proof: By definition,

$$\mu(\Pi_{221}) = \sqrt{\bar{\sigma}[r_2 S_O]\bar{\sigma}[r_3 T_I P^{-1}]} \le \sqrt{\mu_1^2}$$

The proof now follows from (4.4.3) for $N = 2$.

■

Hence, Proposition 4.5.2 reveals that, unlike the problem of maintaining stability robustness with respect to Δ_1 and Δ_2, a feedback design which is robust against Δ_2 and Δ_3 *alone* will tend to be robust with respect to these two uncertainties taken together, independent of the size of the plant condition number.

Lastly, we consider the combined effects of uncertainties Δ_1 and Δ_3.

Proposition 4.5.3 *Let* $\mu(\Pi_{221})$, μ_1 *be defined in (4.5.7). Then, at each frequency,*

$$\mu(\Pi_{221}) \le \sqrt{\mu_1(\mid r_1 \mid + \mu_1)} \tag{4.5.10}$$

$$\mu(\Pi_{221}) \ge \sqrt{\bar{\sigma}[r_3 T_I P^{-1}](\mid r_1 \mid - \bar{\sigma}[r_1 T_I])} \tag{4.5.11}$$

■

Proof: It follows from definition that

$$\begin{aligned}\mu(\Pi_{221}) &= \sqrt{\bar{\sigma}[r_1 T_I P^{-1}]\bar{\sigma}[r_3 S_I]} \\ &= \sqrt{\bar{\sigma}[r_3 T_I P^{-1}]\bar{\sigma}[r_1(I + T_I)]}\end{aligned}$$

The proof is now completed by applying the triangle inequality.

■

The bounds in (4.5.10-11) exhibit that stability robustness with respect to Δ_1 and Δ_3 *together* is potentially much worse than that with respect to either of

67

these uncertainties alone at any frequency for which $| r_1(j\omega) | \gg 1/\gamma$. As shown in [ChF89b], maintaining $\mu(\Pi_{221})$ small at such a frequency imposes a more stringent constraint than what is necessary for achieving stability robustness against Δ_3 alone ($\|r_3 T_I P^{-1}\|_\infty < 1/\gamma$). However, it was shown in [ChF89b that the two parameters $\mu(\Pi_{221})$ and $\mu(\Pi_{211})$ are interrelated in such a way that keeping both of them small at such a frequency imposes *similar* requirements upon the closed-loop transfer functions, and thus maintaining $\mu(\Pi_{211})$ small is also useful for keeping $\mu(\Pi_{221})$ small. Hence, achieving stability robustness with respect to Δ_1 and Δ_2 together also tends to guarantee a certain smaller level of stability robustness with respect to the combined effects of Δ_1 and Δ_3.

Finally, we need to consider the simultaneous effects of *all* three uncertainties. Recall that these effects are determined by the parameters $\mu(\Pi_{311})$ and $\mu(\Pi_{312})$. Fortunately, for this particular problem, requiring μ_1 and μ_2 to be small forces μ_3 to be small as well.

Proposition 4.5.4 *Let μ_1, μ_2, and μ_3 be defined in (4.3.9). Then, at each frequency,*

$$\mu_3 \leq max \ \{\mu_1, \mu_2\} \tag{4.5.12}$$

∎

Proof: First, it is straightforward to show

$$\mu(\Pi_{312}) \leq max \ \{\mu_1, \mu_2\}$$

since

$$\mu(\Pi_{312}) \ = \ \left(\bar\sigma[r_1 T_I P^{-1}]\bar\sigma[r_3 T_I P^{-1}]\bar\sigma[r_2 S_O P]\right)^{1/3}$$

$$= \left(\mu^2(\Pi_{211}) \bar{\sigma}[r_3 T_I P^{-1}] \right)^{1/3}$$

$$\leq \left(\mu_2^2 \cdot \mu_1 \right)^{1/3}$$

Next, following the same line establishes

$$\mu(\Pi_{311}) \leq max \left\{ \mu_1, \mu_2 \right\}$$

since

$$\mu(\Pi_{311}) = \left(\bar{\sigma}[r_1 T_I P^{-1}] \bar{\sigma}[r_3 S_I] \bar{\sigma}[r_2 S_O] \right)^{1/3}$$

$$= \left(\mu^2(\Pi_{331}) \bar{\sigma}[r_2 S_O] \right)^{1/3}$$

$$\leq \left(\mu_2^2 \cdot \mu_1 \right)^{1/3}$$

∎

We now close this section by summing up the analysis procedure demonstrated as above. Essentially, we decompose a complicated robust performance problem into a sequence of more *tractable* problems in which we analyze the interaction parameters. An important step of this method is to study interrelations that exist among all interaction parameters and thus to obtain information useful for purposes of design. For a particular robustness problem, interrelations between blocks of the interconnection matrix do allow us to draw significant insights into the problem. Finally, we note that the analysis in this section also echoes Example 4.3.5 in showing why keeping interaction parameters of order $\leq k$ small is not in general necessary for keeping the kth order effects of uncertainties small.

4.6 Concluding Remarks

We have developed an analysis method for analyzing robustness problems associated with multiple sources of modelling error. We used Mason's gain rule to identify a set of interaction parameters which were shown to capture the essentials of such problems. These parameters were further used to derive bounds upon the structured singular value and their importance was manifested through analyses of certain extreme cases. The analysis methodology we propose is to decompose a robustness problem into a sequence of problems in which we analyze the interaction parameters. An important step of this method is to study interrelations among all interaction parameters and thus draw insights useful in design. A benchmark robust performance problem was analyzed to illustrate this method.

Chapter 5

Achieving Robust Performance via H^∞/H^2 Mixed Sensitivity Optimization

5.1 Introduction

In this chapter we shall consider the robust performance problem of achieving good command following (equivalently, small output sensitivity) despite unstructured multiplicative uncertainty at the plant input. This is a difficult design problem, because achieving robust performance requires that feedback properties at both plant input and output be manipulated simultaneously. This precludes the naive use of multivariable loop-shaping techniques as well as of synthesis techniques such as H^2/H^∞ mixed sensitivity optimization. The goal of robust performance may be translated into one of minimizing the structured singular value (SSV) [Doy85]. However, direct minimization of the SSV is still an experimental procedure, with many difficulties remaining to be resolved [DLP86].

In [Fre89a], [Fre89b], and [Fre90], a multivariable loop-shaping approach to

71

this problem was presented, based upon an earlier version of the bounds derived in Chapter 2. The approach taken was to analyze the interrelations among the blocks of the interconnection matrix to obtain guidelines for compensation selection. In this chapter we shall adopt an alternate approach, and analyze the bounds to obtain guidelines for selecting weighting functions to be used in H^2/H^∞ mixed sensitivity optimization. These weighting functions will depend upon the original weighting functions used to represent design specifications in the robust performance problem, as well as the directional properties of the plant. We shall show that minimizing the H^2 or H^∞ norm of the mixed sensitivity function with these new weightings will lend to minimize the size of the structured singular value for the original robust performance problem. Results summarized in this chapter appear in [LoF88], [LoF89a], [LoF89b].

5.2 Simultaneous Uncertainty and Robust Performance Problems

In this section we review relevant results from [Fre89a] and [Fre89b]. The mathematical problem we study has two distinct physical interpretations, either as a *simultaneous uncertainty* problem or as a *robust performance* problem. In the former, we ask that the system be robustly stable against modelling errors occurring at two points in the feedback loop. In the latter we ask that a performance property defined at one point be robust against uncertainty occurring at the other. Both interpretations are useful in guiding and explaining subsequent developments.

Our first task is to define several important transfer functions. Consider the linear time-invariant feedback system pictured in Figure 5.1. The transfer functions $P(s)$ and $K(s)$ are those of the plant model and compensator, respectively. We shall assume[1] that the plant has n inputs and outputs, and that $\det P(s) \not\equiv 0$. The signals $r(s)$, $e(s)$, and $y(s)$ are the reference input, error signal, and system output, respectively. Properties of this system are governed by two sets of transfer functions. Breaking the loop at the plant input yields the *input open-loop transfer function, sensitivity function,* and *complementary sensitivity function*

$$L_I(s) \triangleq K(s)P(s), \quad S_I(s) \triangleq [I + L_I(s)]^{-1}, \quad T_I(s) \triangleq L_I(s)\,[I + L_I(s)]^{-1} \quad (5.2.1)$$

Breaking the loop at the plant output yields the *output open loop transfer function, sensitivity function,* and *complementary sensitivity function*

$$L_O(s) \triangleq P(s)\,K(s), \quad S_O(s) \triangleq [I + L_O(s)]^{-1}, \quad T_O(s) \triangleq L_O(s)[I + L_O(s)]^{-1} \quad (5.2.2)$$

We shall suppose that the true plant differs from the model due to uncertainty that is present *simultaneously* at the plant input and plant output. Specifically, we suppose that

$$P'(s) = [I + r_2(s)\Delta_2(s)]^{-1} P(s)[I + r_1(s)\Delta_1(s)] \quad (5.2.3)$$

A block diagram of the associated feedback system is in Figure 5.2. The transfer functions $\Delta_1(s)$ and $\Delta_2(s)$ used to model system uncertainty will be referred to

---

[1]Our results extend to nonsquare plants that satisfy the relevant assumption of left or right invertibility.
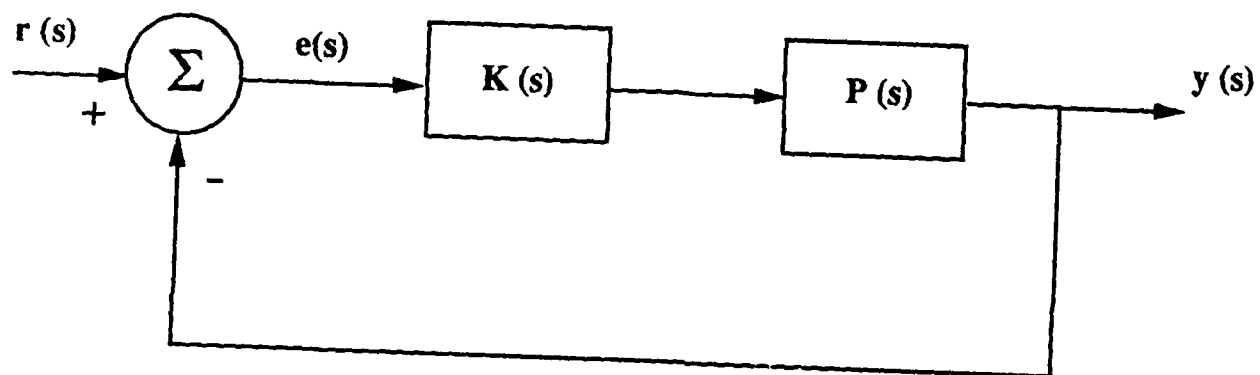
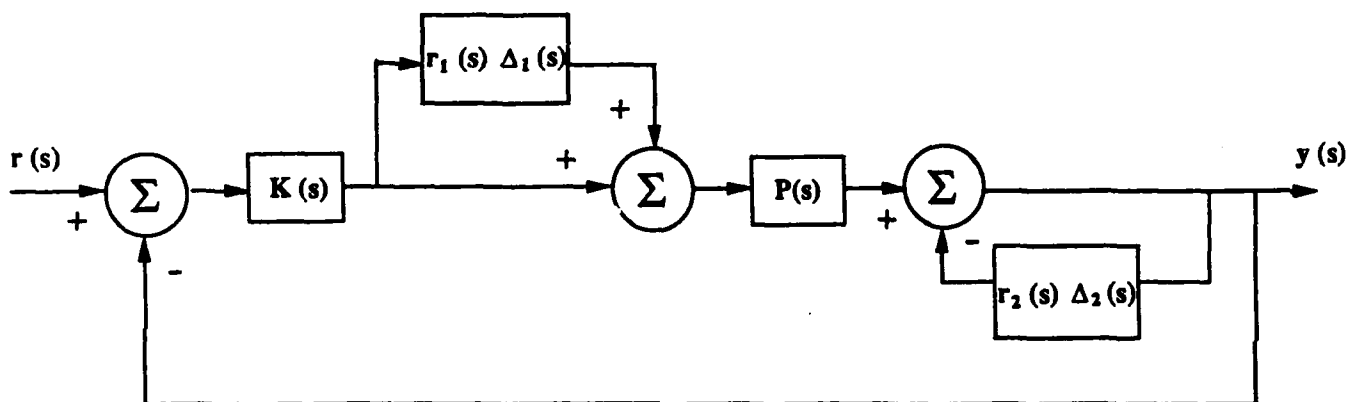Figure 5.1: Block Diagram of Feedback System

74

Figure 5.2: Block Diagram With Uncertainty

75

as input and output perturbations, respectively, and are assumed to be stable and proper. In general, the size of each uncertainty will vary with frequency. This property is modelled by using the weighting functions $r_i(s)$. With no loss of generality, these functions are assumed to be stable and minimum phase, although they may be improper [DWS82]. The sources of each uncertainty are now described.

Uncertainty of the form

$$P_1(s) \triangleq P(s) \left[I + r_1(s)\Delta_1(s) \right] \qquad (5.2.4)$$

is termed *multiplicative input uncertainty*. It typically arises because of unmodelled actuator dynamics or high frequency plant modelling errors. Suppose that the feedback system is nominally stable and that the perturbation Δ_1 may be any stable transfer function satisfying the upper bound $\bar{\sigma}[\Delta_1(j\omega)] \leq \gamma$, $\forall \omega$. Then the system will be robustly stable if and only if the input complementary sensitivity function satisfies the bound [DWS82]:

$$\bar{\sigma}[r_1(j\omega)T_I(j\omega)] < 1/\gamma \ , \ \forall \omega \qquad (5.2.5)$$

Hence $\bar{\sigma}[r_1(j\omega)T_I(j\omega)]$ is inversely proportional to a frequency dependent stability margin against uncertainty (5.2.4)

Uncertainty of the form

$$P_2(s) \triangleq \left[I + r_2(s)\Delta_2(s) \right]^{-1} P(s) \qquad (5.2.6)$$

is termed *divisive output uncertainty*. Its presence may be due to modelling errors at the plant output. For our purposes, however, it is used to represent a

performance specification such as an upper bound upon the response of the error signal to the reference signal shown in Figure 5.1 [DWS82]. Suppose that the feedback system is nominally stable and that the perturbation Δ_2 may be any stable transfer function satisfying the upper bound $\bar{\sigma}[\Delta_2(j\omega)] \leq \gamma$, $\forall\omega$. Then the system will be robustly stable if and only if the output sensitivity function satisfies the bound [DWS82]:

$$\bar{\sigma}[r_2(j\omega)S_O(j\omega) < 1/\gamma \; , \; \forall\omega \qquad (5.2.7)$$

Hence $\bar{\sigma}[r_2(j\omega)S_O(j\omega)]$ is inversely proportional to a frequency dependent stability margin against uncertainty (5.2.6). Alternately, if the output uncertainty arises from an attempt to represent a performance goal, we say that the goal of nominal command following is satisfied if (5.2.7) holds.

Testing for robust performance requires use of the structured singular value [DWS82]. Rearranging the block diagram in Figure 5.2 into the form shown in Figure 2.1, we have[2]

$$M = \begin{bmatrix} r_1 T_I & -r_1 T_I P^{-1} \\ -r_2 S_O P & r_2 S_O \end{bmatrix} \qquad (5.2.8)$$

and

$$\Delta = \text{diag}[\Delta_1, \Delta_2] \qquad (5.2.9)$$

Defining the structured singular value as in Section 2.2, we have that $\bar{\sigma}[r_2 S_O] < 1/\gamma$, $\forall\Delta_1$ such that $\bar{\sigma}[\Delta_1] < \gamma$ if and only if $\mu[M] < 1/\gamma$. Hence the design goal of achieving robust performance can be translated into one of minimizing

---

[2] As usual, we suppress dependence on frequency where convenient.

$\mu_\infty \triangleq \sup_\omega \mu[M(jw)]$. We shall approach this problem by analysing the bounds upon the structured singular value presented in Chapter 2.

Lemma 5.2.1: With M and Δ defined by (5.2.8-9), the structured singular value satisfies the bounds

$$\mu[M] \geq \max \left\{ \begin{array}{c} \bar{\sigma}[r_1 T_I], \bar{\sigma}[r_2 S_O] \ , \\ \sqrt{\bar{\sigma}[r_1 T_I P^{-1}]\bar{\sigma}[r_2 S_(P]} \end{array} \right\}. \qquad (5.2.10)$$

and

$$\mu[M] \leq \sqrt{\bar{\sigma}[r_1 T_I P^{-1}]\bar{\sigma}[r_2 S_O P]} \qquad (5.2.11)$$
$$+ \max\{\bar{\sigma}[r_1 T_I], \bar{\sigma}[r_2 S_O]\}$$

∎

It follows from Corollary 5.2.1 that if

$$\bar{\sigma}[r_1 T_I P^{-1}]\bar{\sigma}[r_2 S_O P] \gg \max\{\bar{\sigma}[r_1 T_I], \bar{\sigma}[r_2 S_O]\}$$

and

$$\bar{\sigma}[r_1 T_I P^{-1}]\bar{\sigma}[r_2 S_O P] \gg 1 \qquad (5.2.12)$$

then performance robustness will be poor even if nominal performance and robust stability are satisfactory. Hence it is desirable to know how a compensator should be selected to prevent (5.2.12) from being satisfied. We approach this problem by deriving a set of upper and lower bounds that are analogous to (5.2.10-11) and that display the plant directionality properties. For simplicity of exposition, we shall restrict our discussion to systems with two inputs and outputs. Extensions

78

to n inputs and outputs are available. The following results are similar in spirit to those of Section 2, [Fre89b].

Denote the plant singular value decomposition by

$$
\begin{aligned}
P &= WTZ^H \\
&= \sum_{i=1}^{2} w_i z_i^H r_i
\end{aligned}
\tag{5.2.13}
$$

where $T = \text{diag}[r_1, r_2]$ contains the singular values with usual ordering, the columns of $W = [w_1 w_2]$ are the left singular vectors, and those of $Z = [z_1 z_2]$ are the right singular vectors. Define the *coupling coefficients*

$$
\mathbb{B}(k,l) = |r_1 r_2| \|S_O w_k\| \cdot \|T_I z_l\|
\tag{5.2.14}
$$

The following result follows similarly to Theorem 2.2 of [Fre89b].

Theorem 5.2.2: For each pair of plant singular values, the structured singular value satisfies

$$
\mu[M] \geq \max \left\{
\begin{array}{c}
\bar{\sigma}[r_1 T_I], \bar{\sigma}[r_2 S_O] \;, \\
\frac{}{\sqrt{\mathbb{B}(k,l) \cdot (r_k/r_l)}}
\end{array}
\right\}
\tag{5.2.15}
$$

∎

Suppose that we desire the structured singular value to satisfy $\mu_\infty < 1$. Then each lower bound implied by (5.2.15) corresponds to a *necessary* condition for robustness. By deriving upper bounds upon the structured singular value, it is also possible to state *sufficient* conditions in terms of the coupling coefficients.

Theorem 5.2.3: For each pair of plant singular values, the structured singular

value must satisfy

$$\mu[M] \leq \sqrt{\sum_{k=1}^{2} \sum_{l=1}^{2} \Xi(k,l)(r_k/r_l)} + \max \left\{ \begin{array}{l} \bar{\sigma}[r_1 T_I], \\ \bar{\sigma}[r_2 S_O] \end{array} \right\} \qquad (5.2.16)$$

∎

A tighter upper bound may be obtained if an additional orthogonality condition is satisfied.

Corollary 5.2.4: Suppose that

$$\begin{array}{ll} \text{(i)} & S_O w_k \perp S_O w_l \quad , \quad k \neq l \\ \text{(ii)} & T_I z_k \perp T_I z_l \quad , \quad k \neq l \end{array} \qquad (5.2.17)$$

Then

$$\mu[M] \leq \max_{k,l} \sqrt{\Xi(k,l)(r_k/r_l)} + \max \left\{ \begin{array}{l} \bar{\sigma}[r_1 T_I] \\ \bar{\sigma}[r_2 S_O] \end{array} \right\} \qquad (5.2.18)$$

∎

Together, Theorems 5.2.2-3 and Corollary 5.2.4 show that requiring each coupling coefficient to be suitably small tends to insure that performance robustness will be satisfactory provided that the bounds $\bar{\sigma}[r_1 T_I] < 1$ and $\bar{\sigma}[r_2 S_O] < 1$ are satisfied.

Note first that each coupling coefficient is the product of the weightings and two terms that are each the gain of a closed-loop transfer function in a particular direction. It follows that the *weighted condition number*

$$\kappa_r[P] \triangleq |r_1 r_2| \cdot \kappa[P] \qquad (5.2.19)$$

is a particularly relevant parameter of the design problem. At frequencies for which (5.2.19) is large, it is necessary that the sensitivity and complementary

80

sensitivity functions be shaped carefully to prevent the structured singular value from becoming large. This imposes constraints upon the open-loop singular values.

Lemma 5.2.5: For each pair of singular values, the coupling coefficients are bounded above and below by

$$|r_1 r_2|\overline{\sigma}[L_O]/|1 - \underline{\sigma}[L_O]|^2 \geq B(k,l) \geq |r_1 r_2|\underline{\sigma}[L_O]/(1 + \overline{\sigma}[L_O])^2 \qquad (5.2.20)$$

$$|r_1 r_2|\overline{\sigma}[L_I]/|1 - \underline{\sigma}[L_I]|^2 \geq B(k,l) \geq |r_1 r_2|\underline{\sigma}[L_I]/(1 + \overline{\sigma}[L_I])^2 \qquad (5.2.21)$$

It also follows from the preceding theorems that the closed loop transfer functions must satisfy certain directionality properties. One approach to achieving these properties is to translate the closed-loop properties into specifications upon the open loop transfer function. This is explored in [Fre89b] and [Fre90]. In the following section we shall pursue an alternate approach.

5.3 Robust Performance via Mixed Sensitivity Optimization

We saw in the preceding section that the goal of robust performance may be translated into one of manipulating the size of the coupling coefficients. In this section we shall show how this may be done using H^2/H^∞ mixed sensitivity optimization techniques. For simplicity of exposition, we shall consider only systems with two inputs and two outputs. In this case, Theorem 5.2.2 reduces as follows.

Corollary 5.3.1: Necessary[3] conditions for achieving

$$\mu[M] < 1 \tag{5.3.1}$$

are that

$$\max\{\bar{\sigma}[r_1 T_I], \ \bar{\sigma}[r_2 S_O]\} < 1 \tag{5.3.2}$$

$$\|r_1 T_I z_2\| \cdot \|r_2 S_O w_1\|(\kappa) < 1 \tag{5.3.3}$$

$$\|r_1 T_I z_1\| \cdot \|r_2 S_O w_2\|(1/\kappa) < 1 \tag{5.3.4}$$

$$\|r_1 T_I z_1\| \cdot \|r_2 S_O w_1\| < 1 \tag{5.3.5}$$

$$\|r_1 T_I z_2\| \cdot \|r_2 S_O w_2\| < 1 \tag{5.3.6}$$

∎

Note first that if (5.3.2) is satisfied, then the only one of conditions (5.3.3-6) remaining of interest is (5.3.3)

We now briefly review the mixed sensitivity minimization problem. Consider the system depicted in Figure 5.3. The transfer function from the disturbance d to the weighted control signal y_1, and system output y_2, is given by

$$\begin{bmatrix} y_1(s) \\ y_2(s) \end{bmatrix} = G(s)d(s)$$

where

$$G(s) = \begin{bmatrix} -W_1(s)P^{-1}(s)T_O(s)W_d(s) \\ W_2(s)S_O(s)W_d(s) \end{bmatrix} \tag{5.3.7}$$

---

[3]Recall that Theorem 5.3.2 and Corollary 5.3.4 imply that making (5.3.2-6) small also tends to insure that (5.3.1) is satisfied.
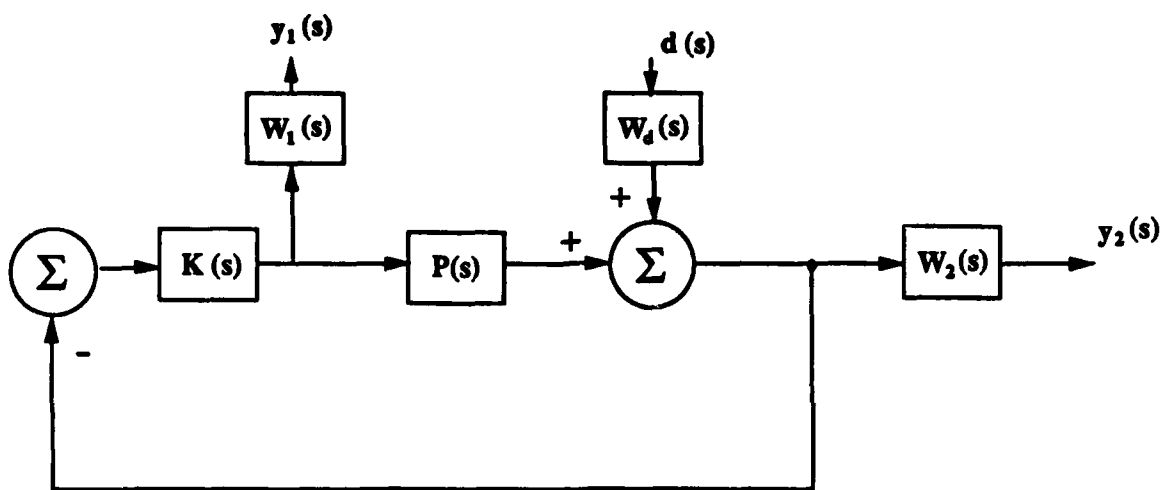
Figure 5.3: Block Diagram for the Mixed Sensitivity Problem

The weighting functions W_1, W_2, and W_d are assumed to be stable and minimum phase. We shall refer to (5.3.7) as the weighted mixed sensitivity function. Define the H^∞ mixed sensitivity problem as that of minimizing

$$\|G\|_\infty = \sup_\omega \bar{\sigma}[G(j\omega)] \tag{5.3.8}$$

over all internally stabilizing controllers. Similarly, we may define the H^2 mixed sensitivity problem as that of minimizing

$$\|G\|_2 = \left[\frac{1}{2\pi}\int_{-\infty}^{\infty} \text{trace } G^T(-j\omega)G(j\omega)\right]^{1/2} \tag{5.3.9}$$

over all internally stabilizing controllers. Computationally tractable solutions to these problems using state-space techniques have recently become available [DGK89].

We shall now show how to pick weighting functions so that minimizing (5.3.8) tends to minize μ_∞. Modifications of this procedure to the problem of minimizing (5.3.9) are found in [LoF89b].

Theorem 5.3.2: Consider $M(s)$ and $G(s)$ defined by (5.2.8) and (5.3.7), respectively, and evaluated at a fixed frequency. Assume that the weightings in (5.3.7) are given by

$$W_d = W \begin{bmatrix} \alpha & 0 \\ 0 & 1 \end{bmatrix} \tag{5.3.10}$$

$$W_1 = r_1 r_2(\kappa/\alpha)I \tag{5.3.11}$$

and

$$W_2 = r_2 I \tag{5.3.12}$$

where W is the matrix of plant left singular vectors (5.2.13), r_1 and r_2 are the weighting functions in (5.2.4) and (5.2.6), r_2 is the smaller plant singular value, κ is the plant condition number, and $\kappa \geq |\alpha| \geq 1$. Suppose that

$$\bar{\sigma}[G] < 1 \qquad (5.3.13)$$

Then (5.3.2-6) are satisfied.

■

Proof: Define $G_1 = -W_1 P^{-1} T_O W_d$ and $G_2 = W_2 S_O W_d$. It is well-known that

$$\bar{\sigma}[G] \geq \max_i \bar{\sigma}[G_i] \qquad (5.3.14)$$

and, for any unit vector x,

$$\bar{\sigma}[G] \geq \|G_i x\| \qquad (5.3.15)$$

Notice that

$$G_1 = -r_1 T_I Z \begin{bmatrix} 1 & 0 \\ 0 & \kappa/\alpha \end{bmatrix} \qquad (5.3.16)$$

Since $\kappa/|\alpha| \geq 1$ by construction, and since Z is unitary, we have from (5.3.14-15)

$$\bar{\sigma}[G] \geq \bar{\sigma}[r_1 T_I] \qquad (5.3.17)$$

and, with $e_2 = [0\ 1]^T$,

$$\begin{aligned} \bar{\sigma}[G] &\geq \|G_1 e_2\| \\ &= \|r_1 T_I z_2(\kappa/\alpha)\| \end{aligned} \qquad (5.3.18)$$

Similarly,

$$G_2 = r_2 S_O W \begin{bmatrix} \alpha & 0 \\ 0 & 1 \end{bmatrix} \qquad (5.3.19)$$

85

which implies that

$$\bar{\sigma}[G] \geq \bar{\sigma}[r_2 S_O] \tag{5.3.20}$$

and

$$\bar{\sigma}[G] \geq \|r_2 S_O w_1\| \tag{5.3.21}$$

From (5.3.17) and (5.3.20), it follows that (5.3.13) implies (5.3.2) and thus also (5.3.4-6). Finally, (5.3.13), (5.3.18), and (5.3.21) taken together imply (5.3.3).

∎

Although these are not *sufficient* conditions, the upper bounds in Theorem 5.2.3 suggest that minimizing $\|G\|_\infty$ also tends to make μ_∞ itself small, and this conjecture appears to be borne out by our design examples.

We now discuss how weighting functions with the properties (5.3.10-12) may be constructed. First, it may not be possible to find a rational matrix $W_d(s)$ so that (5.3.10) holds, because the singular vectors need not be complex analytic and thus need not have frequency responses equal to those of rational transfer functions. However, these vectors can often be approximated sufficiently closely for our purposes by rational functions. (On the other hand, the smallest singular value r_2 and the condition number κ can always be approximated arbitrarily closely by the gain of a stable, rational, minimum phase transfer function.) Finally, we need to select a rational transfer function $\alpha(s)$. To do this we suppose that, as is typical, the weighting functions r_1 and r_2 have the general shape shown in Figure 5.4. Let us now investigate the implications of requiring (5.3.2) to hold at a frequency for which $|r_1(j\omega)| \gg 1$ or $|r_2(j\omega)| \gg 1$.
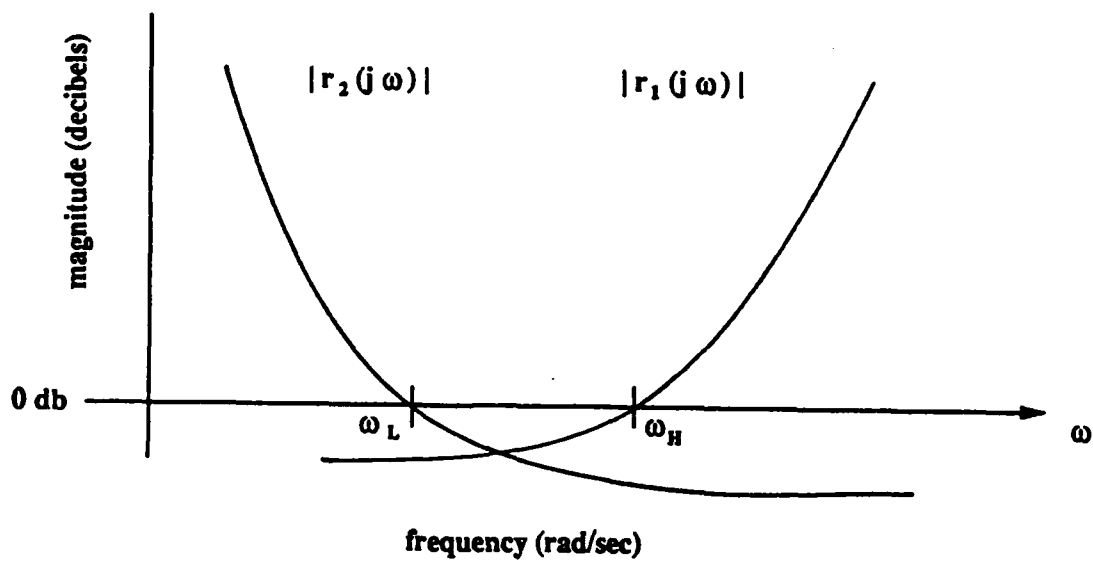
Figure 5.4: Typical Weighting Functions

Lemma 5.3.3: (a) Suppose that $\bar{\sigma}[r_2 S_O] < 1$ and that $|r_2| \gg 1$. Then

$$\|r_1 T_I z_2\| \approx |r_1| \tag{5.3.22}$$

(b) Suppose that $\bar{\sigma}[r_1 T_I] < 1$ and that $|r_1| \gg 1$. Then

$$\|r_2 S_O w_1\| \approx |r_2| \tag{5.3.23}$$

$\blacksquare$

It follows that if we wish to satisfy (5.3.2) and (5.3.3) at low frequencies, for which $|r_2| \gg 1$, then we should require that $\|r_2 S_O w_1 \kappa\| < 1$. Hence we should have $|\alpha| \approx \kappa$ at low frequencies. Similar considerations show that we should require $|\alpha| \approx 1$ at high frequencies. Hence we shall select a function $\alpha(s)$ whose gain decreases from $|\alpha| = \kappa$ to $|\alpha| = 1$.

Of course, the weightings described above may need iteration before a satisfactory design is obtained.

Finally, we state dual results that shall prove useful in our example. To do this, define the mixed sensitivity function

$$\tilde{G}(s) = \begin{bmatrix} -W_1(s) T_I(s) W_d(s) \\ W_2(s) P(s) S_I(s) W_d(s) \end{bmatrix} \tag{5.3.24}$$

corresponding to the block diagram in Figure 5.5.

Theorem 5.3.4: Consider $M(s)$ and $\tilde{G}(s)$ defined by (5.2.8) and (5.3.24), respectively, and evaluated at a fixed frequency. Assume that the weightings in (5.3.24) are given by

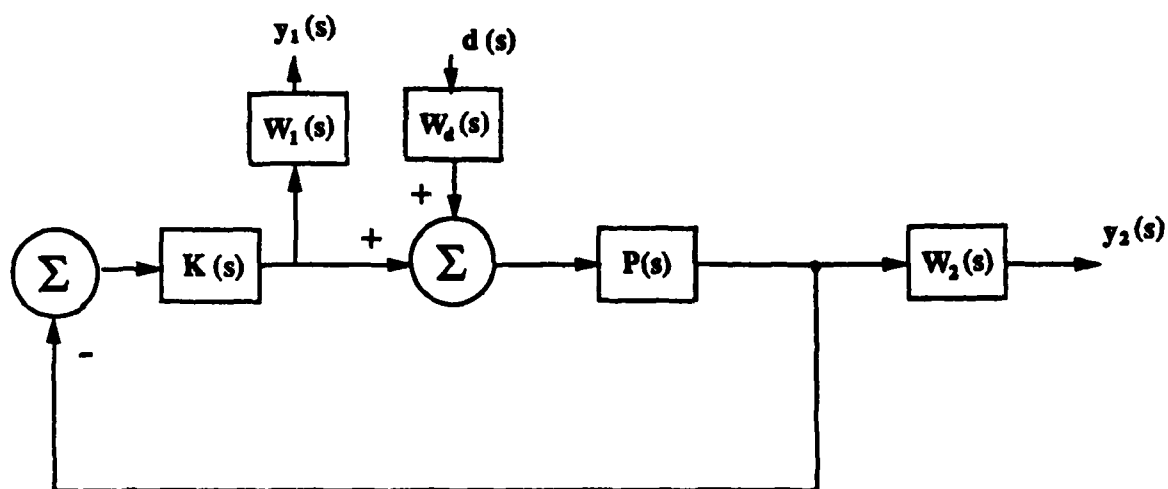$$W_d = Z \begin{bmatrix} 1 & 0 \\ 0 & \beta \end{bmatrix} \tag{5.3.25}$$

Figure 5.5: Block Diagram for Alternate Mixed Sensitivity Problem

$$W_1 = r_1 I \tag{5.3.26}$$

$$W_2 = (r_2/\beta r_2)I \tag{5.3.27}$$

where Z is the matrix of plant right singular vectors (5.2.13), r_1 and r_2 are the weighting functions in (5.2.4) and (5.2.6), r_2 is the smaller plant singular value, κ is the plant condition number, and $\kappa \geq |\beta| \geq 1$. Suppose that

$$\bar{\sigma}[\tilde{G}] < 1 \tag{5.3.28}$$

Then (5.3.2-6) are satisfied. ∎

Proof: Similar to that of Theorem 5.3.2. ∎

The transfer function $\beta(s)$ should increase from 1 at low frequencies to κ at high frequencies.

5.4 Design Example Using H^∞ Mixed Sensitivity

We now apply the procedure developed in the preceding section to the problem of designing a robust performance longitudinal control system for a highly maneuverable aircraft. This example was originally proposed by Stein [Ste84]. The aircraft characteristics and linearized models are discussed in detail in [HBG79]. The aircraft possesses two sets of longitudinal control surfaces: elevators and canards. There are two available measurements: angle of attack and pitch rate. For our discussion, we use the linearized model of the longitudinal dynamics at

Mach 0.9, altitude 25,000 ft:

$$\dot{x} = Ax + Bu$$

$$y = Cx \tag{5.4.1}$$

where

$$A = \begin{bmatrix} -.0226 & -36.6 & -18.9 & -32.1 \\ 0 & -1.9 & -.983 & 0 \\ .0123 & -11.7 & -2.63 & 0 \\ 0 & 0 & 1.0 & 0 \end{bmatrix}$$

$$B = \begin{bmatrix} 0 & 0 \\ -.414 & 0 \\ -77.8 & 22.4 \\ 0 & 0 \end{bmatrix}$$

$$C = \begin{bmatrix} 0 & 57.3 & 0 & 0 \\ 0 & 0 & 0 & 57.3 \end{bmatrix}$$

The plant model in this flight condition is stable and minimum phase. The singular values of the plant are shown in Figure 5.6. Since the plant condition number is equal to the ratio of the larger to smaller singular values, we see from Figure 5.6 that the condition number is large at almost all frequencies. The physical source for the large condition number is the ability of the control surfaces to impart relatively large amounts of rotational energy to the aircraft, combined with an inability to transmit relatively large amounts of kinetic energy to the aircraft. These facts imply that the transfer function from inputs to pitch rate has larger gain than that from inputs to vertical velocity, or angle of attack.

The weighting function for robust stability (5.2.4) is

$$r_1(s) = \frac{1}{2}(.01s + 1) \tag{5.4.2}$$
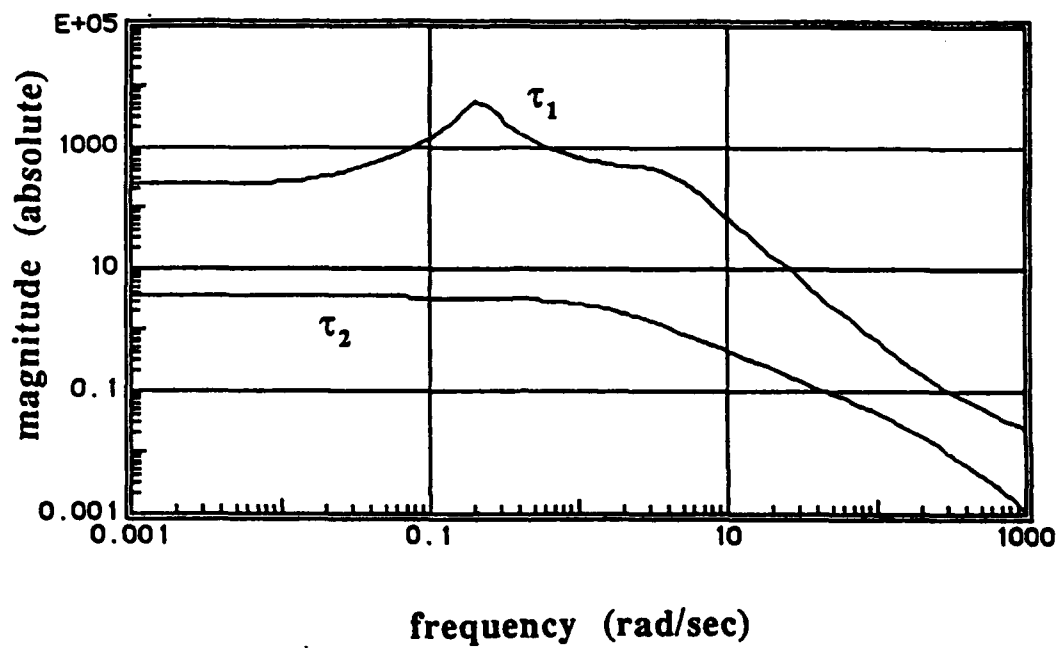
Figure 5.6: Plant Singular Values

while that for tracking performance is

$$r_2(s) = \frac{1}{2}\left(\frac{s+3}{s+.03}\right) \tag{5.4.3}$$

Bode plots of these weighting functions appear in Figure 5.7, and a Bode plot of the weighted condition number (5.2.19) is in Figure 5.8. As shown by [Ste84], the optimal value of $\mu[M]$ for this design is $\mu[M(j)\omega] = 1$, $\forall \omega$.

We shall initially use weighting obtained by approximating those given in Theorem 5.3.4, and then iterating to achieve a final satisfactory design:

$$W_d(s) = \begin{bmatrix} 1 & 0 \\ 0 & .002s+1 \end{bmatrix}\begin{bmatrix} .96 & -.25 \\ -.25 & -.25 \end{bmatrix}\begin{bmatrix} 1 & 0 \\ 0 & \frac{9(s+19)}{s+171} \end{bmatrix} . \tag{5.4.4}$$

$$W_1(s) = r_2(s)I \tag{5.4.5}$$

$$W_2(s) = (1/3.756)r_2(s)I . \tag{5.4.6}$$

The constant factor in (5.4.6) arises from a crude low frequency approximation to the function $\beta(s)r_2(s)$. The structured singular value resulting from these weightings is plotted in Figure 5.9. The key features of this plot are the two peaks, one in the crossover region and one at high frequencies that may be reduced by penalizing the control signal y_1 more heavily by adding a lead filter to W_1:

$$W_1(s) = 2.5\left(\frac{s+80}{s+200}\right)r_1(s)I \tag{5.4.7}$$

while leaving the other design weights unchanged. The structured singular value of the second design (Figure 5.10) has a single large peak in the crossover region. This may be reduced by using a better approximation to the function $\beta(s)r_2(s)$. Such an approximation requires that we introduce a lead filter into (5.4.6):
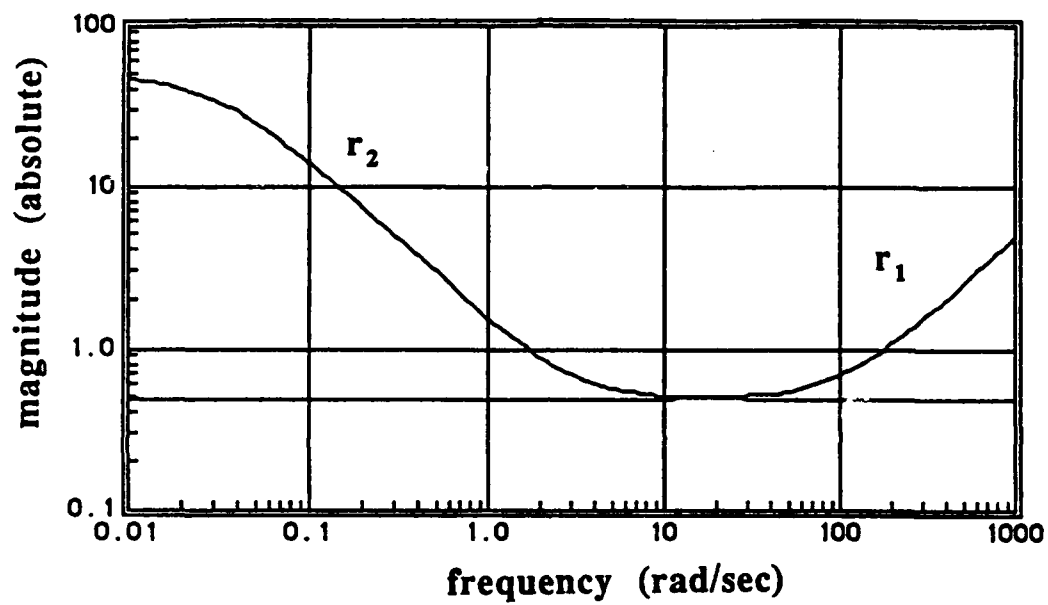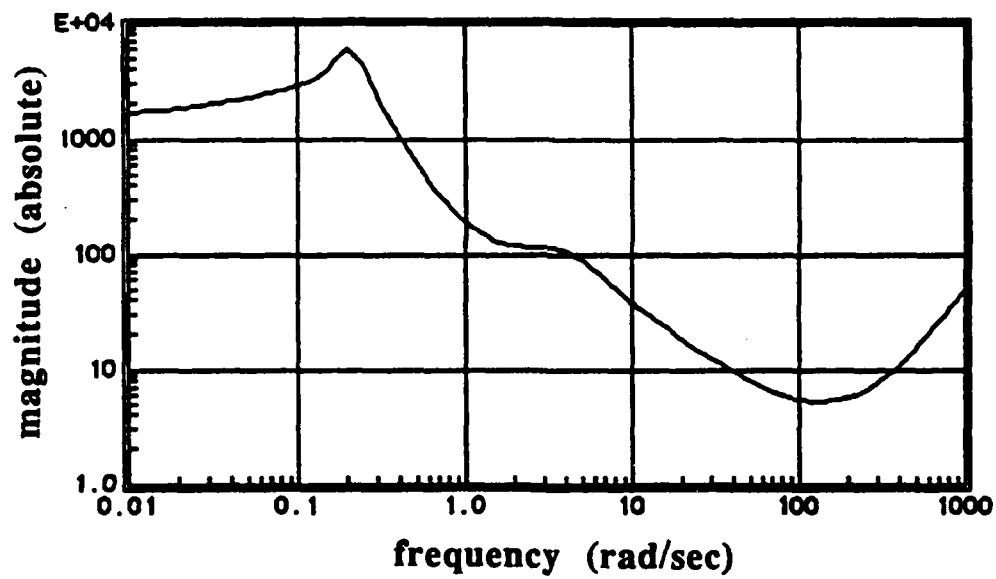
Figure 5.7: Weighting Functions

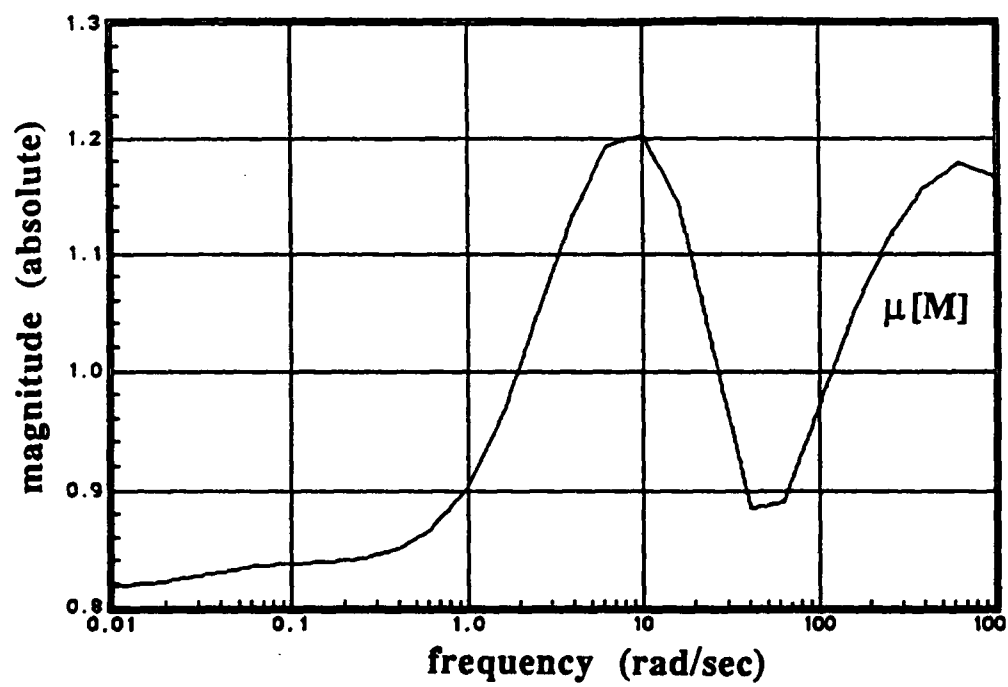Figure 5.8: Weighted Condition Number

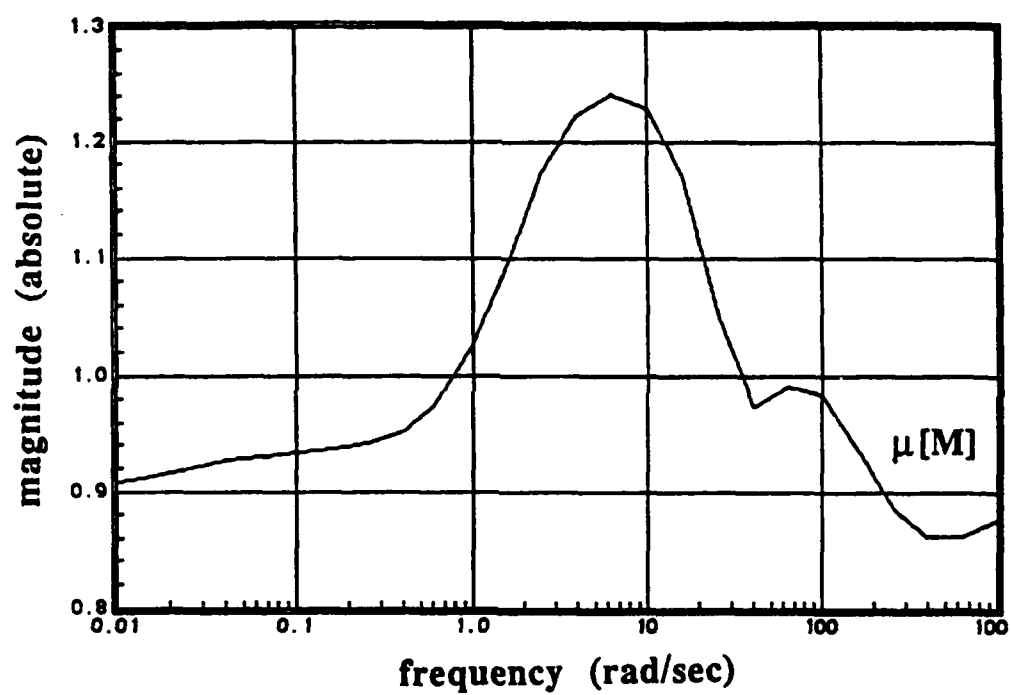Figure 5.9: Structured Singular Value, Design 1.

Figure 5.10: Structured Singular Value, Design 2

$$W_2(s) = \left(\frac{s+1}{s+3.756}\right) r_2(s) I \qquad (5.4.8)$$

The structured singular value for the third design, using (5.4.4), (5.4.7), and (5.4.8) is shown in Figure 5.11. Note that this plot is within 10% of the desired value, and of the optimal value obtained in [Ste84]. If desired, one could reduce this peak further through additional applications of the techniques developed in this chapter. The resulting changes in the compensator will only be minor, however, and are likely to be dominated by effects not incorporated into the linearized design problem.
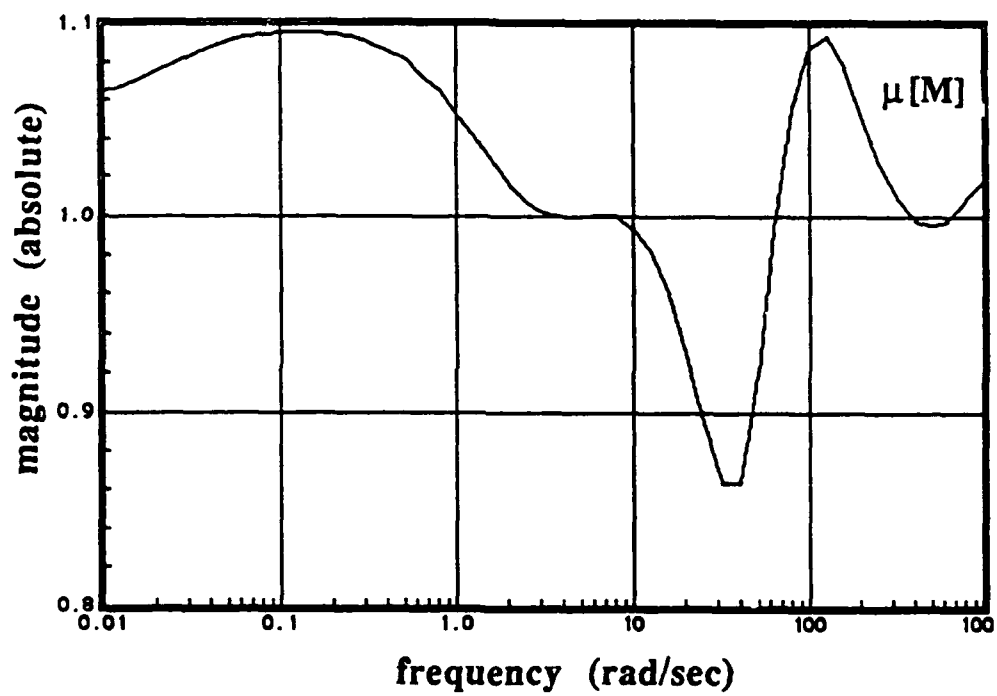
Figure 5.11: Structured Singular Value, Design 3

Chapter 6

Design for Ill-Conditioned Plants Using LQG/LTR Method

6.1 Introduction

Multivariable extensions of classical loop-shaping ideas have recently received much attention [DoS81], [StA87], [SLH81], [HuM82]. The development of these multivariable loop-shaping design methodologies was based upon the introduction of singular value analysis. Since the singular value tests used to analyze stability robustness are applicable only to limited classes of plant uncertainty [FLC82], [Doy82], [DWS82], these design methodologies are most successful only when the design specifications can be precisely formulated in terms of loop transfer functions at one loop breaking point or when the plant has uniform gain in all loops.

Owing to the coupling and the directionality, feedback properties of a multivariable system such as stability margin and sensitivity must be evaluated at more than one loop-breaking point, e.g., at the plant input and plant output. When the

plant transfer function, evaluated at frequencies of interest, is an ill-conditioned matrix, it can happen that nominal properties at one loop-breaking point are unacceptable even though properties at the other are good. It can also happen that nominal properties at one loop-breaking point are extremely sensitive to uncertainty elsewhere [Fre89a], [Fre89b], [NeM87], [SMD88], [Ste85]. Hence, when the plant is ill-conditioned, and when the uncertainties are present simultaneously at different points in the feedback loop, multivariable loop-shaping techniques such as LQG/LTR [StA87] may fail to yield a robust design [Ste84], [Ste85].

Recently, some progress has been made in analyzing how to shape the loop-transfer functions at one loop breaking point to satisfy the design goals formulated in terms of loop transfer functions at different loop breaking points [Fre90] It is shown that the difference between feedback properties at different loop breaking points is closely related to the singular subspace structures of the loop-transfer functions and the plant. These analyses yield conditions that must be satisfied by feedback properties at one loop-breaking point to prevent poor feedback properties at the other or to be robust against uncertainty at the other. It turns out that, to satisfy the design goals, one has to manipulate both the singular values and the singular subspace structures of the loop-transfer functions. However, to the best of our knowledge, no systematic synthesis procedures are available to obtain compensators so that the resultant loops satisfy the loop shaping conditions derived in [Fre90].

The main objective of this chapter is to try to develop such a synthesis procedure. We shall do so by incorporating design insights obtained in [Fre90] into the shaping of the state feedback loop in the LQG/LTR design. We will show

that by properly selecting weighting functions, the LQG/LTR methodology can be an effective loop-shaping technique for ill-conditioned plants.

The rest of the chapter is organized as follows. In Section 6.2, we introduce some notations and preliminaries and formulate the problem considered in this chapter. In Section 6.3, a property of the Kalman equality is discussed which relates the right singular vectors of the return difference function of the state feedback loop with those of the weighting function. In Section 6.4, procedures for selecting weighting functions are suggested for the LQG/LTR target state feedback loop design which ensure that the resultant LQG/LTR design has good stability robustness against simultaneous uncertainties at the plant input and output. Design examples are given in Section 6.5 to illustrate the procedures.

6.2   Preliminaries and Problem Formulations

Consider the linear time-invariant feedback system shown in Figure 6.1. $P(s)$ and $F(s)$ denote the transfer functions of the plant model and the compensator, respectively. We assume that $P(s)$ is an $m \times m$ rational matrix and is invertible. The signals $u(s)$ and $y(s)$ are the plant input and measured output, respectively. Let the singular value decomposition of the plant model be denoted[1] $P = WTZ^H$, where $T = diag[\tau_1, \tau_2, \ldots, \tau_m]$ contains the singular values with usual ordering $\bar{\sigma}[P] = \tau_1 \geq \tau_2 \geq \cdots \geq \tau_m = \underline{\sigma}[P]$, $W = [w_1, w_2, \ldots, w_m]$ and $Z = [z_1, z_2, \ldots, z_m]$ are unitary matrices whose columns are the left and right singular vectors, respectively. We shall use a boldface letter to denote the col-

---

[1]We suppress dependence upon frequency whenever appropriate.

umn space generated by the matrix (or vector) denoted by the corresponding uppercase (lowercase) letter. The condition number of the plant is defined as $\kappa[P] := \bar{\sigma}[P]/\underline{\sigma}[P]$. If the condition number is very large at some frequency, we say the plant is ill-conditioned at that frequency. The plant condition number is not invariant under scaling, or a change of units. Hence we must assume throughout this chapter that physically meaningful units have been chosen. It follows that, if a plant is ill-conditioned with respect to these units, then the ill-conditioning cannot be removed simply by scaling.

For this system, the feedback system properties are governed by the following two sets of transfer functions:

1. Input open-loop transfer function $L_I(s) := F(s)P(s)$

   Input sensitivity function $S_I(s) := [I + L_I(s)]^{-1}$

   Input complementary sensitivity function $T_I(s) := L_I(s)[I + L_I(s)]^{-1}$

2. Output open-loop transfer function $L_O(s) := P(s)F(s)$

   Output sensitivity function $S_O(s) := [I + L_O(s)]^{-1}$

   Output complementary sensitivity function $T_O(s) := L_O(s)[I + L_O(s)]^{-1}$.

When all design specifications can be accurately formulated in terms of the transfer functions at one loop breaking point, then multivariable loop-shaping design methods (e.g., [StA87]) can be applied to manipulate the shape of the transfer functions so that the design specifications are satisfied as well as possible. However, when design specifications are formulated in terms of transfer functions at different loop breaking points, then the multivariable loop-shaping methods may
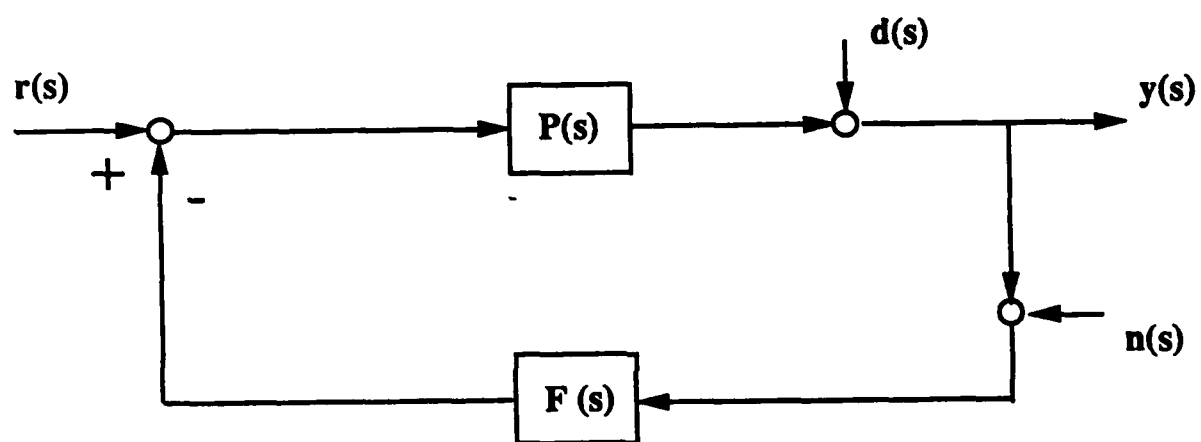
103

Figure 6.1: Linear Feedback System

not be so readily applicable. For the problem we consider in this chapter, the design specifications have to be formulated in terms of transfer functions at different loop-breaking points. The following is the problem description. It is the same as that discussed in Chapter 5, and is restated here for ease of discussion.

Suppose that the true plant is given by

$$\tilde{P}(s) = [I + r_2(s)\Delta_2(s)]P(s)[I + r_1(s)\Delta_1(s)] \qquad (6.2.1)$$

where the unstructured uncertainties $\Delta_i, i = 1, 2$ lie in the set

$$\mathbf{D}_\gamma := \{\Delta \in C^{m \times m} : \Delta \text{ is stable and } \bar{\sigma}[\Delta] < \gamma\} \qquad (6.2.2)$$

and the weighting functions $r_1(s)$ and $r_2(s)$ describe how the size of each uncertainty varies with frequency. $\Delta_1(s)$ is called input uncertainty and is assumed to arise from plant or actuator modelling errors. $\Delta_2(s)$ is called output uncertainty. It may arise either from modelling error or from the use of fictitious uncertainty to represent an equivalent performance specification [DWS82]. Hence, the problem we are to consider next can be interpreted either as robust stability against simultaneous plant input and output uncertainties or as robust performance at the plant output against uncertainty at the plant input. Our goal is to find a compensator $F(s)$, for given design specifications $r_1(s)$ and $r_2(s)$, such that the feedback system in Figure 6.1 is stable when the plant model $P(s)$ is replaced by the true plant $\tilde{P}(s)$ described in (6.1) and (6.2), i.e., we would like to achieve stability robustness against simultaneous input and output uncertainty. This problem is equivalent to finding a compensator such that the structured singular value satisfies

$$\mu[M(j\omega)] < 1/\gamma, \forall \omega \qquad (6.2.3)$$

105

where

$$M = \begin{bmatrix} r_1 T_I & -r_1 T_I P^{-1} \\ -r_2 S_O P & r_2 S_O \end{bmatrix} \qquad (6.2.4)$$

and the structured singular value is defined at each frequency by [2]

$$\mu[M] := \begin{cases} 0, & \text{if no } \Delta \in \mathbf{D}_\infty \text{ exists with } \det[I + M\Delta] = 0 \\ 1/\min\{\bar{\sigma}[\Delta] : \det[I + M\Delta] = 0 \text{ and } \Delta \in \mathbf{D}_\infty\}, & \text{otherwise.} \end{cases} \qquad (6.2.5)$$

However, the structured singular value can only be used to judge our compensator design and it does not give insights into how we should construct compensators such that (6.2.3) is satisfied. To obtain such insights, bounds on the structured singular value have been derived (see Chapters 2–4) in terms of the singular values and vectors of the plant transfer functions together with the sensitivity and complementary sensitivity functions used to perform singular value analysis. Specifically, we have for M defined in (6.2.4) that

$$\max\{\mu_1, \mu_2\} \leq \mu[M] \leq \mu_1 + \mu_2 \qquad (6.2.6)$$

where

$$\mu_1 := \max\{\bar{\sigma}[r_1 T_I], \bar{\sigma}[r_2 S_O]\} \qquad (6.2.7)$$

$$\mu_2 := \sqrt{\bar{\sigma}[r_2 P S_I]\bar{\sigma}[r_1 T_I P^{-1}]} \qquad (6.2.8)$$

Hence, to satisfy (6.2.3), it is necessary and sufficient to keep the parameters μ_1 and μ_2 small.

It is useful to decompose an ill-conditioned plant into higher and lower gain subsystems at frequencies of interest. Hence we partition the plant singular value decomposition as

$$P = W_1 T_1 Z_1^H + W_2 T_2 Z_2^H \qquad (6.2.9)$$

---

[2]For details about structured singular value, see [Doy82].

where $T_1 = diag[\tau_1, \ldots, \eta], T_2 = diag[\eta_{l+1}, \ldots, \tau_m]$, and W_i and $Z_i, i = 1, 2$, are partitons of W and Z of dimensions compatible with those of T_1 and T_2. We shall assume that $\eta \gg \eta_{l+1}$. In this case, it can happen that μ_2 is very large even if μ_1 is small, which means that the system stability is much more sensitive to simultaneous input and output uncertainties than to either uncertainty acting alone [Fre89a]. Assume that the gain in each subsystem given by partition (6.9) is uniform, i.e., $\bar{\sigma}[T_i] \approx \underline{\sigma}[T_i], i = 1, 2$. Then it is shown [Fre90] that to prevent μ_2 from being large, the compensator has to be chosen so that the closed-loop transfer functions satisfy

$$\bar{\sigma}[Z_1^H S_I] \bar{\sigma}[T_I Z_2] \ll 1 \qquad (6.2.10)$$

at frequencies for which the weighting product $| r_1 r_2 |$ is large.

Hence, if we apply a multivariable loop-shaping design method at the plant input and would like to have stability robustness against simultaneous input and output uncertainties or robust performance at the plant output, we must manipulate the loop shape to satisfy the condition (6.2.10) as well as possible in addition to meeting the design specifications at the plant input.

6.3   Properties of the LQ Regulators

The LQG/LTR procedure consists of two basic steps. The first step is called the target state feedback loop design. In this step a state feedback loop is designed to meet all stability and performance requirements. The second step is called the recovery procedure where an LQG/LTR compensator is designed to asymptotically recover the state feedback loop. The quality of recovery is governed by

107

the nonminimum phase characteristics of the plant [ZhF90]. Hence, to find an LQG/LTR compensator so that condition (6.2.10) is satisfied, it is necessary for the target state feedback loop to satisfy condition (6.2.10). In the following we shall re-examine some properties of the LQ regulators and use those properties to guide us in the LQ weighting selection so that the resulting state feedback loop satisfies condition (6.2.10).

Consider a state-space realization of the plant model $P(s)$

$$\dot{x}(t) = Ax(t) + Bu(t) \qquad (6.3.1)$$

$$y(t) = Cx(t) \qquad (6.3.2)$$

where $x(t) \in R^n$ is the state, $u(t) \in R^m$ is the control input, $y(t) \in R^m$ is the measured output. It is assumed that (C, A) is observable and (A, B) is controllable.

Suppose an LQ regulator is designed for the system. Hence the feedback law is given by

$$u(t) = -K_c x(t) \qquad (6.3.3)$$

where $K_c = R^{-1}B^T P$, and P is the unique positive definite solution of the Riccati equation

$$PA + A^T P - PBR^{-1}B^T P + H^T H = 0 \qquad (6.3.4)$$

In equation (6.3.4) H is a design parameter and is chosen such that (H, A) is observable and $R > 0$ is a given weighting matrix.

Denote the transfer function of the LQ-optimal state feedback loop by

$$L(s) \triangleq K_c \Phi(s) B \qquad (6.3.5)$$

108

where $\Phi(s) = (sI - A)^{-1}$, and let the corresponding sensitivity and complementary sensitivity functions be denoted by

$$S(s) = (I + L(s))^{-1} \tag{6.3.6}$$

and

$$T(s) = L(s)[I + L(s)]^{-1} \tag{6.3.7}$$

respectively. It is well known that $L(s)$ satisfies the following Kalman equality:

$$[I + L(j\omega)]^H R[I + L(j\omega)] = R + [H\Phi(j\omega)B]^H[H\Phi(j\omega)B] \tag{6.3.8}$$

Define the transfer function from control inputs to weighted states by

$$Q(s) \triangleq H(sI - A)^{-1}B \tag{6.3.9}$$

By an abuse of terminology we shall call $Q(s)$ a *weighting function*; our motivation for this nomenclature is that we shall shape properties of the optimal state feedback loop (6.3.5) by manipulating $Q(s)$. Denote the singular values of the matrix $M \in \mathbb{C}^{n \times n}$ by $\sigma_i[M]$; $i = 1, \ldots, n$.

Lemma 6.3.1: Suppose that $R = \rho I$ in (6.3.8). Then

(i) $$\sigma_i[I + L(j\omega)] = \sqrt{1 + (1/\rho)\sigma_i^2[Q(j\omega)]} \tag{6.3.10}$$

(ii) If u_i is a right singular vector of $Q(j\omega)$ associated with singular value $\sigma_i[Q(j\omega)]$, the u_i is also a right singular vector of $I + L(j\omega)$ associated with the singular value $\sigma_i[I + L(j\omega)]$.

Proof: Straightforward. ∎

109

The first part of this lemma is well-known (e.g. [DoS81]) and has been used extensively in multivariable loop-shaping via the LQG/LTR methodology. The second part appears to be less well known. We shall use this result to shape the right singular subspaces of the return difference function $I + L(j\omega)$, and thus the left singular subspaces of the sensitivity function (6.3.6).

Now suppose that the singular value decomposition of the weighting function (6.3.9) may be separated into high- and low-gain parts dimensioned compatibly with those of the plant (6.2.9):

$$Q = V_q \Sigma_q U_q = \begin{bmatrix} V_{q1} & V_{q2} \end{bmatrix} \begin{bmatrix} \Sigma_{q1} & 0 \\ 0 & \Sigma_{q2} \end{bmatrix} \begin{bmatrix} U_{q1}^H \\ U_{q2}^H \end{bmatrix} \qquad (6.3.11)$$

where $\Sigma_{q1} = diag[\sigma_1, \cdots, \sigma_l]$, $\Sigma_{q2} = diag[\sigma_{l+1}, \cdots, \sigma_m]$, and V_{qi} and U_{qi} are partitions of V_q and U_q whose dimension are compatible with those of Σ_{q1} and Σ_{q2}.

Proposition 6.3.2: Assume that $R = \rho I$, and suppose that the weighting function (6.3.11) satisfies

$$\underline{\sigma}[\Sigma_{q1}]/\sqrt{\rho} \gg 1 \qquad (6.3.12)$$

and

$$U_{qi} = Z_i , \; i = 1, 2 \qquad (6.3.13)$$

Then the state feedback sensitivity function (6.3.6) satisfies

$$\bar{\sigma}[Z_1^H S] \ll 1 \qquad (6.3.14)$$

∎

Proof: It follows from (6.3.11) and Lemma 6.3.1 that the singular value de-

110

composition of the return difference matrix can be written as

$$I + L = \begin{bmatrix} V_1 & V_2 \end{bmatrix} \begin{bmatrix} \Sigma_1 & 0 \\ 0 & \Sigma_2 \end{bmatrix} \begin{bmatrix} Z_1^H \\ Z_2^H \end{bmatrix} \qquad (6.3.15)$$

where $\Sigma_1 = diag[\sqrt{1 + \sigma_1^2/\rho}, \ldots, \sqrt{1 + \sigma_l^2/\rho}]$, $\Sigma_2 = diag[\sqrt{1 + \sigma_{l+1}^2/\rho}, \ldots, \sqrt{1 + \sigma_m^2/\rho}]$, and $V = \begin{bmatrix} V_1 & V_2 \end{bmatrix}$ is a unitary matrix. Hence the singular value decomposition of (6.3.6) is

$$S = (I + L)^{-1} = \begin{bmatrix} Z_1 & Z_2 \end{bmatrix} \begin{bmatrix} \Sigma_1^{-1} & 0 \\ 0 & \Sigma_2^{-1} \end{bmatrix} \begin{bmatrix} V_1^H \\ V_2^H \end{bmatrix} \qquad (6.3.16)$$

The result follows from (6.3.12).   ∎

Recall that the complementary sensitivity function of the LQ state feedback loop must satisfy $\bar{\sigma}[T(j\omega)] < 2$, $\forall \omega$ (e.g. [DoS81]). It follows from this fact and (6.3.14) that if the plant is minimum phase so that the LTR procedure may be successfully applied, then we can insure that (6.2.10) holds by requiring that (6.3.12-13) hold.

It is not possible to require that (6.3.14) hold at all frequencies, because this condition requires that some open-loop gains be large. In particular, it is not possible for loop gains to be large at high frequencies. In such situations, an alternate approach is to require that $\bar{\sigma}[T_I Z_2] \ll 1$. (Recall that $\bar{\sigma}[S(j\omega)] < 1$, $\forall \omega$.) This may be accomplished, for a minimum phase weighting $Q(s)$, by using cheap state feedback control. The following result is well-known (e.g. [DoS81]).

Lemma 6.3.3: Let $R = \rho I$ in (6.3.8), and suppose that $Q(s)$ in (6.3.9) is minimum phase. Then as $\rho \to 0$, the state feedback loop transfer function satisfies, at each frequency,

$$L(j\omega) \longrightarrow (1/\sqrt{\rho})WQ(j\omega) \qquad (6.3.17)$$

111

when W is a unitary matrix. ∎

This result shows that asymptotically the open-loop state feedback singular values satisfy $\sigma_i[L(j\omega)] \approx \sigma_i[Q(j\omega)]/\sqrt{\rho}$ and the right singular subspaces of L are approximately equal to those of Q. Suppose that Q has the form (6.3.11), where $\mathcal{U}_{qi} = Z_i, i = 1, 2$, and $\bar{\sigma}[\Sigma_{q2}(j\omega)]/\sqrt{\rho} \ll 1$. Then it follows from the results of [FrL86], [Fre90] that the state feedback complementary sensitivity function satisfies $\bar{\sigma}[T(j\omega)Z_2] \ll 1$. Again, if the plant is minimum phase, we can apply the LTR procedure so that the (6.2.10) holds.

Hence, by properly choosing the weighting $Q(s)$ in the state feedback loop design, the LQG/LTR procedure can be applied to achieve stability robustness against simultaneous input and output uncertainties.

6.4 Weighting Selection in the LQG/LTR Procedure

We can see from previous discussions that one way to meet requirement (6.2.10) in the LQG/LTR design is to choose the LQ weighting function $Q(s)$ so that it has the same spread in gains and the same corresponding right singular subspaces as the plant.

It is clear that if we let $H = C$, then $Q(s) = C(sI - A)^{-1}B = P(s)$ and the above requirements on $Q(s)$ are trivially satisfied. This is the simplest way to achieve the requirements. However, it restricts the loop shapes we can have at the input loop-breaking point. To have more freedom in selecting the loop shape at plant input, we have to augment proper dynamics to the plant.

1. Dynamics Augmentation at the Plant Output

One way to augment the plant is to add extra dynamics at the plant output (see Figure 6.2). In this case the augmented system can be described by

$$\left[\begin{array}{c} \dot{x} \\ \dot{x}_w \end{array} \right] = A_a \left[\begin{array}{c} x \\ x_w \end{array} \right] + B_a u, \ \tilde{y} = C_a \left[\begin{array}{c} x \\ x_w \end{array} \right] \tag{6.4.1}$$

where

$$A_a = \left[\begin{array}{cc} A & 0 \\ B_w C & A_w \end{array} \right], \ B_a = \left[\begin{array}{c} B \\ 0 \end{array} \right], \ C_a = \left[\begin{array}{cc} 0 & C_w \end{array} \right] \tag{6.4.2}$$

and $W(s) := C_w(sI - A_w)^{-1}B_w$ is the dynamics we add to the plant. If we select $H = [0 \ C_w]$, then the singular value and singular vector properties of the resultant LQ feedback loop are essentially determined by the augmented plant. This can be verified by writing down the Equation (6.3.8) for the augmented system with the above weighting and using Lemma 6.3.1. We can see in this case that $Q(s) = H(sI - A_a)^{-1}B_a = W(s)P(s)$. Hence, $W(s)$ should be chosen such that the product $W(s)P(s)$ preserves the right singular subspace structure and the spread in gains of the plant $P(s)$ and such that $W(s)P(s)$ has the desired loop shape. The following are some suggestions in how to choose $W(s)$.

(1) The plant $P(s)$ is ill-conditioned at all frequencies, i.e., the partition (6.2.9) holds at all frequencies. In this case, we may choose $W(s)$ to be

$$W(s) = g(s)I$$

where $g(s)$ is a stable minimum phase transfer function that can be used to manipulate the loop shape at the plant input. If the matrix of plant left singular vectors W can be well approximated by a constant real matrix, [3] say $\tilde{W}$, then

---
[3] When W varies sufficiently slowly with frequency, it can usually be well approximated by a real matrix. Techniques of approximating a complex matrix by a real matrix can be found in [MaK77], [EdK79].
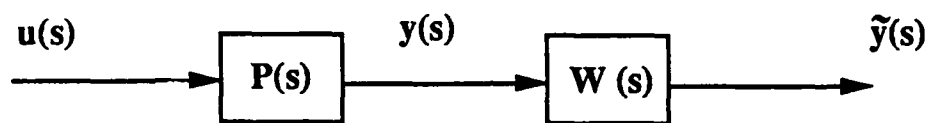
Figure 6.2: Augmenting the Plant at the Output

we may let $W(s)$ be of the following form.

$$W(s) = diag[g_1(s), g_2(s), \ldots, g_m(s)]\tilde{W}^T$$

where scalar transfer functions $g_i(s)$, $i = 1, 2, \ldots, m$, are selected to be stable and minimum phase. They can be manipulated to achieve their desired loop shape.

(2) The plant $P(s)$ is ill-conditioned only around some frequency ω_0, i.e., the partition (6.2.9) holds only around frequency ω_0. A procedure to obtain the desired augmenting dynamics is as follows:

  (i) Compute the singular value decomposition of $P(j\omega_0)$ to obtain its left singular matrix W.

 (ii) Approximating W by a real matrix $\tilde{W}$.

(iii) Select scalar transfer functions $g_i(s)$, $i = 1, 2, \ldots, m$, such that they are stable and minimum phase. They can be manipulated to achieve the desired loop shape at $s = j\omega_0$.

(iv) Form the augmenting dynamics $W(s)$ as follows

$$W(s) = diag[g_1(s), g_2(s), \ldots, g_m(s)]\tilde{W}$$

 (v) Manipulate free parameters in $g_i(s)$ to achieve desired loop shape for $W(s)P(s)$.

The weighting selection procedure will be repeated in the LQG/LTR design until a satisfactory result is obtained.

2. Formal Loop Shaping

This dynamics augmentation procedure is adopted from [StA87], [Enn84] which makes it very easy to manipulate the loop shape at one loop breaking point. Suppose that the plant is stable and the desired loop shape at the plant input can be denoted by $W(s) = C_w(sI - A_w)^{-1}B_w$. If the plant is augmented as in Figure 6.3, then the state space representation of the augmented plant is given by

$$A_a = \begin{bmatrix} A & 0 \\ 0 & A_w \end{bmatrix}, \ B_a = \begin{bmatrix} B \\ B_w \end{bmatrix}, \ C_a = \begin{bmatrix} C & 0 \end{bmatrix} \qquad (6.4.3)$$

The LQ optimal feedback gain for the augmented system is obtained by solving the Riccati equation (6.3.4) with the weighting matrices being chosen as $R = I$ and $H = [0 \ C_w]$.

As we have shown in the previous sections, feedback properties of the resultant state feedback system are basically determined by the weighting $Q(s) = H(sI - A_a)^{-1}B_a = C_w(sI - A_w)^{-1}B_w$. Note that by selecting different A_w, B_w, C_w, we now have complete freedom in specifying the weighting function $Q(s)$. To illustrate how to select $Q(s)$, we again consider the following two cases.

(1) The plant $P(s)$ is ill-conditioned at all frequencies. In this case we may select

$$Q(s) = g(s)P(s)$$

The scalar transfer function $g(s)$ can be manipulated to obtain satisfactory loop shape at the plant input. Such a selection trivially implies that high gain/low gain structure of P is present in Q.

(2) The plant $P(s)$ is ill-conditioned only around some frequency ω_0. In this

116
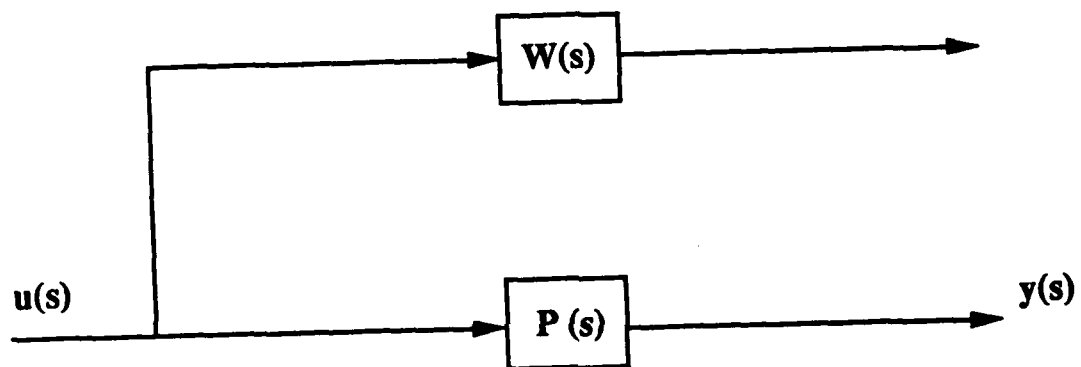
Figure 6.3: Formal Loop Shaping

case, an algorithm to obtain the desired weighting function is as follows:

(i) Compute the singular value decomposition of $P(j\omega_0)$ to obtain its right singular matrix Z.

(ii) Approximate Z by a real matrix $\tilde{Z}$.

(iii) Select stable transfer functions $g_i(s)$, $i = 1, 2, \ldots, m$, so that $\mid g_i(j\omega) \mid$ resembles the desired loop shapes at the plant input, $\mid g_i(j\omega) \mid \geq \mid g_k(j\omega) \mid$, if $i \geq k$ and $\mid g_l(j\omega_0) \mid / \mid g_{l+1}(j\omega_0) \mid \approx \kappa[P(j\omega_0)]$.

(iv) Form the weighting function $Q(s)$ as follows

$$Q(s) = diag[g_1(s), g_2(s), \ldots, g_m(s)]\tilde{Z}^H$$

Again, the weighting selection procedure will be repeated in the LQG/LTR design until a satisfactory result is obtained. Comparing with the output dynamics augmentation, the formal loop shaping method gives us more flexibility in manipulating the loop shapes to achieve design specifications. However, it usually results in higher order controllers. As regards to which dynamics augmantation procedure should be followed, the selection may be based on whether the right or the left singular vectors can be better approximated by real vectors.

6.5 Design Examples

In this section, we illustrate the results of previous sections by designing a LQG/LTR compensator for two aircraft control problems.

Example 6.5.1 We first consider the aircraft control problem studied in [Ste84]. The plant has two inputs and two outputs, and it is stable and minimum phase. It has strong directionality properties that vary with frequency. The problem formulation is the same as the one in Section 6.2. The state space representation of the plant is given by

$$A = \begin{bmatrix} -0.0226 & -36.6000 & -18.9000 & -32.1000 \\ 0.0000 & -1.9000 & 0.9830 & 0.0000 \\ 0.0123 & -11.7000 & -2.6300 & 0.0000 \\ 0.0000 & 0.0000 & 1.0000 & 0.0000 \end{bmatrix}$$

$$B = \begin{bmatrix} 0.0000 & 0.0000 \\ -0.4140 & 0.0000 \\ -77.8000 & 22.4000 \\ 0.0000 & 0.0000 \end{bmatrix}, \quad C = \begin{bmatrix} 0.0000 & 57.3000 & 0.0000 & 0.0000 \\ 0.0000 & 0.0000 & 0.0000 & 57.3000 \end{bmatrix}$$

The uncertainty is as described in (6.2.1) and (6.2.2) with weighting functions given by

$$r_1(s) = \frac{s + 100}{200}$$
$$r_2(s) = \frac{s + 3}{2(s + 0.03)}$$

Plots of the plant singular values and condition number are given in Figure 6.4-5. Note that the plant is ill-conditioned. Plots of weighting functions $r_1(s)$ and $r_2(s)$ are given in Figure 6.6.

Our objective is to design an LQG/LTR compensator with the property that $\mu[M(j\omega)] < 1/\gamma, \forall \omega$, for γ as large as possible. We shall try to achieve this by manipulating the bounds for $\mu[M]$, i.e., the quantities μ_1 and μ_2. From the discussion of Section 6.2 and 6.3, it follows that as long as Q shares the high gain/low gain structure of the plant, we can simply simply concentrate on making μ_1 small. The weighting selection can be judged by the structured singular value plots of the resulting design.
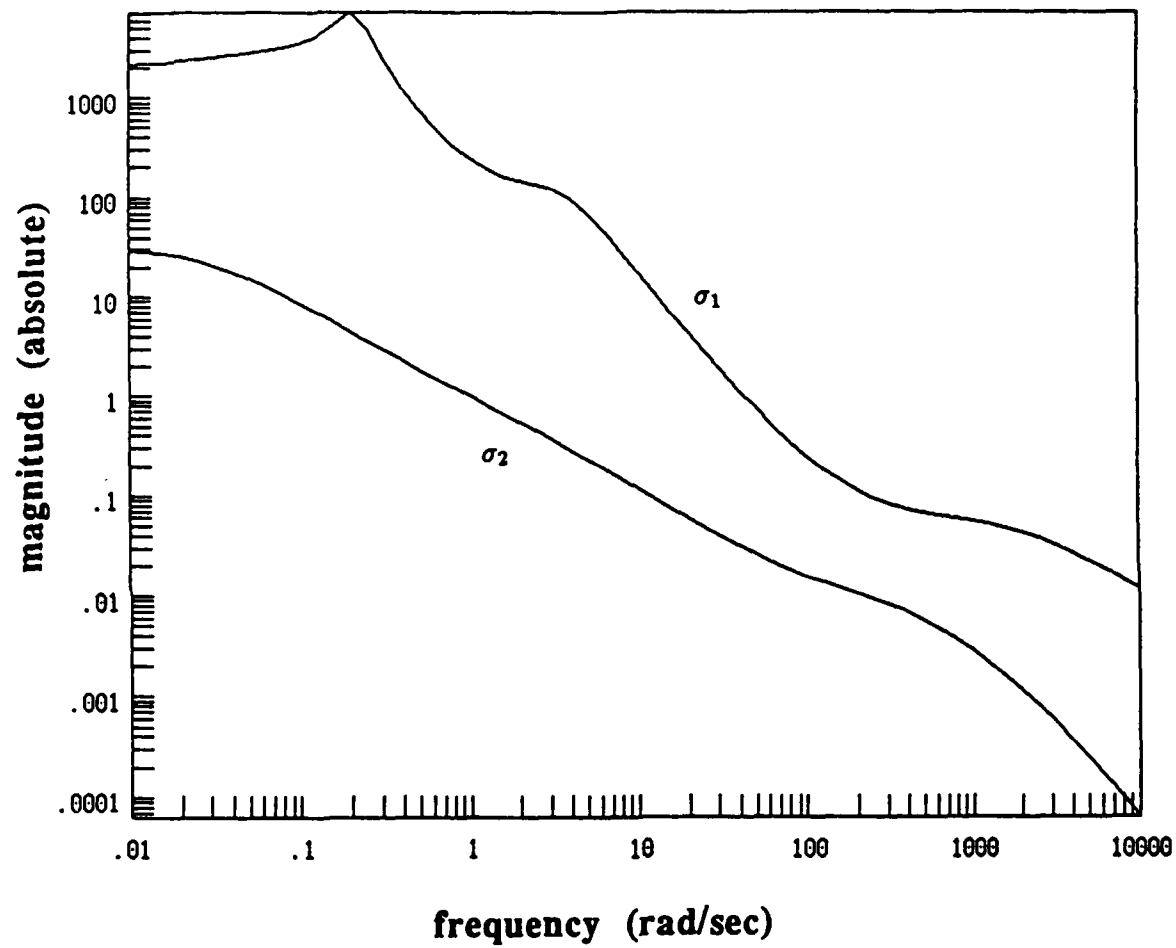
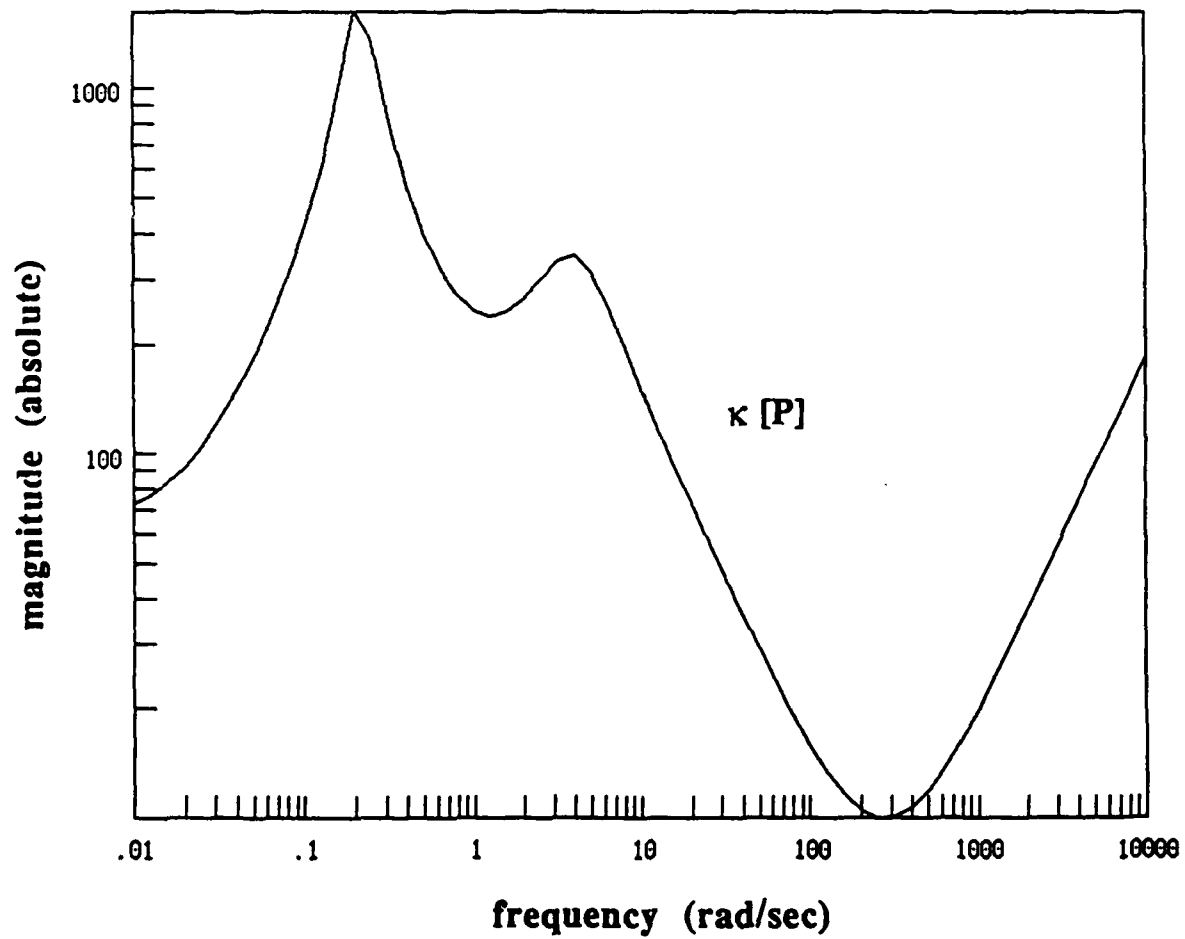Figure 6.4: Plant Singular Values, Example 6.5.1

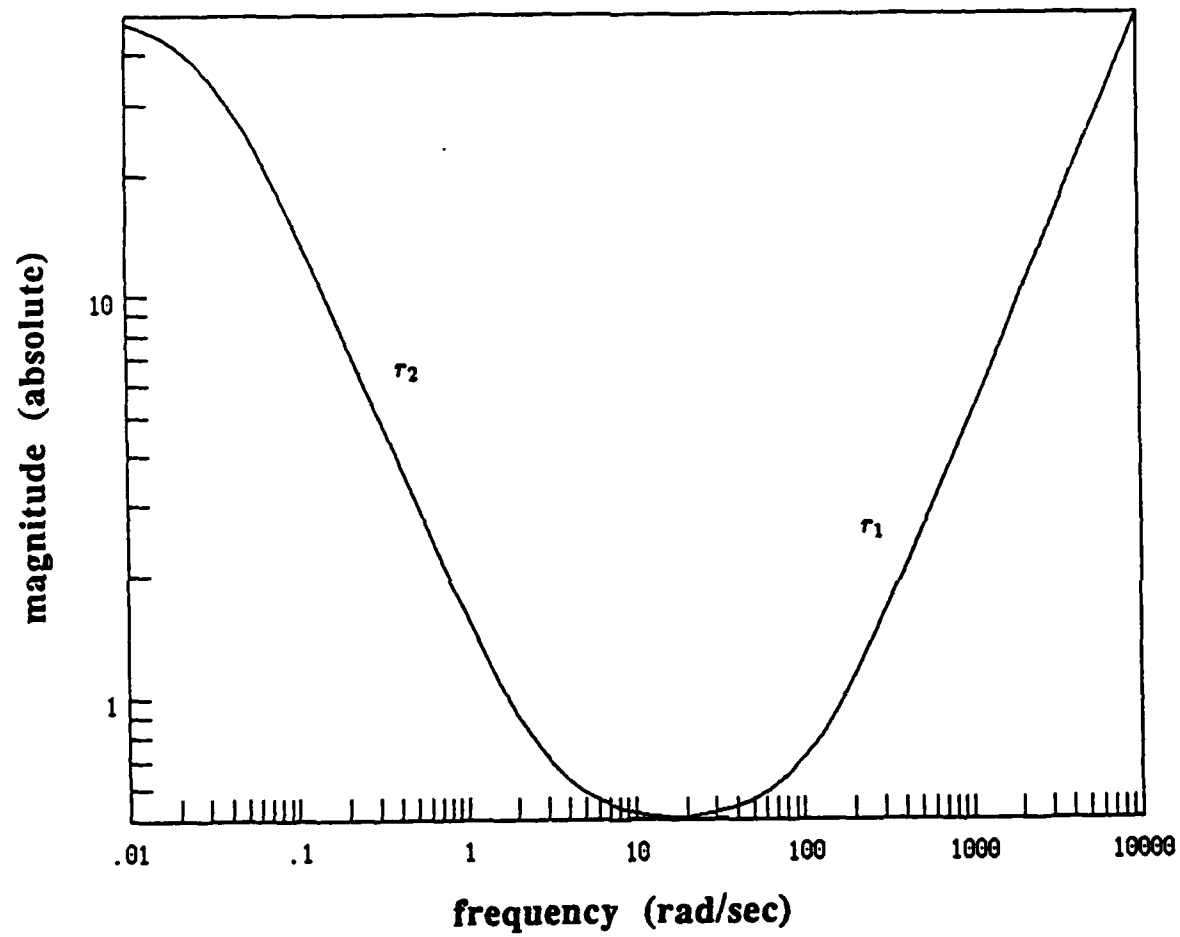Figure 6.5: Plant Condition Number, Example 6.5.1

Figure 6.6: Weighting Functions, Example 6.5.1

For our case, we first augment the plant by a scalar factor

$$g(s) = 5 \cdot \frac{s+1}{s+0.03} \cdot \frac{s+100}{s+2000}$$

at the plant output. This will not change the gain spread in each loop and the plant condition number remains the same.

The target state feedback loop is obtained from (6.3.3) and (6.3.4) with A, B, C replaced by A_a, B_a, C_a and $R = I$ and $H = C_a$. The loop-transfer recovery is obtained using the Kalman filter with the parameter $q^2 = 1000$. The structured singular value of the resulting design is given in Figure 6.7. One can see that for this design, $\mu[M(j\omega)] < 1.26, \forall \omega$, i.e., the system will remain stable for simultaneous input and output uncertainties whose magnitudes are less than $\frac{1}{1.26} \approx 0.8$. Hence, a decent result can be obtained throug` `he relatively simple LQG/LTR procedure.

Example 6.5.2 We now consider the drone lateral attitude control problem studied by Ridgely and Banda [RiB86]. We shall use this example to illustrate that when the plant is ill-conditioned, the singular value balancing method suggested in [Ath86] may result in a nonrobust design. The state space representation of the plant is given by

$$A = \begin{bmatrix} -0.08527 & -0.0001423 & -0.9994 & 0.04142 & 0 & 0.1862 \\ -46.86 & -2.757 & 0.3896 & 0 & -124.3 & 128.6 \\ -0.4248 & -0.06224 & -0.06714 & 0 & -8.792 & -20.46 \\ 0 & 1 & 0.0523 & 0 & 0 & 0 \\ 0 & 0 & 0 & 0 & -20 & 0 \\ 0 & 0 & 0 & 0 & 0 & -20 \end{bmatrix}$$

$$B = \begin{bmatrix} 0 & 0 & 0 & 0 & 20 & 0 \\ 0 & 0 & 0 & 0 & 0 & 20 \end{bmatrix}^T, \quad C = \begin{bmatrix} 1 & 0 & 0 & 0 & 0 & 0 \\ 0 & 0 & 0 & 1 & 0 & 0 \end{bmatrix}$$
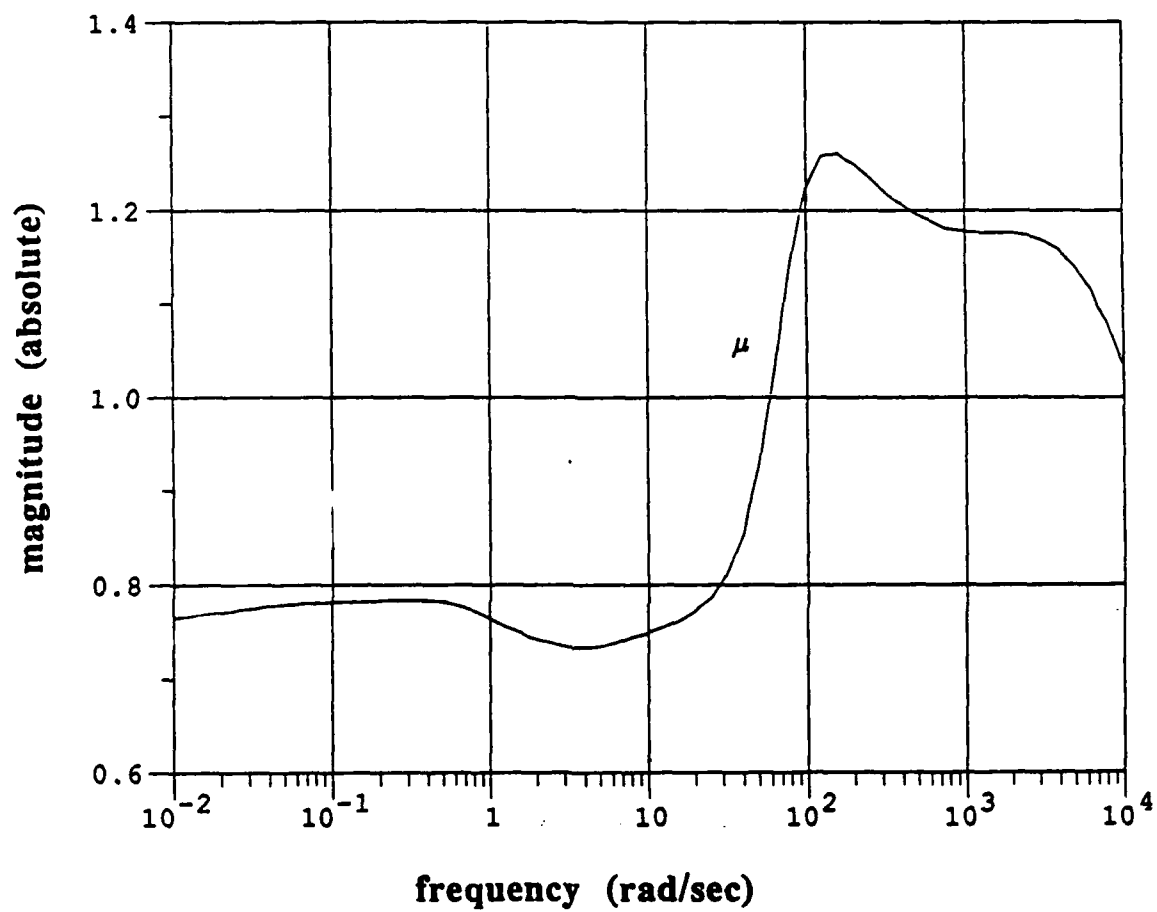
Figure 6.7: Structured Singular Value, Example 6.5.1

124

The plant is minimum phase, but unstable. The design specifications can be represented by the following weighting functions on the input and output uncertainties

$$r_1(s) = \frac{0.5s + 1}{10}$$

$$r_2(s) = \frac{0.5(s + 2)}{s}.$$

Plots of the plant singular values and condition number are given in Figures 6.8-9. Note that the plant is ill-conditioned. Plots of weighting functions $r_1(s)$ and $r_2(s)$ are given in Figure 6.10.

First, we examine two designs given in [RiB86]. Design 1 (see Table 13.6 in [RiB86]) uses the singular value balancing method where the plant is augmented by adding an integrator in each loop and the weighting function in the LQ design was chosen in such a way that the singular values of the state feedback loop were squeezed together at low frequencies. The authors of [RiB86] noticed that even though this design satisfied design specifications at the plant input, it failed to meet design specifications at the plant output. Design 2 (see Table 13.7 in [RiB86]) also augments the plant by adding an integrator in each loop. In this case the weighting functions in the LQ design is simply chosen as the plant, i.e., $Q(s) = C(sI - A)^{-1}B$ in our notation. The authors of [RiB86] noticed that, for this design, the design specifications were not only satisfied at the plant input but also at the plant output. Using our results in previous sections, we are able to explain the above observations. Clearly, the weighting selection in Design 2 happens to satisfy the directionality requirements, hence the resulting design meets condition (6.2.10), which implies a robust design against both input and
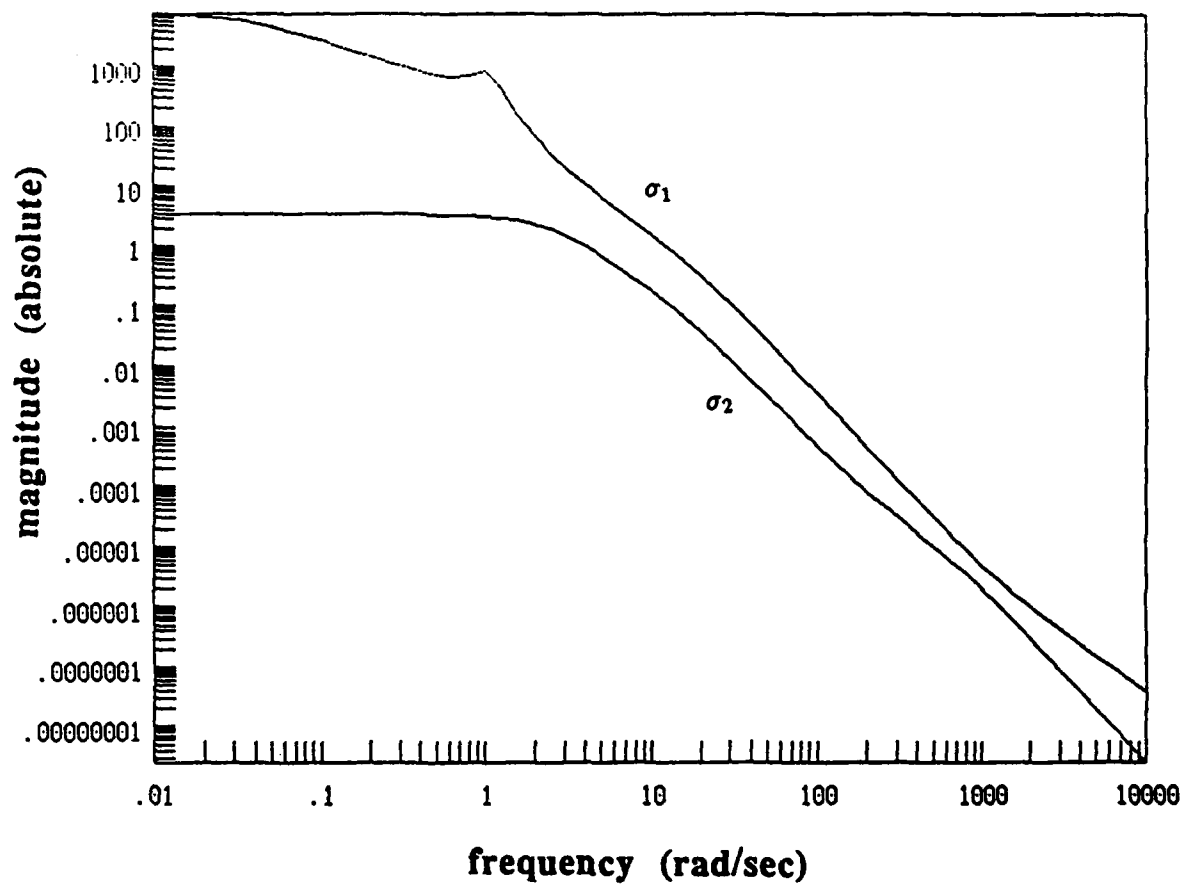
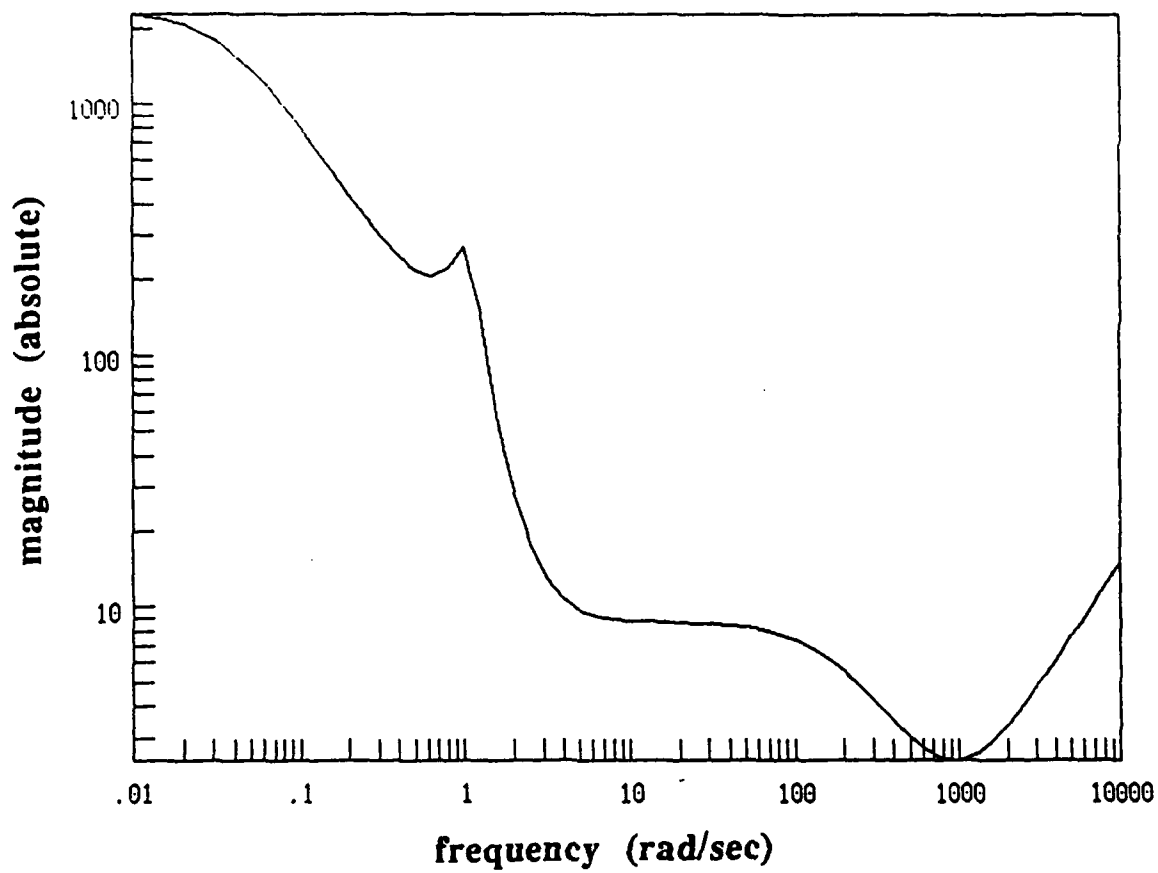Figure 6.8: Plant Singular Values, Example 6.5.2

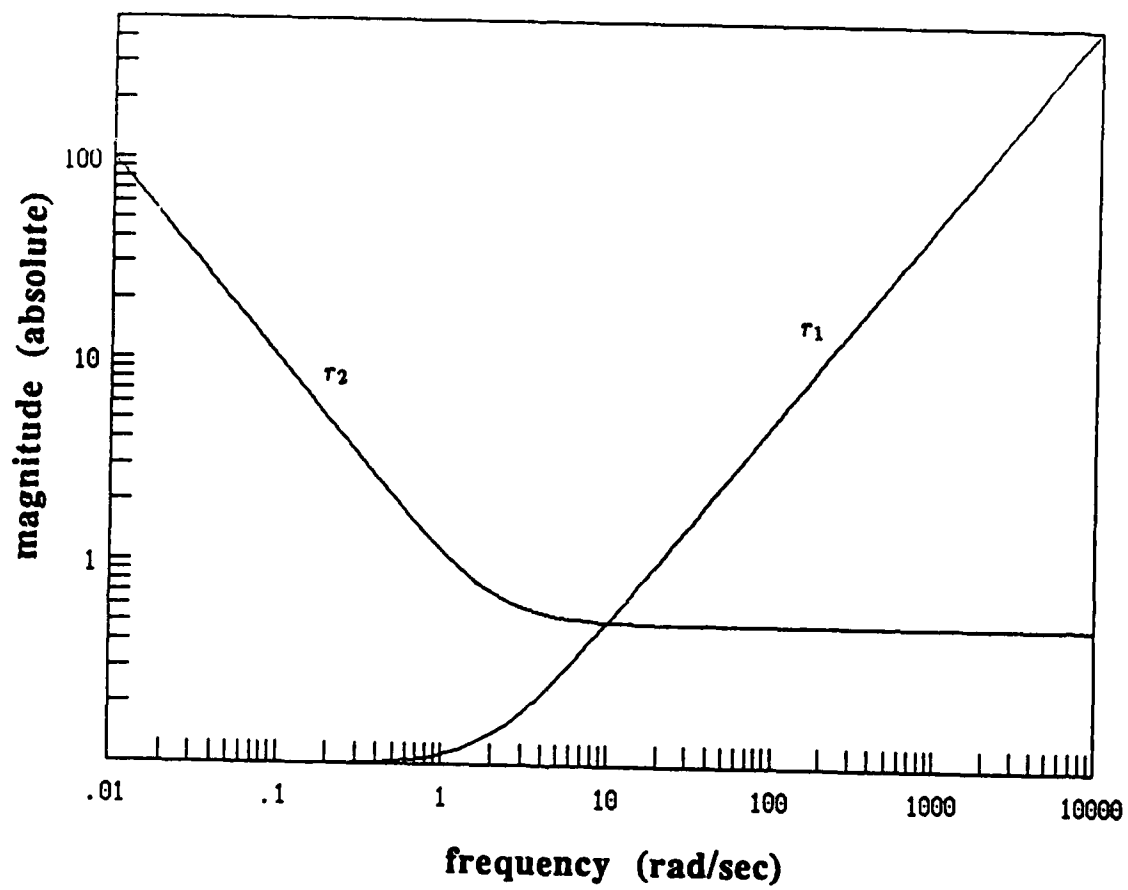Figure 6.9: Plant Condition Number, Example 6.5.2

Figure 6.10: Weighting Functions, Example 6.5.2

output uncertainties. On the other hand, since the weighting selection of Design 1 does not meet these directionality conditions and the plant is ill-conditioned, it is not surprising that Design 1 results in a nonrobust design. In Figures 6.11-12, we plot the bounds for the structured singular values of the two designs. One can see that Design 1 indeed has much larger structured singular values than Design 2.

Next, we illustrate that, by adding a little more dynamics to the plant output, we can further improve Design 2. We first augment the plant by a scalar factor

$$g(s) = \frac{10(s+2)(s+3)}{s(s+200)}$$

at the plant output. The target state feedback loop is obtained from (6.3.3) and (6.3.4) with A, B, C replaced by A_a, B_a, C_a and $R = I$ and $H = C_a$. This weighting selection satisfies the directionality criteria. The loop-transfer recovery is obtained using the Kalman filter with the parameter $q = 1000$. The bounds for structured singular values of the resulting design is given in Figure 6.13. One can see that for this design, the upper bound for $\mu[M(j\omega)]$ is less than 1.65, $\forall \omega$, while the lower bound for $\mu[M(j\omega)]$ of Design 2 is greater than 1.7 at some frequencies.

6.6   Concluding Remarks

In this chapter, we have considered the problem of obtaining stability robustness in the presence of simultaneous input and output uncertainties. We demonstrate how the LQG/LTR design methodology can be effectively applied to this problem. The key in the application is the weighting selection in the LQ optimal state feedback loop design. It is shown that the right singular subspaces of the return
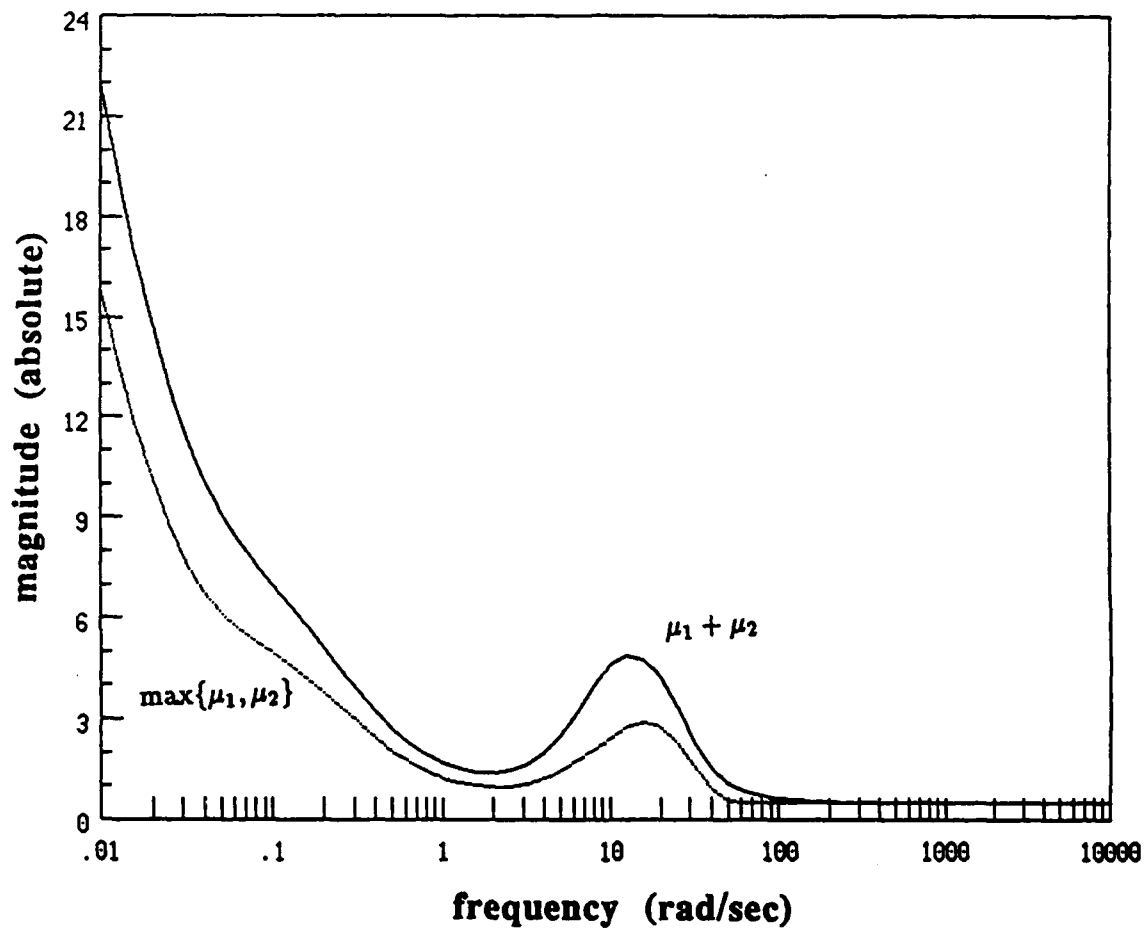
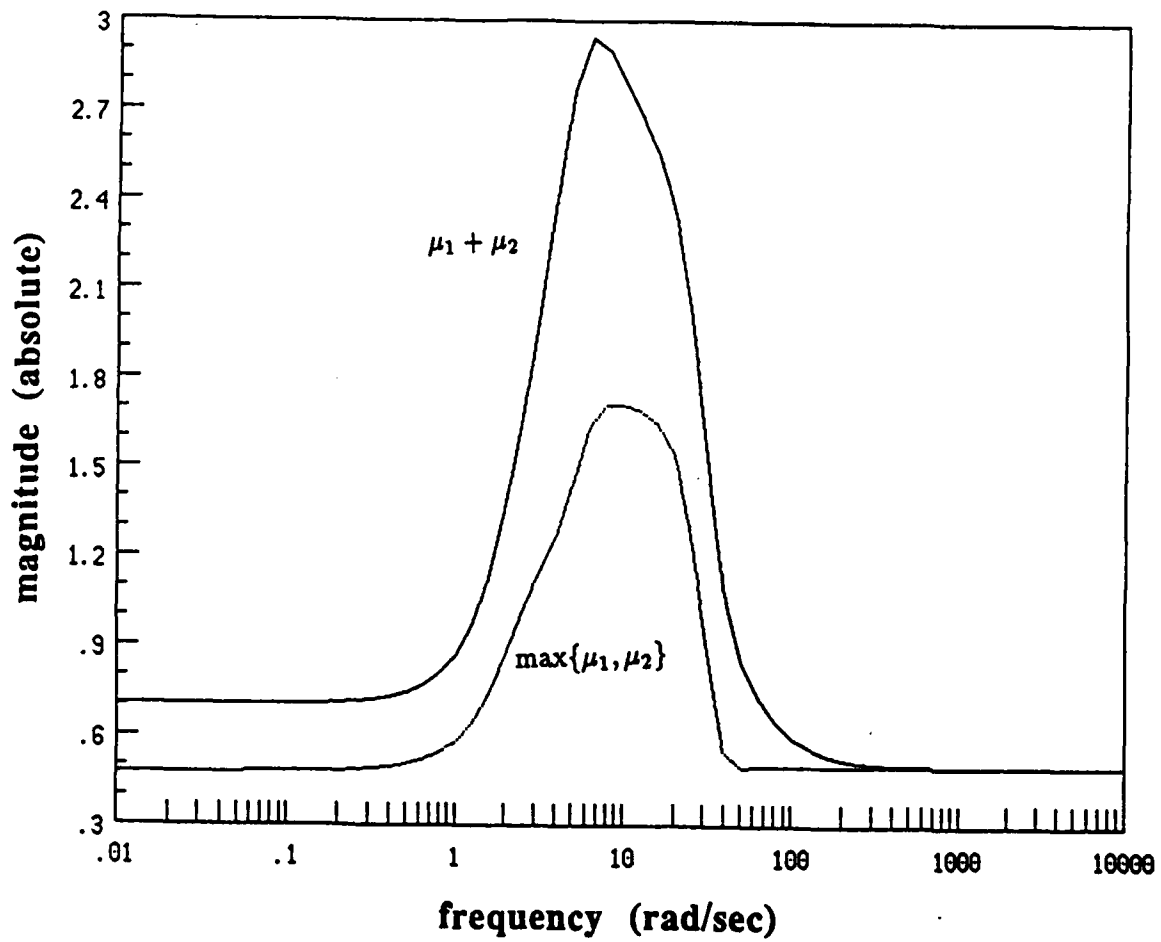Figure 6.11: Bounds for SSV, Design 1, Example 6.5.2

130

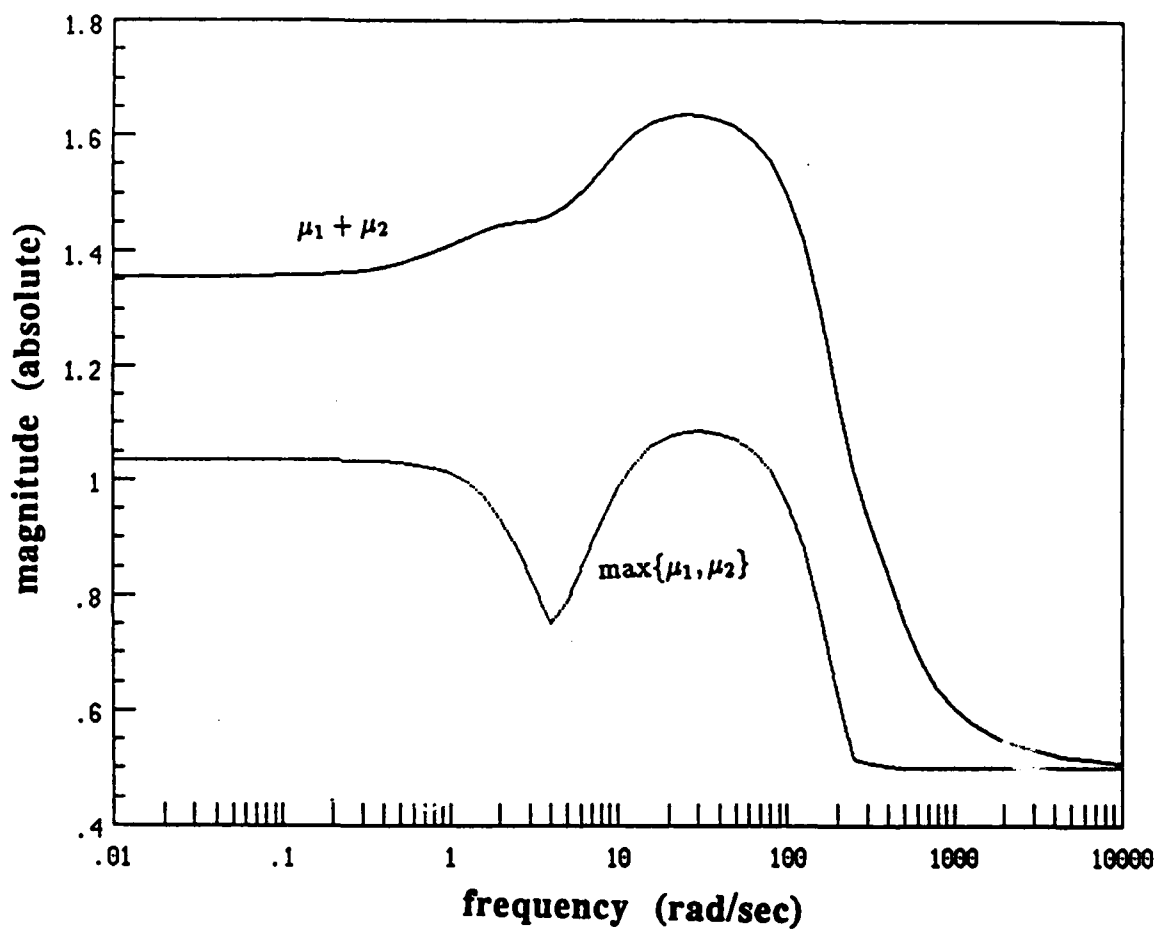Figure 6.12: Bounds for SSV, Design 2, Example 6.5.2

131

Figure 6.13: Bounds for SSV, Design 3, Example 6.5.2

difference matrix of the target LQ optimal state feedback loop are uniquely determined by that of the weighting functions of the LQ design. This provides an effective means to obtain a compensator which achieves the loop-shaping conditions derived in [Fre90]. To achieve stability robustness against simultaneous input and output uncertainties, the singular subspace structure of the plant must be taken into account in the weighting selection. Hence, both singular values and singular subspace structures of the loop-transfer functions should be manipulated to achieve a satisfactory design.

Chapter 7

Conclusions and Recommendations for Future Research

A number of problems remain before a satisfactory robust multivariable design methodology is available. Some of these problems are now described.

It appears that ill-conditioned plants may be inherently difficult to robustly control for some classes of uncertainty. However, the size of the plant condition number depends upon the units chosen with which to measure the plant input and output signals. This fact is somewhat disturbing, as inherent difficulty of a design problem should be independent of units. A little thought, however, suggests that changing units to reduce the size of the plant condition number may increase the size of the plant uncertainty. Hence the difficulty of the design problem would be preserved under scaling. Further research is necessary to resolve this matter.

The results described above focus on analyzing system properties at a fixed

frequency. Yet it is crucial to understand design tradeoffs that must be performed between system properties in different frequency ranges. For example, it appears that the inherent difficulty associated with ill-conditioned plants takes the form of a frequency dependent design tradeoff. A tentative conjecture is that the loop singular values must be separated by an amount proportional to the plant condition number, and that the requirement for this separation aggravates the tradeoff imposed by the Bode gain-phase relation. Verifying this conjecture seems to require use of the multivariable gain-phase relations developed in [FrL:88].

Design limitations that are due to unstable poles and nonminimum phase zeros are fundamental in classical control design. These tradeoffs are governed by integral relations. An important avenue of research is to extend these results to multivariable systems using the mathematical tools developed in [FrL88].

The preceding analysis problems, and others, appear to lie at the heart of understanding multivariable design tradeoffs. Once such an understanding is available, it will be possible to incorporate it into design methodologies. This should proceed along two lines. First, for systems with two or three inputs and outputs it should be possible to develop a direct multivariable loop-shaping methodology. Secondly, as was done in Chapters 5 and 6 of this report, methods must be found to manipulate feedback properties expeditiously through weighting function selection for formal synthesis procedures.

Chapter 8

References

[Ath86] M. Athans, "A Tutorial on the LQG/LTR Method," *Proc. American Contr. Conf.*, pp. 1289-1296, Seattle, WA, June 1986.

[BJG73] Å. Björck and G. H. Golub, "Numerical Methods for Computing Angles Between Linear Subspaces," *Mathematics of Computation*, vol. 27, no. 123, pp. 579-594, July 1973.

[Bri66] E. H. Bristol, "On a New Measure of Interaction for Multivariable Process Control," *IEEE Trans. Aut. Contr.*, vol. AC-11, pp. 133-134, Jan. 1966.

[ChF89a] Chen and J.S. Freudenberg, "Robust Performance with Respect to Diagonal Input Uncertainty," *Proc. 28th IEEE Conf. on Decision and Contr.*, Tampa, Florida, Dec. 1989, also submitted to *IEEE trans. Auto. Contr.*.

[ChF89b] J. Chen and J.S. Freudenberg, "Robust Performance in the Presence of Additive and Multiplicative Uncertainties," *Proc. 1989 Allerton Conf.*, Monticello, Illinois, Sept. 1989.

[ChF89c] J. Chen and J. S. Freudenberg, "Bounds on the Three-Block Structured Singular Value," *7th Annual OSU Control Workshop*, Columbus, OH, April 1989, also submitted to *Contr.-Theory and Advanced Technology*.

[ChF90] J. Chen and J.S. Freudenberg, "Robustness Problems with Several Sources of Modelling Uncertainty," to appear, American Control Conference, 1990.

[Dem88] J. Demmel, "On Structured Singular Values," *Proc. 27th IEEE Conference on Decision and Control*, Austin, Texas, 2138-2143, 1988.

[DGK89] J.C. Doyle, K. Glover, P.P. Khargonekar, and B.A. Francis, "State-Space Solutions to Standard H^2 and H^∞ Control Problems" *IEEE Trans. on Automatic Control*, vol. AC-34, no. 8, pp. 831-847, 1989.

[DLP86] J.C. Doyle, K. Lenz, and A. Packard, "Design Examples Using μ-synthesis: Space Shuttle Lateral Axis FCS During Reentry. *Proc. 25th IEEE Conference on Decision and Control*, Athens, Greece, 2218-2223.

[DoS81] J. C. Doyle and G. Stein, "Multivariable Feedback Design: Concept for a Classical/Modern Synthesis," *IEEE Trans. Aut. Contr.*, vol. AC-26, pp. 4-16, Feb. 1981.

[Doy82] J. C. Doyle, "Analysis of Feedback Systems with Structured Uncertainties," *IEE Proc.*, vol. 129, Pt.D, no. 6, pp. 242-250, Nov. 1982.

[Doy85] J. C. Doyle, "Structured Uncertainty in Control System Design," *Proc. 24th IEEE Conf. on Decision and Contr.*, pp. 260-265, Ft. Lauderdale, Florida, Dec. 1985.

[Doy87] J.C. Doyle, *Lecture Notes of Workshop on Robust Multivariable Control*, Minneapolis, MN, June 1987.

[DWS82] J. C. Doyle, J. E. Wall, and G. Stein, "Performance and Robustness Analysis for Structured Uncertainty," *Proc. 21st IEEE Conf. on Decision and Contr.*, pp. 629-636, Orlando, Florida, Dec. 1982.

[EdK79] J. Edmund and B. Kouvaritakis, "Extensions of the Frame Alignment Technique and Their Use in the Characteristic Locus Design Method," *Int. J. Control*, vol. 29, no. 5, pp. 787-796, 1979.

[Enn84] D. Enns, "Model Reduction for Control System Design," Ph.D. dissertation, Stanford Univ., Standard, CA, June 1984.

[Enn87] D. F. Enns, "Multivariable Flight Control for an Attack Helicoptor," *IEEE Contr. Systems Magazine*, pp. 34-38, April 1987.

[FaT86] M.D.H. Fan and A. Tits, "Characterization and Efficient Computation of the Structured Singular Value," *IEEE Trans. Aut. Contr.*, vol. AC-31, pp. 734-743, 1986.

[FaT88] M.K.H. Fan and A. Tits, "Characterization and Efficient Computation of the Structured Singular Value," *IEEE Trans. Aut. Contr.*, vol. AC-33, pp. 284-289, 1988.

[FLC82] J.S. Freudenberg, D.P. Looze and J.B. Cruz, "Robustness Analysis Using Singular Value Sensitivities," *Int. J. Control*, vol. 35, no. 1, pp. 95, 1982.

[Fra87] B.A. Francis, *A Course in H_∞ Control Theory*, Lecture Notes in Control and Information Sciences, No. 88, Springer-Verlag, Berlin, 1987.

[Fre89a] J.S. Freudenberg, "Analysis and Design for Ill-Conditioned Plants, Part 1: Lower Bounds on the Structured Singular Value." *Int. J. Control*, 49, 851-871, March 1989.

[Fre89b] J.S. Freudenberg, "Analysis and Design for Ill-Conditioned Plants, Part 2: Directionally Uniform Weightings and an Example." *Int. J. Control*, 49, 873-903, March 1989.

[Fre90] J.S. Freudenberg, "Plant Directionality, Coupling and Multivariable Loop-Shaping," To appear, *Int. J. Contr.*, 1990.

[FrL86] J. S. Freudenberg and D. P. Loose, "The Relation Between Open Loop and Closed Loop Properties of Multivariable Feedback Systems," *IEEE Trans. Aut. Contr.*, vol. AC-31, no. 4, pp. 333-340, April 1986.

[FrL88] J. S. Freudenberg and D. P. Loose, *Frequency Domain Properties of Scalar and Multivariable Feedback Systems*, Springer-Verlag Lecture Notes in Control and Information Sciences, 1988.

[GoV83] G. H. Golub and C. F. Van Loan, *Matrix Computations*, Baltimore, MD: Johns Hopkins Univ. Press, 1983.

[HBG79] G.L. Hartmann, M.F. Barrett, and C.S. Greene, "Control Design for an Unstable Vehicle," Contract Report NAS 4-2578, NASA Dryden Flight Research Center, December 1979.

[Hel88] W. Helton, "A Numerical Method for Computing the Structured Singular Value," *Sys. and Contr. Letters*, vol. 10, pp. 21-26, 1988.

[HuM82] Y.S. Hung and A.G.J. MacFarlane, *Multivariable Feedback: A Quasi-Classical Approach*, Lecture Notes in Control and Information Sciences, vol. 40, Springer-Verlag, Berlin, 1982.

[Kai80] T. Kailath, *Linear Systems*, Englwood Cliffs, NJ: Prentice-Hall, 1980.

[LoF88] D.P. Loose and J.S. Freudenberg, "Linear Quadratic Gaussian Design for Robust Performance Objectives," *Procedings 27th IEEE Conference Decision and Control*, Austin TX, December 1988.

[LoF89a] D.P. Loose and J.S. Freudenberg, "H^∞-Optimal Design for Robust Performance," Proceedings 1989 Hopkins Conference, March 1989.

[LoF89b] D.P. Loose and J.S. Freudenberg, "Linear Quadratic Gaussian Design for Robust Performance of a Highly Maneuverable Aircraft", *Proc. 1989 AIAA Guidance and Control Conference*

[MaK77] A.G.J. MacFarlane and B. Kouvaritakis, "A design technique for linear multivariable feedback systems," *Int. J. Control*, vol. 25, pp. 837-874, 1977.

[NeM87] C. N. Nett and V. Manousiouthakis, "Euclidean Condition and Block Relative Gain: Connections, Conjectures, and Clarifications," *IEEE Trans. Aut. Contr.*, vol. AC-32, no. 5, pp. 405-407, May 1987.

[NeU88] C.N. Nett and J.A. Uthgenannt, "An Explicit Formula and an Optimal Weight for the 2-Block Structured Singular Value Interaction Measure". *Automatica*, 24, 261-265, 1988.

[PFD88] A. Packard, M.K.F. Fan, and J.C. Doyle, "A Power Method for the Structured Singular Value, *Proc. 27th IEEE Conf. on Decision and Contr.*, pp. 2132-2137, Atlanta, Georgia, Dec. 1988.

[RiB86] D.B. Ridgely and S.S. Banda, "Introduction to Robust Multivariable Control," Tech. Report, Flight Dynamics Lab., Wright-Patterson Airforce Base, Ohio, 1986.

[SkM87] S. Skogestad and M. Morari, "Implications of Large RGA Elements on Control Performance," *Ind. Eng. Chem. Res.*, vol. 26, pp. 2323-2330, 1987.

[SLH81] M.G. Safonov, A.J. Laub and G.L. Hartman, "Feedback Properties of Multivariable Systems: the Role and Use of the Return Difference Matrix," *IEEE Trans. on Auto. Contr.*, vol. AC-26, 1981.

[SMD88] S. Skogestad, M. Morari, and J. C. Doyle, "Robust Control of Ill-Conditioned Plants: High-Purity Distillation," *IEEE Trans. Aut. Contr.*, vol. AC-33, no. 12, pp. 1092-1105, Dec. 1988.

[StA87] G. Stein and M. Athans, "The LQG/LTR Procedure for Multivariable Feedback Control Design", *IEEE Trans. Aut. Contr.*, vol. AC-32, No. 2, pp. 105-114, Feb. 1987.

[Ste77] G. W. Stewart, "On the Perturbation of Pseudo-Inverse, Projections and Linear Least Squares Problems," *SIAM Review*, vol. 19, no. 4, pp. 634-662, Oct. 1977.

[Ste84] G. Stein, Notes, ONR/Honeywell Workshop, Oct. 1984.

[Ste85] G. Stein, "Beyond Singular Values and Loop Shapes," Report No. LIDS-P-1504, MIT, Cambridge, MA, August 1985.

[Ste87] G. Stein, *Lecture Notes of Workshop on Robust Multivariable Control*, Minneapolis, MN, June 1987.

[Vid85] M. Vidyasagar, *Control Systems Synthesis: A Factorization Approach*, Cambridge, MA: MIT Press, 1985.

[ZaD63] L.A. Zadeh and C.A. Desoer, *Linear System Theory*, McGraw-Hill, New York, 1963.

[ZhF90] Z. Zhang and J.S. Freudenberg, "Loop Transfer Recovery for Nonminimum Phase Plants," to appear, *IEEE Trans. Automat. Contr.*, May 1990.

Appendix A. Proof of Proposition 3.5.4

We shall first need several preliminary lemmas in order to prove Proposition 5.4. For convenience, we shall also denote $T_I = \begin{bmatrix} t_{11} & t_{12} \\ t_{21} & t_{22} \end{bmatrix}$.

Lemma A.1 *Let M be given in (3.4.3) with $n = 2$, $k = 1$. Then,*

$$rank[M] \leq 2 \tag{A.1}$$

Proof: It can be readily verified that

$$M = diag[r_1, r_2, r_3 I_2] \cdot \begin{bmatrix} T_I P^{-1} \\ -S_O \end{bmatrix} [P \ - I_2].$$

∎

Lemma A.2 *Let M be given in (3.4.3) with $n = 2$, $k = 1$, and let $U = diag[u_1, u_2, u_3]$, $V = diag[v_1, v_2, v_3]$, where $u_1, u_2, v_1, v_2 \in \mathbf{C}$, $u_3, v_3 \in \mathbf{C}^{2 \times 1}$, $\|u_i\| = \|v_i\| = 1$. Then,*

$$rank[V^H MU] \leq 2 \tag{A.2}$$

Proof: Noting that $rank[U] = rank[V] = 3$, and $rank[M] \leq 2$, the lemma follows immediately from the well-known Sylvester inequality.

∎

Lemma A.3 *Let the interaction parameters be given in (3.4.11-13), and (3.4.17-18). Suppose that $n = 2$, $k = 1$. Then these parameters are related via*

(i)

$$
\begin{aligned}
\mu^3(1,2,3) \ \leq \ & \mu^3(1,3,2) + \mu^2(1,2) \cdot \bar{\sigma}[r_3 S_O] + \mu^2(2,3) \cdot | \, r_1 t_{11} \, | \\
& + \ \mu^2(1,3) \cdot | \, r_2 t_{22} \, | + | \, r_1 t_{11} \, | \cdot | \, r_2 t_{22} \, | \, \bar{\sigma}[r_3 S_O]
\end{aligned} \tag{A.3}
$$

140

(ii)

$$\mu^3(1,3,2) \leq \mu^3(1,2,3) + \mu^2(1,2) \cdot \bar{\sigma}[r_3 S_O] + \mu^2(2,3) \cdot |r_1 t_{11}|$$

$$+ \mu^2(1,3) \cdot |r_2 t_{22}| + |r_1 t_{11}| \cdot |r_2 t_{22}| \bar{\sigma}[r_3 S_O] \qquad \text{(A.4)}$$

Proof: By symmetry, it suffices to show Part (i). Toward this end, choose $u_1 = u_2 = v_1 = v_2 = 1$, $u_3 = (r_2 e_2^H P^{-1} T_O)^H / \| r_2 e_2^H P^{-1} T_O \|$, and $v_3 = (r_3 S_O P e_1)/\| r_3 S_O P e_1 \|$ in Lemma A.2. Consider the Laplace expansion of $det[V^H M U] = 0$. The result follows by noting that

$$|r_1 t_{12}| \| r_2 t_{21} \| v_3^H r_3 S_O u_3 | \leq \mu^2(1,2) \cdot \bar{\sigma}[r_3 S_O]$$

$$|r_1 t_{11}| \| v_3^H r_3 S_O P e_2 | \bar{\sigma}[r_2 e_2^H P^{-1} T_O] \leq \mu^2(2,3) \cdot |r_1 t_{11}|$$

$$|r_2 t_{22}| \| r_1 e_1^H P^{-1} T_O u_3 | \bar{\sigma}[r_3 S_O P e_1] \leq \mu^2(1,3) \cdot |r_2 t_{22}|$$

$$|r_2 t_{21}| \| v_3^H r_3 S_O e_2 \| r_1 e_1^H P^{-1} T_O u_3 | \leq \mu^3(1,3,2)$$

$$|r_1 t_{11}| \| r_2 t_{22} \| v_3^H r_3 S_O u_3 | \leq |r_1 t_{11}| \cdot |r_2 t_{22}| \cdot \bar{\sigma}[r_3 S_O]$$

and applying the triangle inequality.

■

Proof of Proposition 3.5.4

Proof: By symmetry, we assume $\mu(1,2,3) = \mu_3$ with no loss of generality. Then, it suffices to prove

$$\mu(1,2,3) \leq 1.62 \, max \{\mu_1, \mu_2\} \qquad \text{(A.5)}$$

Noticing that

$$\mu^3(1,2,3) \cdot \mu^3(1,3,2) = \mu^2(1,2) \cdot \mu^2(1,3) \cdot \mu^2(2,3) \qquad \text{(A.6)}$$

141

by definition, it follows from Part (i) of Lemma A.3 that

$$\mu^3(1,2,3) \leq \frac{\mu^2(1,2)\mu^2(2,3)\mu^2(1,3)}{\mu^3(1,2,3)} + \mu^2(1,2) \cdot \partial[r_3 S_O]$$
$$+ \mu^2(2,3) \cdot |r_1 t_{11}| + \mu^2(1,3) \cdot |r_2 t_{22}|$$
$$+ |r_1 t_{11}| \cdot |r_2 t_{22}| \, \partial[r_3 S_O]$$

For convenience, let $\theta = max\{\mu_1, \mu_2\}$. The above inequality then reduces to

$$(\mu_3^3)^2 - 4\theta^3(\mu_3^3) - \theta^6 \leq 0$$

Solving this inequality yields

$$\mu_3^3 \leq (\sqrt{5} + 2)\theta^3$$

This completes the proof.

■

Appendix B. Proof of Proposition 3.5.6

Proof: First note that the lower bound in (3.5.15) is a restatement of (3.4.14). In order to show the upper bound, consider instead that $M = diag[M_{11}, M_{22}, M_{33}] + M_1$, where

$$M_1 = \begin{bmatrix} 0 & 0 & M_{13} \\ 0 & 0 & M_{23} \\ M_{31} & M_{32} & 0 \end{bmatrix}$$

It follows from Chapter 2 that $\mu[M] \leq \mu_1 + \mu[M_1]$. From [?], it follows that $\mu[M_1] = \max_{X,Y} \rho[X^H M_1 Y]$ for $X = diag[x_1, x_2, x_3]$ and $Y = diag[y_1, y_2, y_3]$, where x_i and y_i are unit vectors with appropriate dimensions. It can then be readily verified that $\mu[M_1] \leq \sqrt{\mu^2(1,3) + \mu^2(2,3)}$. The proof is now completed by noticing that (3.5.16-18) follow from straightforward calculations.

■

Appendix C. Proof of Proposition 4.4.2

Before proving Proposition 4.4.2, we first consider a partition

$$M = \sum_{l=1}^{N} M(l), \tag{C.1}$$

where $M(l)$ satisfies

$$M_{ij}(l) = \begin{cases} M_{ij} & \text{For } i = 1, \cdots, N+1-l, \ j = i+l-1; \\ M_{ij} & \text{For } i = N+2-l, \cdots, N, \ j = i+l-1-N; \\ 0 & \text{Otherwise} \end{cases} \tag{C.2}$$

Note that $M(l)$ has all blocks being zero, except $M_{1l}, M_{2,l+1}, \cdots, M_{N+1-l,N}, M_{N,l-1} \cdots,$ $M_{N+2-l,1}$. Specifically, there is only one block possibly being nonzero along each block-row and block-column. To illustrate, consider $N = 4$.

Example C.1: Let $N = 4$. Then,

$$M(1) = diag[M_{11}, M_{22}, M_{33}, M_{44}], \qquad M(2) = \begin{bmatrix} 0 & M_{12} & 0 & 0 \\ 0 & 0 & M_{23} & 0 \\ 0 & 0 & 0 & M_{34} \\ M_{41} & 0 & 0 & 0 \end{bmatrix},$$

$$M(3) = \begin{bmatrix} 0 & 0 & M_{13} & 0 \\ 0 & 0 & 0 & M_{24} \\ M_{31} & 0 & 0 & 0 \\ 0 & M_{42} & 0 & 0 \end{bmatrix}, \qquad M(4) = \begin{bmatrix} 0 & 0 & 0 & M_{14} \\ M_{21} & 0 & 0 & 0 \\ 0 & M_{32} & 0 & 0 \\ 0 & 0 & M_{43} & 0 \end{bmatrix}.$$

Proof of Proposition 4.4.2: With no loss of generality, we assume $\mu_N = (\sigma_{12}\sigma_{23} \cdots \sigma_{N1})^{1/N}$.

Note first that

$$\mu_N = \inf_{D \in \mathcal{D}} \bar{\sigma}[DM(2)D^{-1}]$$

$$= \inf_{d_1, \cdots, d_N} \ max \ \left\{ \frac{d_1}{d_2}\sigma_{12}, \ \frac{d_2}{d_3}\sigma_{23}, \ \cdots, \ \frac{d_N}{d_1}\sigma_{N1} \right\}.$$

The solution to this minimization problem is obtained by setting

$$d_1 = 1$$

$$d_i = \frac{\sigma_{12} \cdots \sigma_{i-1,i}}{\mu_N^{i-1}}, \quad \forall i \geq 2.$$

144

This leads to

$$\frac{\hat{d}_i}{\hat{d}_j}\sigma_{ij} = \begin{cases} \frac{\mu_{i-j+1}^{i-j+1}}{\mu_N^{i-j}} & if\ i > j \\ \frac{\mu_{N-(j-i)+1}^{N-(j-i)+1}}{\mu_N^{N-(j-i)}} & if\ i < j \end{cases}$$

and in turn to

$$\begin{aligned} \bar{\sigma}[\hat{D}M(l)\hat{D}^{-1}] &= max\left\{\frac{\hat{d}_1}{\hat{d}_l}\sigma_{1l},\ \frac{\hat{d}_2}{\hat{d}_{l+1}}\sigma_{2,l+1},\cdots,\ \frac{\hat{d}_{N+2-l}}{\hat{d}_1}\sigma_{N+2-l,1}\right\} \\ &\leq \frac{\mu_{N+2-l}^{N+2-l}}{\mu_N^{N+1-l}}. \end{aligned}$$

Next, notice that

$$\mu[M] \leq \inf_{D\in\mathcal{D}}\bar{\sigma}[DMD^{-1}] \leq \mu_1 + \mu_N + \sum_{l=3}^{N}\bar{\sigma}[\hat{D}M(l)\hat{D}^{-1}].$$

Hence

$$\mu[M] \leq \mu_1 + \mu_N + \sum_{l=3}^{N}\frac{\mu_{N+2-l}^{N+2-l}}{\mu_N^{N+1-l}}.$$

This proves (4.4.3), and (4.4.4) is immediate.